The Effect of Housing Temperature and a High-fat, High-carbohydrate Diet on Maternal Interscapular Brown Adipose Tissue

By

Dr Enas AlHarethi

Division of Child Health, Obstetrics and Gynaecology

School of Medicine

Faculty of Medicine and Health Sciences

University of Nottingham

Thesis submitted to the University of Nottingham for the degree of Master of Philosophy

November 2018

Abstract

Brown adipose tissue (BAT) has a role in energy balance and the utilization of fatty acids and glucose, but the extent to which its composition may be modulated by housing temperature is unknown, especially during gestation. BAT activity decline during gestation to enable conservation of maternal energy. This study aimed to investigate the effect of the standard housing temperature (20°C) as compared to a thermoneutral environment (~27°C) on obesity during gestation. The hypothesis is the impact of gestation and high-fat, high-sucrose (HFHS) diet on BAT and white adipose tissue (WAT) would be pronounced on thermoneutral temperature conditions and these changes would be mediated by changes in BAT.

Several methods were employed in this study to produce the outcomes, including immunohistochemistry on a BAT for visualisation and quantification of mitochondrial UCP1 abundance. The qPCR (quantitative polymerase chain reaction) was performed to investigate the mRNA expression of several BAT-related genes, including *UCP1,* proximal proliferator-activated receptor *(PPARγ),* PPARγ coactivator *(PGC1α),* beta-3 adrenergic receptor (*β_3-ARs)* and transient receptor potential vanilloid subfamily 1 *(TRPV1)*. Other genes were also investigated, such as the lipid-transporter gene adipocyte triglycerides lipase *(ATGL)*, the energy-sensing gene (*leptin)* and the UCP1-independent thermogenesis sarco/endoplasmic reticulum ATPase2b *(SERCA2b).* Some plasma metabolites were measured including the use of enzyme linked immune assay for plasma insulin hormone.

The HFHS diet had the greatest effect on body weight gain and fat mass deposition in the gestational group. Throughout gestation, both HFHS diet and housing at 20°C increased interscapular BAT weight. The mitochondrial UCP1 abundance in the animals housed at 20°C increased in the pre-gestation and 10-days gestation groups. Before gestation, the mRNA expression of the *UCP1* followed a similar pattern to the UCP1 protein abundance, *PGC1* mRNA expression increased and *leptin* expression decreased as compared to 27°C. In the 19-day gestation group, the mRNA expression of *PPARγ* decreased and the expression of *PGC1α* increased. The (*ATGL*) mRNA expression increased at 27 °C in the pre-gestation and 19-day gestational groups.

In conclusion, these results suggest that the standard housing temperature conditions under which rat are normally maintained impact UCP1 abundance and fat mass deposition although this effect is partially modified by gestation. Only modest changes were shown in plasma metabolites, which emphasize the subtle but important role of housing temperature when examining the effect of HFHS diet. Standard housing temperature do not reflect rat thermoneutrality and may have consequences for metabolic research results. Therefore, thermoneutrality remains the ideal housing temperature that could model human conditions for metabolic research.

Acknowledgement

This thesis is the summary of my MPhil journey and for that; I would like to express my greatest gratitude to my father Dr Mohammed AlHarethi, my first love, my role model and my source of inspiration for showing faith in me and providing all the financial support for this degree. I thank my mother Mrs Mariam Aqlan for loving me unconditionally and supporting me. I thank my beloved husband, Dr Mohammed Badawi, for your continued and unfailing love, being there for me, comforting me, and supporting me financially to travel and stay in England throughout my studies. I thank my brother M.Eng Shaker AlHarethi for sacrificing hours of his busy schedule and travel long distances to ensure that my paper work was completed for the studies and the visa, thank you for believing in me. I can never repay all of you, my family, back.

I would like to express my appreciation to my principle supervisor, Prof Michael Symonds, for his valuable advice, criticism and positive feedback that kept me going. Thank you for your support during the difficulties I passed through, and guiding me throughout my degree. I thank my second supervisor, Prof Helen Budge, for her scientific advice, guidance and support. I thank Dr Neele Dellschaft for performing the animal study experimentation and the laboratory advice.

I cannot express my gratitude to my colleague who become a dear friend Dr Reham Alagal for her support and help since the day I started my degree. Thank you for proofreading my thesis although all of your responsibilities, teaching me and giving me valuable advices throughout my study.

Special thanks to Mrs Layla Albustanji for sharing this research journey with me, for opening your heart and home for me, for all the warm moments with you and your lovely family, you have been and continue to be a great friend.

I thank Dr Ian Bloor, a Child Health division staff, who helped me during my research, planning my thesis and preparing for the viva. This work would not be completed without the very tolerant technical staff Mr Mark Pope and Ms Catherin Pincott, thank you I appreciate all the help and support you offered me.

To my friend Ms Shimaa Almozyn, thank you for being the wonderful friend and neighbour I could ever ask for, all the Sunday morning coffees will lasts in my heart and mind forever. To Ms Afnan Alshenbari, my friend since the childhood, thank you for supporting me and celebrating my achievements. I thank the friends who made my stay in Nottingham enjoyable, Dr Ahmed Meliebary, Mrs Fadiah Almonajed and Mr Hassan Bawabiji for the amazing nights we spend talking about our dreams and hopes, and for being such a great family for my husband and me. Thank you my colleagues, Mr Saleh Algarni, Dr Amna Nasuf, Dr Zainab Elfzzani, Dr Ahmed Alhaddad for sharing this journey with me and showing support and care.

Finally, I thank my siblings, my closet friends, Amal, Eman, Shaker, Afrah, Sharaf, Shehab and Shaheen and their children for their continue unparalleled love, support and prayers.

Declaration

The work in this thesis was performed within the Academic Child Health Division, Obstetrics and Gynaecology at University of Nottingham, Queens Medical Centre between February 2017 and November 2018.

Unless otherwise stated, this thesis illustrates my own work, completed under the supervision of Prof Michael Symonds and Prof Helen Budge of the University of Nottingham.

This thesis is an accurate representation of the work performed and no other study reproducing this work, to my knowledge, has been carried out within the University of Nottingham.

Enas AlHarethi

November 2018

Table of contents

Abstract I

Acknowledgements I

Declaration III

Table of contents IV

List of abbreviations I

Chapter 1 – Introduction 1

1.1 Overweight and Obesity 1

1.2 Adipose Tissue 9

1.2.1 White Adipose Tissue 11

1.2.2 Brite Adipocyte Tissue 12

1.2.3 Brown Adipose Tissue 14

1.2.4 Genes expressed in BAT 26

1.3 General physiology and physiological changes with gestation 32

1.4 Maternal obesity 35

1.4.1 Obesity programming 35

1.5 Rats as an experimental model 39

1.6 Study aims and hypothesis 41

Chapter 2 - Material and methods 43

2.1 Procedural and legal declaration 43

2.2 Study design 44

2.2.1 Animals, diets and ambient temperature 45

2.2.2 Post-mortem analysis and plasma sampling 47

2.2.3 Tissue analysis 47

2.3 Histology 48

2.3.1 The principle of the technique 48

2.3.2 Histological tissue processing 48

2.3.2 Immunohistochemistry 50

2.4 Insulin assay 56

2.4.1 Sandwich Enzyme-Linked Immuno-Sorbent Assay (ELISA) principle 56

2.4.2 Sandwich ELISA procedure steps 58

2.5 Ribonucleic acid extraction 59

2.5.1 RNA extraction procedures 61

2.5.2 Polymerase chain reaction 63

2.5.3 Reverse transcription polymerase chain reaction 64

2.5.3.1 Principle of RT-PCR 64

2.5.4 Quantitative polymerase chain reaction 65

2.5.4.1 The principle of the Q-PCR technique 65

2.5.4.2 Development of oligonucleotide primers for Q-PCR 68

2.5.4.3 RT-PCR technique 73

2.5.4.4 Selection of housekeeping genes in Q-PCR 73

2.5.4.5 Quantitative polymerase chain reaction procedure 74

2.6 Statistical analysis 78

2.6.1 Power calculation 79

Chapter 3 - The effect of different housing temperature condition and dietary intervention on body composition and plasma metabolites 80

3.1 Introduction and aims 80

3.2 Material and methods 81

3.3 Results 82

3.3.1 The effect of the HFHS diet and standard housing temperature and their contribution to whole body weight and fat deposition 82

3.2.2 The effect of the housing temperature and diet on plasma metabolites 92

3.3 Discussion 96

3.3.1 The impact of standard housing temperature and a HFHS diet on the body composition of female rodents 96

3.3.2 Metabolic adaptation to the HFHS and standard housing temperature 100

3.4 Conclusion 104

Chapter 4 - The effect of temperature and dietary intervention on BAT thermogenic capacity 105

4.1 Introduction and aims 105

4.2 Material and methods 106

4.3 Results 107

4.3.1 The effect of housing temperature and diet on interscapular BAT morphology 107

4.3.2 The effect of housing temperature and diet on the interscapular BAT genotype 114

4.4 Discussion 123

4.4.1 The effect of the housing temperature and the HFHS on the interscapular BAT phenotype 123

4.4.2 The effect of the housing temperature and HFHS diet on the interscapular BAT genotype 128

4.5 Conclusions 133

Chapter 5 – Conclusion 135

5.1 General aims 135

5.2 Main methods 135

5.3 Summary of findings 136

5.3.1 The HFHS diet increased TBW and adiposity 136

5.3.2 Modest effect of HFHS diet and housing temperature on plasma metabolites 137

5.3.3 Standard housing temperature modified BAT thermogenic capacity 137

5.4 Study limitations 140

5.4.1 Rats as a model for human 140

5.4.2 Challenges in measuring food intake 141

5.4.3 Limitations of laboratory techniques and power calculation 141

5.4.4 Moderate high-fat content in the HFHS diet 143

5.5 Future work 143

5.6 Final remarks 144

Appedix: List of suppliers 174

Table of figures:

Figure 1.1: The distribution of obesity worldwide. 3

Figure 1.2: Hospital admissions in England per 100,000 people in which obesity was a factor. 3

Figure 1.3: Summary of the insulin-signalling pathway in adipose tissue. 6

Figure 1.4: Histological image and main morphological characteristics of white adipocytes. 12

Figure 1.5: BAT depots anatomical distribution in A) rodent, B) Human infant C) Human adult. 16

Figure 1.6: Histological image and the main morphological characteristics of brown adipocytes. 17

Figure 1.7: BAT activation by SNS cascade. 21

Figure 1.8: White, brite and brown adipocytes. 14

Figure 1.9: Scheme of adipocytes' developmental pathway. 11

Figure 1.10: Scheme representing UCP1 regulation by PPARα, PPARγ and PGC1α. 28

Figure 2.1: Schematic overview of the number of rodents involved in the study. 45

Figure 2.2: Direct and indirect immunostaining methods. 51

Figure 2.3: Example of (A, B) a negative and (C) a positive controls. 53

Figure 2.4: Illustration of selection areas for IHC analysis. 56

Figure 2.5: Schematic design of sandwich ELISA principle. 57

Figure 2.6: Insulin ELISA standard curve. 58

Figure 2.7: Reverse transcription of polymerase chain reaction. 65

Figure 2.8: Standard curve generated by Q-PCR's software. 67

Figure 2.9: The melt curve generated by Q-PCR software. 68

Figure 3.1: Cumulative body weight prior to gestation. 83

Figure 3.2: 10-days gestation cumulative body weight showing a trend towards increased weight gain in the animals fed HFHS diet. 84

Figure 3.3: 19-days gestation cumulative body weight showing a trend towards increased weight gain in the animals fed HFHS diet. 85

Figure 3.4: Absence of correlation between TBWs and BAT weight before gestation. 89

Figure 3.5: There was a correlation between TBW and BAT weight at 10 days of gestation in the animals fed the control diet and housed under standard housing temperature. 90

Figure 3.6: Correlation between TBW and BAT weight in 19 days of gestation in the animals fed the control diet and housed under standard housing temperature. .91

Figure 3.7: The effect of housing temperature and diet on fasting plasma insulin (ng/ml). 92

Figure 3.8: The effect of housing temperature and diet on fasting plasma glucose (µg/ml) at the three time points. 93
Figure 3.9: The effect of housing temperature and diet on fasting plasma triglycerides (mg/dl)..... 94
Figure 3.10: The effect of housing temperature and diet on fasting plasma NEFA (mmol/L)..... 95

Figure 4.1: Representative examples of the IHC stained histological sections in the pre-gestation. 108
Figure 4.2: Representative examples of the IHC stained histological sections in the mid gestational period (10-days gestation). 109
Figure 4.3: Representative examples of the IHC stained histological sections in the late gestational period (19-days gestation). 110
Figure 4.4: The effect of housing temperature and diet on UCP1 abundance (%) at the three time points. 111
Figure 4.5: The effect of housing temperature and diet on adipocyte area at the three time points. 112
Figure 4.6: The effect of housing temperature and diet on the mean adipocyte count at the three time points. 113
Figure 4.7: The effect of housing temperature and diet on the relative mRNA expression of UCP1 gene in interscapular BAT at the three time points. 115
Figure 4.8: The effect of housing temperature and diet on the relative mRNA expression PPARγ gene in interscapular BAT at the three time points. 116
Figure 4.9: The effect of housing temperature and diet on the relative mRNA expression of PGC1α gene in interscapular BAT at the three time points. 117

Figure 4.10: The effect of housing temperature and diet on the relative mRNA expression of β_3-ARs gene in interscapular BAT at the three time points. 118
Figure 4.11: The effect of housing temperature and diet on the relative mRNA expression of SERCA2b gene in interscapular BAT at the three time points. ..119
Figure 4.12: The effect of housing temperature and diet on the relative mRNA expression of TRPV1 gene in interscapular BAT at the three time points. 120
Figure 4.13: The effect of housing temperature and diet on the relative mRNA expression of leptin gene in interscapular BAT at the three time points. 121
Figure 4.14: The effect of housing temperature and diet on the relative mRNA expression of ATGL gene in the interscapular BAT at the three time points. ...122

Figure 5.1: Summary of hypotheses, methods, and main results. 139

Table of tables:

Table 2.1 Summary of the processing programme used for BAT. 49

Table 2.2. General criteria for optimal PCR primer design. 64

Table 2.3. Reference genes primer sequences for mRNA quantification. 70

Table 2.5. Target genes probes for TaqMan. 72

Table 2.6. Q-PCR reaction mix for SYBER green. 75

Table 2.7. Master Mix reaction mixture for SYBR Green. 75

Table 2.8. Q-PCR reaction mix for TaqMan. 76

Table 2.9. TaqMan Master Mix used for ATGL, PGC1α, TNFα and TRPV1α gene. 77

Table 2.10. Q-PCR programme for SYBR Green. 77

Table 2.11. TaqMan Q-PCR programme required 40 minutes only for each plate. 78

Table 3.1. The effect of housing temperature and diet on WAT and BAT relative weight to body weight. 87

Table 3.2. The effect of housing temperature and diet on organ weight. 88

List of abbreviations

AC – Adenylyl cyclase

ATGL – Adipose triglyceride lipase

ADP – Adenosine diphosphatase

ANOVA – Analysis of variance

ATP – Adenosine triphosphates

BAT – Brown adipose tissue

BLAST - Basic Local Alignment Search Tool

BMI – Body mass index

BMP – Bone morphogenetic protein 7

BMR – Basal metabolic rate

C_p - Crossing point

cAMP – Cyclic adenosine monophosphate

cDNA – complementary deoxyribonucleic acid

C/EBPs – CCAT/enhancer binding protein

CNS – Central nervous system

Cpt1 - Carnitine palmitoyl transferase 1

CRP – C-reactive protein

C_p – crossing-point

Ct - cycle threshold

CV% - Coefficient of variance

DAB - 3-3’-diaminobenzidine

DIT – Diet-induced thermogenesis

DNA - Deoxyribonucleic acid

EDTA – Ethylenediaminetetraacetic acid

ELISA – Enzyme linked immunoassay

ER – Endoplasmic reticulum

ETC – Electron transport chain

FA – Fatty acid

FFA – Free fatty acid

FDG – 18 F-fluorodeoxyglucose

gDNA – Genomic deoxyribonucleic acid

GLUT 4 – Glucose transporter 4

HFD – High-fat diet

HFHS – High-fat and high-sucrose

HIER – Heat-induced epitope retrieval

HRP – Horseradish peroxidase

HSL – Hormone sensitive lipase

IHC – Immunohistochemistry

IL-6 – Interleukin 6

IRS – Insulin receptor substrate

Kg – kilogram

LGA – Large for gestational age

LPL – lipoprotein lipase

M^2 – Meter square

MAPK - Ras-mitogen-activated protein kinase

mRNA – Messenger ribonucleic acid

MSC – Mesenchymal stem cell

MYF5 - Myogenic factor 5

NCBI – National centre for biotechnology information

NE – Norepinephrine

NEFA – Non- esterified fatty acid

NHS – National Health Service

NIH – National Institution of Health

NRTC – No reverse transcriptase control

NST – Non-shivering thermogenesis

NTC – No template control

PCR – Polymerase chain reaction

PDH – Pyruvate dehydrogenase

PDP1c – Pyruvate dehydrogenase phosphate

PDK1 – Phosphotidylinostiol-dependent protein kinase 1

PET – Positron emission tomography

PI3K - phosphatidylinositol 3-kinase

PIP_2 - Phosphatidylinositol 4,5-bisphosphate

PIP_3 - Phosphatidylinositol 3,4,5-trisphosphate

PGC1α - The proximal proliferator-activated receptor co activator alpha

PKA – Protein kinase A

PKB – Protein kinase B

PPARα - The proximal proliferator-activated receptor alpha

PPARγ – The proximal proliferator-activated receptor gamma

PPRE - Peroxisome proliferator response element

PRDM16 – Transcriptional protein domain 16

qPCR – Quantitative polymerase chain reaction

RMR – Resting metabolic rate

RNA – Ribonucleic acid

RPM – Round per minute

RT – Reverse transcription

RT-PCR – Reserve transcription polymerase chain reaction

RyR2 - Ryanodine receptor 2

SERCA2B - Sarco/endoplasmic reticulum ATPase2b

SEM – Standard error of mean

SH domain - Src homology domain

SHOX2 - Short stature homeobox 2

SNS – Sympathetic nervous system

T2DM – Type 2 diabetes mellitus

TBW – Total body weight

TBP – TATA box binding protein

TBX1 - T-box protein 1

TCA - Tricarboxylic acid cycle

TG – Triglyceride

TMB – Tetramethylbenzidine

TMEM26 - Transmembrane protein 26

TNFα – Tumour necrosis factor alpha

TRPV1 - Transient receptor potential vanilloid subfamily 1

VMH – Ventromedial hypothalamus

UCP1 – Uncoupling protein 1

UV- Ultra violet

WAT – White adipose tissue

WHO – World health organisation

YWHAZ – Tyrosine 3 – monooxygenase/ tryptophan 5-monooxygnase axctivation protein zeta

α1-AR – Alpha 1 adrenergic receptor

β-AR – Beta adrenergic receptor

μm^2 – Micrometre square

Chapter 1 – Introduction

This thesis aimed to investigate the effect of standard housing temperature on obesity during gestation among rats. This chapter will discuss and summarise the current knowledge and epidemiological findings about obesity and BAT in relation to standard housing temperature, diet-induced obesity and gestation.

1.1 Overweight and Obesity

Overweight and obesity are medically identified health risk factors that affect all age groups around the globe. Although their aetiologies are well identified, the negative effects of these risks upon human health are continuing to grow.

1.1.1 Definition and incidence

Overweight and obesity are characterised by greater energy intake compared to energy expenditure (i.e., a positive energy balance) leading to excess fat storage. Obesity is defined as the excess accumulation of triglycerides in adipose tissue and is a part of the metabolic syndrome, which is associated with type 2 diabetes mellitus (T2DM) and cardiovascular disease (Galassi et al., 2006, Eckel et al., 2005). The World Health Organisation (WHO) classifies obesity using body mass index (BMI), which is derived by dividing an individual's weight in kilograms (kg) by with their height (m^2) (WHO, 2018).

Although BMI is a widely accepted measurement of the body fat mass, it does not distinguish between muscular and fat mass, and it is often used in

conjunction with other measurements such as waist circumference (NICE, 2006), waist to hip ratio and body composition measurements. Worldwide, the cut-off point is a BMI of ≥ 25 for overweight and of ≥ 30 for obesity. In 2016, more than 1.9 billion adults were overweight, of which 650 million were obese, worldwide. The same year, 41 million children under the age of five were either overweight or obese, as were 340 million children between the ages of 5 and 19 (WHO, 2016). According to the National Health Service (NHS), obese adults made up 26% of the population in England, a 15% increase from 1993. However, childhood obesity prevalence was at about 10% in children aged 4 to 5 years, 20% in those aged between 10 and 11 years (NHS, 2018).

1.1.2 Overweight and obesity: A Global Health crisis

The WHO describes obesity as one of the most obvious yet nonetheless neglected public health issues that threatens to overwhelm industrialised countries. Overweight and obesity occur worldwide in all age groups, regardless of socioeconomic status (WHO, 2018). Figure 1.1 illustrates the global distribution of obesity.

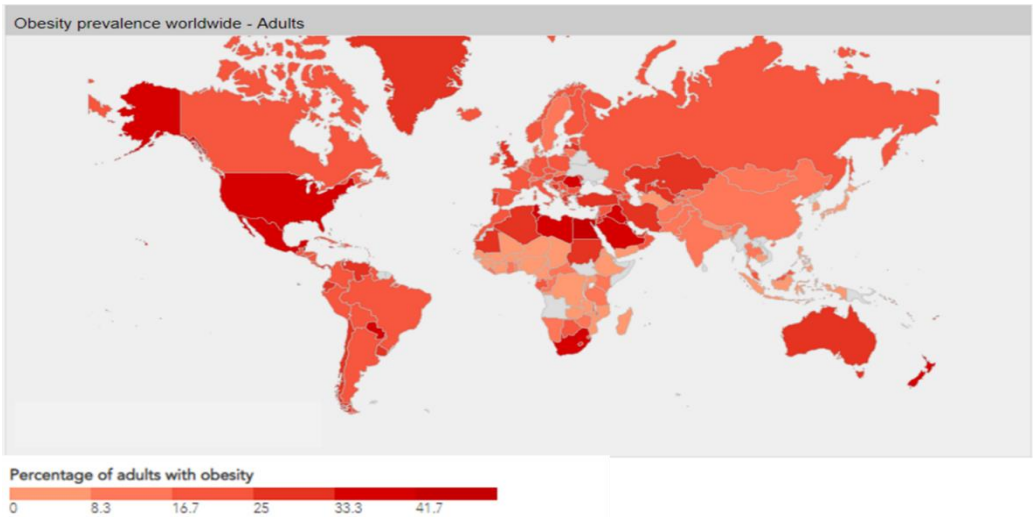


Figure 1.1: The distribution of obesity worldwide.

Data obtained from more than 50 countries by the World Obesity Federation (WOF); grey areas indicate unavailable data.

The increasing prevalence of obesity places a large burden on health-care system use and costs. In 2016/2017, obesity was a factor in 617,000 hospital admissions in England, a figure that is 18% higher than that of 2015/2016 (NHS, 2018) (Figure 1.2).

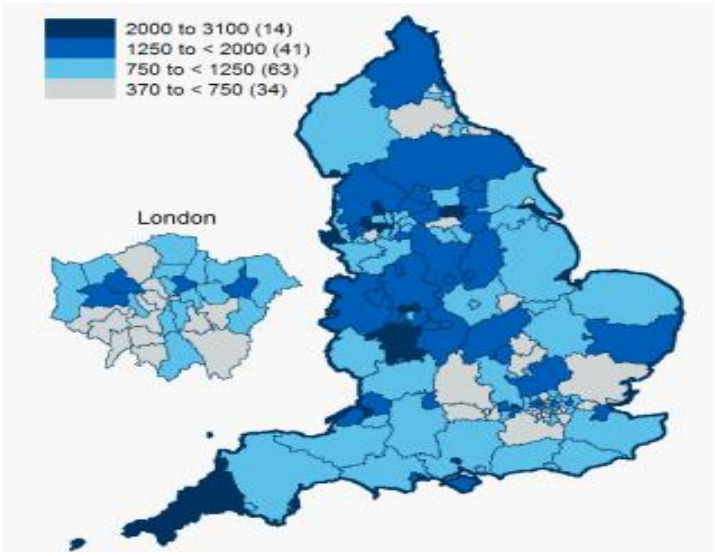


Figure 1.2: Hospital admissions in England per 100,000 people in which obesity was a factor.

Data obtained from the NHS and reported by local authorities.

1.1.3 The impact of being overweight or obese on pregnancy

Pregnancy carries its own complications according to the National Institution of Health (NIH), including, preeclampsia, infections and preterm labour (NIH, 2017). For pregnant women, obesity carries many health risks, such as impaired glucose tolerance, gestational diabetes and hypertension (Leddy et al., 2008). Foetal risks include increased incidence of large for gestational age (LGA) and stillbirth (Hull et al., 2008). Children born to obese mothers may be at greater risk of metabolic, respiratory, cardiovascular diseases and childhood obesity (Harpsoe et al., 2013).

1.1.4 Aetiology and complications

The aetiology of overweight and obesity occur because of triglyceride (TG) accumulation and deposition in adipose tissue following long-term positive energy balance (i.e., eating too much or not being active enough). The current obesity epidemic is occurring in part because of interactions between lifestyle and inherited genes (Symonds et al., 2011). Several other factors contribute to the obesity epidemic, including the level of education, medical conditions, lifestyle, and psychological issues (FRAC, 2015). Factors that facilitate a negative energy balance will lead to weight loss (Fruhbeck et al., 2009).

Obese children are more likely to be obese adults and experience a greater risk of morbidity, disability and premature mortality. Obesity increases the risk of developing metabolic syndrome, a medical condition with five criteria for diagnosis, described by an expert group in the modified national cholesterol education programme adult treatment panel III (NCEP ATP III)

as abdominal obesity, hypertriglyceridemia; low high-density lipoproteins (HDL) cholesterol; impaired fasting glucose and elevated blood pressure (Alberti et al., 2005, Moy and Bulgiba, 2010). Furthermore, an obese adult can develop dyslipidaemia, and other diseases involving the cardiovascular, pulmonary, cerebrovascular, gastrointestinal or reproductive system (Segula, 2014).

1.1.5 Obesity and insulin resistance

The association between obesity and insulin resistance was identified a long time ago. Insulin resistance is a feature of metabolic syndrome and a predictor of the development of T2DM (Lillioja et al., 1993). Insulin resistance occurs when cells fail to respond to the released insulin, which results in impaired glucose uptake. Insulin stimulates TG storage in adipose tissue using several mechanisms, including promoting pre-adipocytes' differentiation to adipocytes, increasing glucose uptake, free fatty acid (FFA) uptake derived from circulating lipoprotein lipase (LPL) activity, lipogenesis and inhibiting lipolysis (Kahn and Flier, 2000). The metabolic effect of insulin is initiated when insulin binds to its receptor, leading to the phosphorylation of insulin receptor substrate (IRS) proteins. This activates two signalling pathways: the phosphatidylinositol 3-kinase (PI3K)-AKT/ protein kinase B (PKB) pathway, which is the most important metabolic pathway for insulin action and the Ras-mitogen-activated protein kinase (MAPK) pathway. IRS-1 is phosphorylated by the insulin receptor and binds to PI3K, its src homology (SH) domain. PI3K converts phosphatidylinositol 4,5-bisphosphate (PIP_2), to phosphatidylinositol-(3,4,5)-triphosphate (PIP_3), a lipid second messenger that activates phosphotidylinostiol-

dependent protein kinase 1 (PDK1), which enrols AKT/PKB to the cell membrane. PI3K-AKT/PKB signalling events then result in the translocation of glucose transporter 4 (GLUT 4) to allow for glucose uptake by the adipocytes. Insulin has an anti-lipolystic action on adipocytes whereas, PI3K activity, through several steps, limits FFA release by reducing TGs catabolism. The MAPK pathways are involved in mediating the growth and mitogenic effects of insulin (Jung and Choi, 2014) (Figure 1.3).

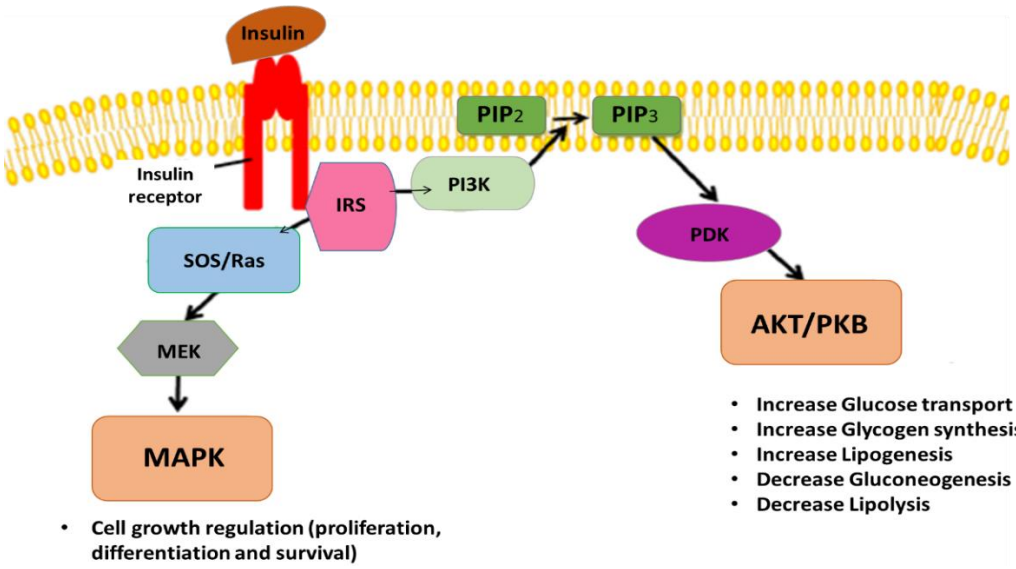


Figure 1.3: Summary of the insulin-signalling pathway in adipose tissue.

Insulin binds to the insulin receptor on the cell membrane and triggers phosphorylation and the activation of IRS, which forms a joining site for PI3K at the membrane. Bound PI3K converts PIP_2 to PIP_3, which is a second messenger that activates PDK1, which in turn recruits AKT/PKD. Ultimately, the PI3K -AKT/PKB signalling pathway regulates the metabolic process.

Several mechanisms are involved in insulin resistance with obesity. One is low-grade inflammation, characterised by an elevated white blood cell count or increased proinflammatory cytokines in the circulation and tissues. Inflammation accompanied obesity begins in adipose tissue and the liver,

with an increase in macrophage infiltration and cytokines (Ye and McGuinness, 2013). The association between proinflammatory cytokines such as tumour necrosis factor alpha (TNFα) and insulin resistance was highlighted the adipose tissue of mice (Hotamisligil et al., 1993). Furthermore, other inflammatory mediators were found to be raised in the circulation of those with obesity, for instance, C reactive protein (CRP) and interleukin 6 (IL-6) (Kershaw and Flier, 2004, Halberg et al., 2008). Inflammation inhibits insulin signalling in adipocytes and hepatocytes either by inhibiting IRS-1, which in the insulin signalling pathway, receives signals from insulin receptors (White, 2002, Ye and Gimble, 2011). The other is the inhibition of peroxisome proliferator-activated receptor gamma (PPARγ) whose function is to drive lipid synthesis and fat storage in adipocytes (Ye, 2008, Ye and Gimble, 2011). The final pathway is the increase of FFA lipolysis and inhabitation of TG synthesis (Ye, 2007). These three effects are found in adipocytes and hepatocytes; however, the insulin action of muscle was not found to be affected by inflammation (Ye, 2013).

Abnormal energy production is one of the major causes of the development of diabetes complications both microvascular and macrovascular diseases (Forbes and Cooper, 2013). These abnormalities include switching cell fuel sources among glucose intermediates, amino acids and fatty acids, changes in respiratory chain function and the respiration produced by uncoupling protein (Forbes et al., 2008). This could terminate ATP production by mitochondrial membrane that can potentially lead to heat loss. The loss of ATP with diabetes may occur late in the development of the disease (Forbes and Cooper, 2013). Although the mitochondrial

abnormalities may be early manifestations of the disease, the loss of ATP generation could be the reason for end-organ damage and cellular apoptosis in the latter stages of the disease (Brooks et al., 2009, Forbes and Cooper, 2013). This could contribute to the changes that enhance energy production from excesses glucose and free fatty acids, which play an important role in the early development of diabetes complications. Glycaemic control is very effective in controlling vascular complication of the disease by decreasing the delivery of glucose into tissues to prevent utilizing other fuel source such as free fatty acids under inappropriate conditions such as oxidative stress (Yan et al., 2009). Reduced postprandial glucose uptake because of the impaired insulin signalling mobilizes fatty acids from adipose tissue as an alternative source of energy and upregulating gluconeogenesis and glycogenolysis (Forbes and Cooper, 2013). Subsequently, accumulation of free fatty acids and hyperglycaemia modulate the localization and expression of glucose transporters (GLUTs) at the sites of diabetic complications. These complications are preventable using selective inhibition of sodium/glucose transport protein 2 for microvascular complications and GLUT 1 and 4 for diabetic nephropathies and cardiomyopathy complications, respectively (Forbes and Cooper, 2013).

Impaired FFA metabolism as in adipose tissue hypoxia can account for several changes in those with obesity, such as leptin elevation, adipocyte death, macrophage infiltration and lipolysis (Ye, 2009). Hypoxia may induce the expression of proinflammatory cytokines in fat (Kershaw and Flier, 2004, Halberg et al., 2008). Hyperinsulinemia results from insulin

resistance, and represents the body's efforts to control hyperglycaemia (Ye, 2007, Corkey, 2012).

1.1.6 Overweight and obesity: Cost and management

The Net Ingredient Cost (NIC) for obesity treatment in 2017 was £6.9 million (NHS, 2018). Obese pregnant women are more likely to require an operative delivery than women with normal BMI (Leddy et al., 2008, Athukorala et al., 2010, Hollowell et al., 2014). Maternity costs for women with a normal BMI is £3,546, which increases by £1,171 with obesity. The overall health service costs increase by 23% for overweight and 39% for obese pregnant women (Morgan et al., 2014).

To aid the management of obesity, a better understanding of the causative mechanisms is required to achieve effective prevention and treatment strategies. Reducing the amount of stored lipids in white adipose tissue (WAT) will reduce the number of complications associated obesity. Several studies have recognised the biochemical abilities of BAT to consume energy. Recently, BAT received an increased amount of attention, as it was found to have a potential role in combating obesity (Symonds et al., 2011, Carey and Kingwell, 2013, Vosselman et al., 2013).

1.2 Adipose Tissue

In mammals, there are at least two types of adipose tissue: WAT and BAT. These tissues have variable amounts of TG, different morphological features, different colours and different anatomical locations (Cinti, 2001, Cannon and Nedergaard, 2004, Cinti, 2006).

Each type of adipocyte (BAT, WAT and brite) is derived from mesenchymal stem cells (MSCs) although the exact mechanism by which this occur unknown (Guilak et al., 2006). BAT shares the same precursor, myogenic factor 5 (MYF5+) with the skeletal muscles (Lepper and Fan, 2010). BAT production requires the MYF5+ precursor to induce bone morphogenetic protein 7 (BMP7), proximal proliferator-activated receptor gamma (PPARγ) and CCAT/enhancer binding protein (C/EBPs) with the transcriptional protein domain 16 (PRDM16) and proximal proliferator-activated receptor gamma coactivator 1 alpha (PGC1α) (Tanaka et al., 1997, Barbera et al., 2001, Jimenez-Preitner et al., 2011, Townsend and Tseng, 2012). WAT adipocytes develop from MYF5- progenitors, and they share this precursor with brite adipocytes (Park et al., 2014). This differentiation is induced by bone morphogenetic protein 2 and 4 (BMP2) (BMP4), C/EBPα,β and PPARγ (Zhang et al., 2004, Rosen and MacDougald, 2006) (see Fig. 1.9). The origin of brite adipocytes is still under debate; a previous study has shown that they could emerge from a smooth muscle-like origin (Long et al., 2014), while another has suggested that the origin is heterogeneous of that of both progenitor cells MYF5+ and MYF5- (Sanchez-Gurmaches and Guertin, 2014).

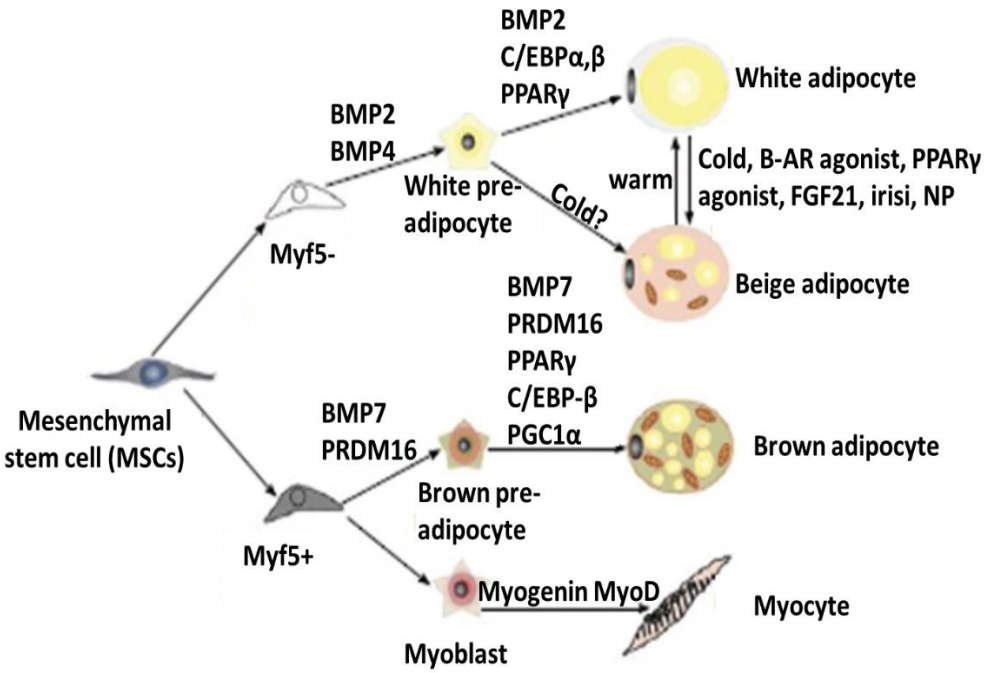


Figure 1.4: Scheme of adipocytes' developmental pathway.

White, brown and brite adipocytes are all derived from the same origin: the pluripotent stem cell MSCs. White and brite are derived from MYF5- precursor cells, whereas brown adipocytes arise from MYF5+ precursor cells. Scheme adapted from (Park et al., 2014).

1.2.1 White Adipose Tissue

WAT is the main depot for excess energy storage and expands with a positive energy balance (Cinti, 2001, Cinti, 2012). WAT is mainly found in visceral and subcutaneous depots. Visceral depots surround the organs, for instance, in the intra-abdominal region, whereas, subcutaneous depots are located beneath the skin in abdominal, inguinal and gluteal areas (Gesta et al., 2007). The main functions of WAT are to store energy in form of TG and to provide insulation to maintain body temperature (McManus and Mitchell, 2014). WAT is a metabolically dynamic organ that synthesises and secrets bioactive compounds, including adipokines such as leptin,

which is a hormone that influences eating behaviour and energy balance (Cinti, 2006). Furthermore, WAT utilises up to 15% of the glucose after a meal, thus, it plays a role in glucose homeostasis (Kahn, 1996).

In periods of fasting, WAT releases FFA from stored TG, a metabolic effect that is regulated by endocrine, paracrine and autocrine signals (Lopez et al., 2007).

WAT morphology is spherical cells that vary in size, are unilocular and have a large lipid droplet; the majority of the cytoplasm is occupied with lipids, with a small number of mitochondria (Cinti, 2006) (see Fig. 1.4).

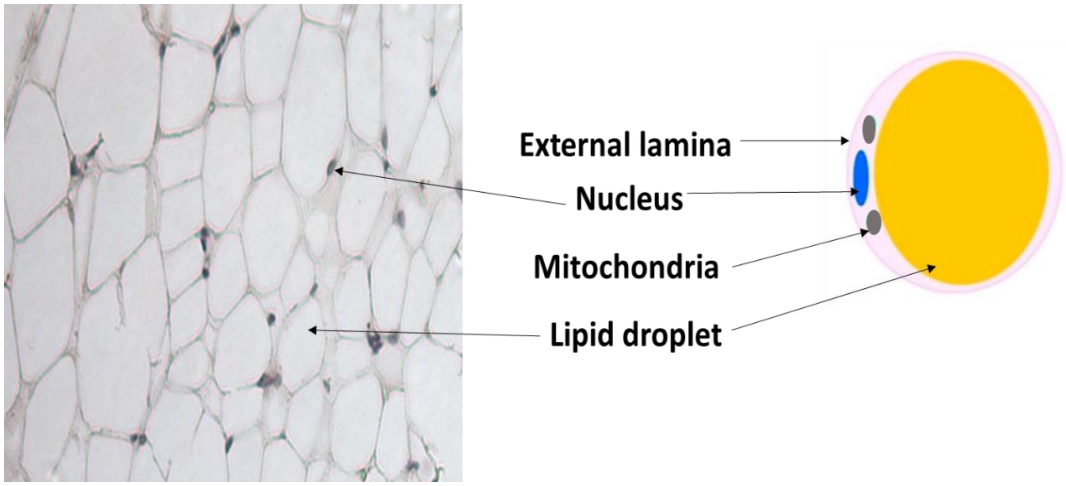


Figure 1.5: Histological image and main morphological characteristics of white adipocytes.

Immunohistochemistry-stained microscopic section from interscapular WAT depot in a rat at 19-days of gestation. White adipocytes contain a spherical, unilocular lipid droplet surrounded by cytoplasm that contains a nucleus and a small number of mitochondria, the external lamina enclose the cell. The histological image magnification is 20X.

1.2.2 Brite Adipocyte Tissue

Another type of adipose tissue has been found within white adipocytes (i.e., brown-in-white), called "brite" or "beige" fat (Klingenspor, 2012, Chen et

al., 2016). This was first discovered in rodents (Young et al., 1984). Brite adipocytes are inducible and have a reversible thermogenic capacity affected by the ambient temperature (Berry et al., 2016). In mice, brite adipocytes are scattered within the subcutaneous depots such as the inguinal and anterior subcutaneous WAT (Ikeda et al., 2018). In contrast, in an adult human, brite adipocytes are located within BAT depots and can develop in WAT under appropriate stimulation (Wu et al., 2012, Walden et al., 2012). Brite adipocytes are inducible with prolonged cold exposure or β_3-AR agonist administration (Loncar, 1991, Cousin et al., 1992). Morphologically, brite adipocytes share some characteristics with the classical brown adipocytes, for instance, in terms of their mitochondrial content and UCP1 expression (Fig. 1.8) (Cousin et al., 1992). However, multilocular brite adipocytes are subjected to variation in the cellular content such as lipid droplet and cell size, and the amount of UCP1-positive mitochondria (Bostrom et al., 2012). Brite adipocytes develop from the same myogenic factor 5- (MY5-) precursor, as white adipocytes (Seale et al., 2008). This will be discussed in detail below, in section 1.2.4. Although brite adipocytes express some BAT-specific genes, such as UCP1, they express their own markers, such as short stature homeobox (SHOX2) (Lidell et al., 2013), transmembrane protein 26 (TMEM26) and T-box protein 1 (TBX1) (Wu et al., 2012).

The browning process is inducible and reversible, meaning that when the ambient temperature rewarms after a cold stimulant, the brite adipocytes convert to white adipocytes and BAT gene expression decreases (Rosenwald et al., 2013). Studies are now focusing on brite adipocytes, as

they may play a role in managing obesity by expending energy when induced (Wu et al., 2012, Okamatsu-Ogura et al., 2013, Shabalina et al., 2013).



Figure 1.6: White, brite and brown adipocytes.

1.2.3 Brown Adipose Tissue

BAT has also received increased attention recently, following its rediscovery in human adults (Nedergaard et al., 2007). The increased interest in BAT is due to its being estimated to contribute up to 5% of the basal metabolic rate (BMR) (Cypess and Kahn, 2010). BAT was thought to be present and functioning only in the neonate (Cannon and Nedergaard, 2004).

The function of BAT is to utilise energy and produce heat, by a process known as non-shivering thermogenesis (NST) through uncoupling protein 1 (UCP1), which is found in the mitochondria. During thermogenesis, mitochondria oxidise FFA obtained from the surface of the lipid droplet rapidly, forming a proton gradient, then protonophore UCP1 facilitate the lowering of the proton gradient and heat production as the FFA burn (Cinti, 2006). Furthermore, BAT releases Batokines such as nerve growth fibre

(NFG) and fibroblast growth factor 2 (FGF2), which may increase sympathetic innervation and preadipocytes count in BAT (Villarroya et al., 2017).

The interscapular BAT is the main depot in rodent whereas in human adults, the main depot is the supraclavicular depot. In infants, BAT appears as a thin layer between shoulder blades.

1.2.3.1 Anatomical distribution

The location of BAT varies between mammals, for instance, the major depot in humans is the supraclavicular area, whereas in rats it is in the interscapular area (Nedergaard et al., 2007, Vosselman et al., 2013). Human new-borns have been found to have interscapular BAT that gradually diminishes with age (Enerbäck, 2010) (see Fig. 1.5). Furthermore, humans have BAT located in tracheal, para-aortic, para-vertebral, supra and perirenal depots (Enerbäck, 2010, Vosselman et al., 2013).

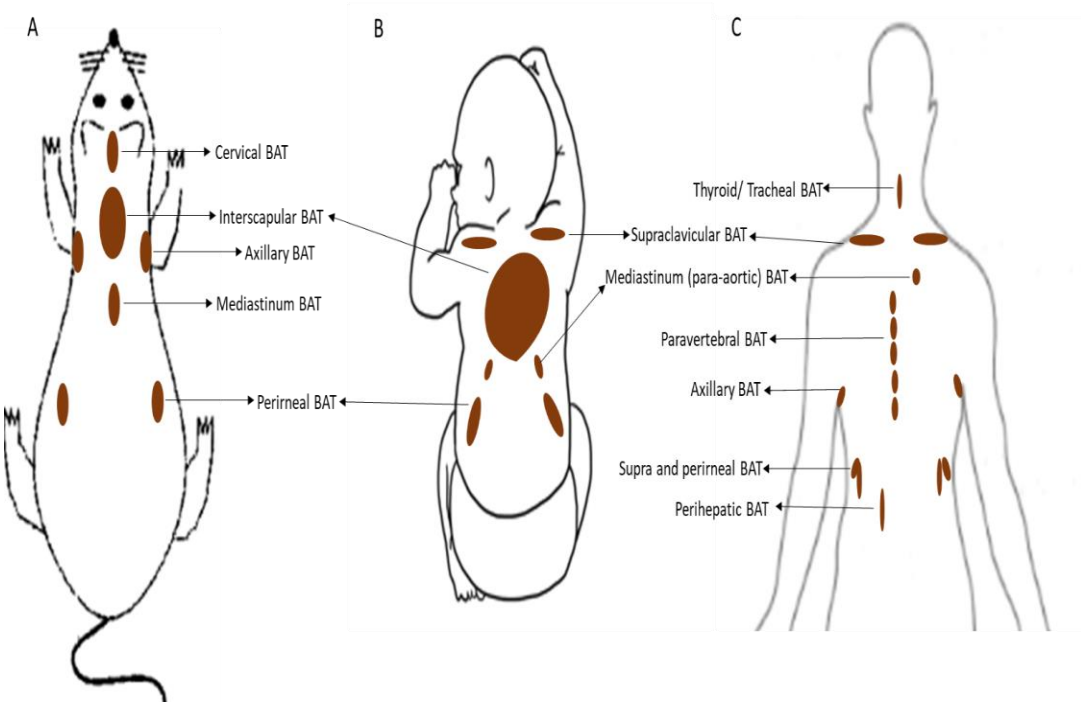


Figure 1.7: BAT depots anatomical distribution in A) rodent, B) Human infant C) Human adult.

1.2.3.2 BAT Morphology

Brown adipocytes are multilocular and contain small lipid droplets that are rich in mitochondria and are highly vascularised, and have central nuclei (Ovalle, 2013, Cinti, 2006) (see Figure. 1.6). These features make BAT histologically different from WAT, as summarised in Table 1.1.

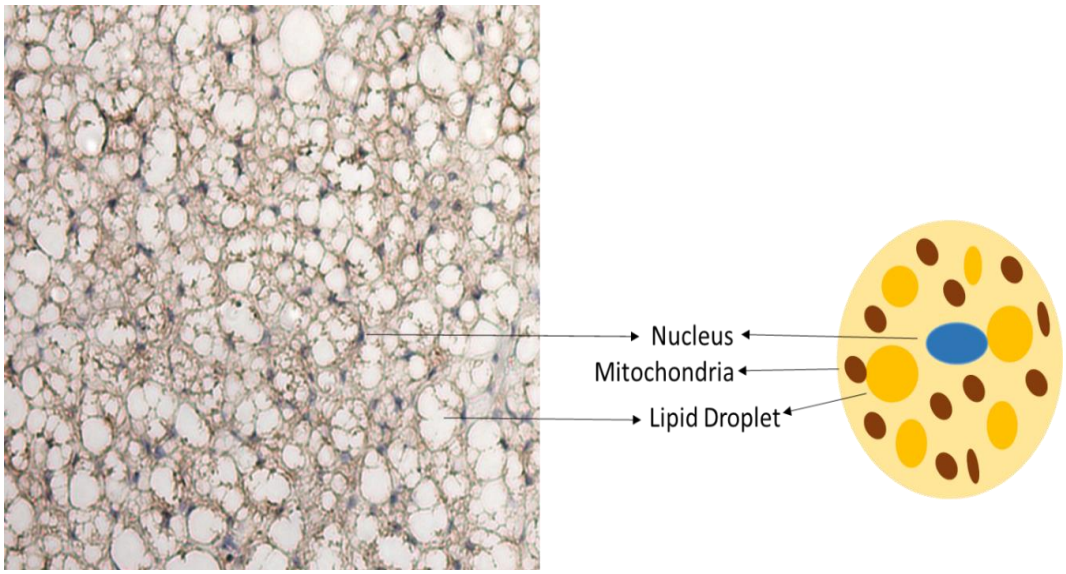


Figure 1.8: Histological image and the main morphological characteristics of brown adipocytes.

Immunohistochemistry-stained microscopic section from interscapular BAT depot in a rat at the unmated time point. Brown adipocytes, within the cytoplasm, contain multilocular lipid droplets, central nuclei, and an abundance of mitochondria. The histological image magnification is 20X.

Table 1.1: Illustration of the difference between brown and white adipocyte characteristics, adapted from (Fruhbeck et al., 2009, Park et al., 2014, Villarroya et al., 2017).

Characteristic	BAT	WAT
Location	Interscapular, axillary, mediastinum and perirenal areas	Visceral depots: retroperitoneal, omental, perirenal, inguinal, perigonadal areas. Subcutaneous depots: Abdominal, inguinal and gluteal areas.
Function	Thermogenesis (non-shivering) and secreting batokines (e.g., NGF & FGF2)	Energy storage in the form of TG and adipokines release (e.g., leptin)
Cell morphology	Multilocular/small lipid droplets and polygonal in shape	Unilocular/large lipid droplet and spherical in shape
Nucleus	Central and round or oval	Peripheral and flattened
Mitochondria	Abundant, large, rounded and with high iron content	Few, small, elongated and with low iron content
UCP1	Abundant	Undetectable
Vascularisation	Abundant	Adequate

1.2.3.3 Non-shivering thermogenesis in BAT activation

NST is defined by (Himms-Hagen, 1984, Cannon and Nedergaard, 2011) as a heat production in response to cold exposure, without shivering. At birth, in humans and mammals, UCP1 is activated in the mitochondria as the new-born is exposed to the cold of the extra-uterine environment (Cannon and Nedergaard, 2004).

BAT activation is inducible by the sympathetic nervous system (SNS), which promotes glucose and lipid uptake (Cannon and Nedergaard, 2004). In humans, BAT activity (i.e. glucose uptake) in the neck was reported by several clinical studies using positron emission tomography (PET) scans and 18 F-fluorodeoxyglucose (FDG) in healthy adults (Saito et al., 2009, van Marken Lichtenbelt et al., 2009, Hwang et al., 2015). Further, increased glucose uptake was observed with cold exposure (Au-Yong et al., 2009, Cypess et al., 2009).

In response to cold, the SNS is activated and releases norepinephrine (NE), which acts upon beta-adrenergic receptors (β-AR), located on the BAT cell membrane (van Marken Lichtenbelt et al., 2009, Cypess et al., 2015). The activation adrenergic receptor has a great effect on metabolism this include: increased lipolysis and elevated fatty acids levels in plasma, increased gluconeogenesis by the liver to provide fuel for the brain, and a moderate inhibition of insulin to conserve glucose and to shift fuel metabolism of muscle to fatty acids oxidation (Ciccarelli et al., 2013). The activation of β-AR catalyses adenylyl cyclase (AC), which is an enzyme that regulates the conversion of adenosine triphosphate (ATP) to cyclic adenosine

monophosphate (cAMP). Protein kinase A (PKA) then phosphorylate Perilipin (Plin 1). Adipose TG lipase (ATGL) is then activated, which regulates the rate-limiting step of TG hydrolysis alongside Plin1. This activates PKA, which activates and phosphorylates hormone-sensitive lipase (HSL) inducing lipolysis and FFA released from TG degradation. Then, carnitine palmitoyl transferase 1 (Cpt1) carries FFA to the mitochondria. Once the FFA binds to UCP1, the proton conductance pathway is activated, thereby bypassing the need to convert ADP to ATP, as occurs in all other cells. β-oxidation (which is a multistep process in which, FFAs are broken down to produce energy by the tricarboxylic acid cycle [TCA]) produce respiration, and UCP1 then uncouples respiration from ATP synthesis (Okada et al., 2016, Cannon and Nedergaard, 2004) (see Fig. 1.7).

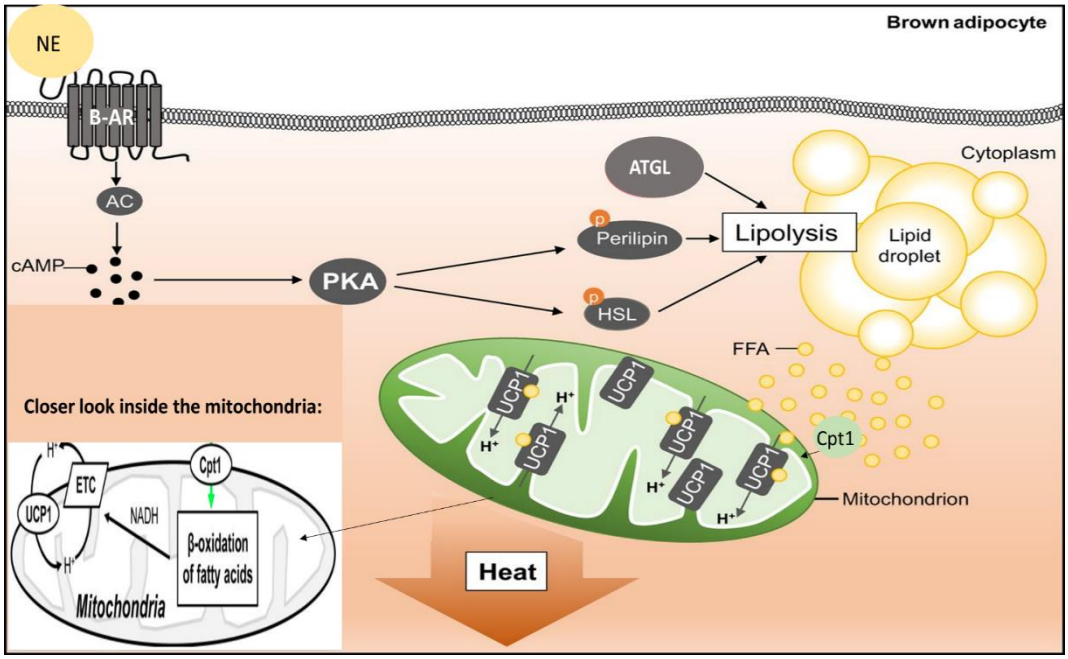


Figure 1.9: BAT activation by SNS cascade.

In response to cold, the SNS releases NE that binds to β-AR, which catalyses AC, which regulates the conversion of ATP to cAMP, which activates PKA, which in turn activates and phosphorylate HSL, which allows that FAs to be released from the stored TG. Cpt1 then, carries FFA into the mitochondria, and the FAs activate UCP1 to uncouple the proton gradient from the oxidative phosphorylation. In this way, energy is released in the form of heat. Diagrams are adapted from (Braun et al., 2018, Okada et al., 2016) and modified for details.

1.2.3.4 BAT regulation and ambient temperature

BAT was thought to be available only in human new-borns, and it was believed to disappear with age (Heaton, 1972). However, as imaging modalities advanced, this enabled researchers to look further for BAT activity in adult human.

BAT activity was detected in studies that exposed adults to cold temperatures of 17 ± 1°C (Saito et al., 2009, Saito, 2013). Furthermore, BAT activity was undetectable at higher temperatures using F-FDG-

PET/CT and Infrared thermography (Hanssen et al., 2016, Yoneshiro et al., 2016, Law et al., 2018).

In rats, BAT activity was detected in studies that exposed animals to cold temperature in the range of 5 ± 1°C (Thornhill and Halvorson, 1990, Jakus et al., 2008, Wang et al., 2015, Hiroshima et al., 2018) to 10°C (Fukano et al., 2016). However, it has been argued that rodents should be housed within their thermoneutral temperature zone, which falls in the range 28 ± 1°C for rats and 30 ± 1°C for mice, to mimic human thermoneutral temperature conditions (Poole and Stephenson, 1977, Speakman and Keijer, 2013, Maloney et al., 2014, Fischer et al., 2018, Symonds et al., 2018, L Small, 2018). Moreover, it was suggested that housing temperature conditions could affect lipid deposition and glucose homeostasis (Feldmann et al., 2009, Overton, 2010, Stemmer et al., 2015). The current rodent studies utilise 21 ± 1°C as a standard housing temperature for rodents, and this is unequal to the human thermoneutral temperature (~21°C) and not an accurate representation of human metabolic, physiological or pathological conditions (Cinti, 2006, Havenaar, 2001, NRC, 2011, Speakman and Keijer, 2013, Fischer et al., 2018, Symonds et al., 2018). For laboratory rodents, the standard housing temperature applies a mild to moderate cold stress because the temperature used is 8 to 10°C lower than the equivalent in human thermoneutrality (Speakman and Keijer, 2013).

The importance of housing temperature has been clarified in past metabolic studies; for instance, a previous study reported that the outcomes were significantly dependent on housing temperature in UCP1-deficient mice (Enerback et al., 1997). These mice showed cold intolerance but did not

became obese at a standard housing temperature (21°C) relative to wild-type mice, when both were fed a high-fat diet (HFD) (Enerback et al., 1997). However, when maintained at the thermoneutral temperature (30°C), UCP1-deficient mice became obese on a chow diet and showed greater fat deposition than did wild-type mice on a HFD (Feldmann et al., 2009). Housing temperature influences the experimental outcome in many different studies such as those involving chemical toxicity (Malcolm and Alkana, 1983, Finn et al., 1989) and responses to a HFD (Enerback et al., 1997, Liu et al., 2003, Feldmann et al., 2009). Hence, it is suggested that rodents should be housed at thermoneutral conditions in laboratory-based studies because it mimics human thermoneutral conditions, unlike the standard housing temperature.

1.2.3.4.1 Food component and BAT activity

The most effective physiological inducer of BAT activity to date, is cold exposure through activating β-ARs (Cannon and Nedergaard, 2004, Saito et al., 2009, Sakamoto et al., 2014) and the transient receptor potential channel subfamily vanilloid 1 (TRPV1) (Szallasi and Blumberg, 1999, Caterina, 2007), which is also stimulated by capsaicin. This induces thermogenesis by increasing the release of catecholamines from SNS activity (Kawada et al., 1986, Watanabe et al., 1987, Yoshioka et al., 2001).

Diet-induced thermogenesis (DIT) is the production of heat following a meal which contributes to an increase in resting metabolic rate (RMR) above basal fasting level divided by the energy content of the food consumed (Weststrate, 1989, Westerterp, 2004), which means part of the calories intake will be expended as energy (Cannon and Nedergaard, 2012). The

rate of DIT is different based on the macronutrient type (Westerterp, 2004). Previous studies reported the DIT values for macronutrients are 0 to 3% for fat, 5 to 10% for carbohydrates, 20 to 30% for protein and 10 to 30% for alcohol (Acheson, 1993, Westerterp et al., 1999).

To induce obesity and the associated metabolic changes in rats, the combination of high-fat and high-sucrose (HFHS) diet was utilized in this study. Rats fed a high-carbohydrates showed dyslipidaemia, impaired glucose tolerance and hypertension but failed to develop central obesity (Thirunavukkarasu et al., 2004, Pang et al., 2008), whereas, rats fed a high-fat showed central obesity (Buettner et al., 2006), therefore, the combination of both diets is used in metabolic research to elicit obesity and the associated changes of metabolic parameters. Furthermore, HFHS diet is more relevant to the diet responsible for human metabolic syndrome (K. Panchal et al., 2011).

1.2.3.4.2 BAT and obesity

BAT activity reduces as BMI increases in healthy children and adults (Saito, 2013, Robinson et al., 2014). A study of 24 healthy adults, where 10 of the participants had a BMI of < 25 and 14 were either overweight or obese (BMI ≥ 25), reported an inverse relationship between BAT activity and BMI (van Marken Lichtenbelt et al., 2009).

It is clear that obese individuals can manage to loses large portion of their weight, but upon this weight loss, many factors challenge the maintenance of the new weight (Carey and Kingwell, 2013). One such challenge is the reduction of the BMR (Sumithran et al., 2011). BMI reduced by 20% in

obese patients who lost 10 -20% of their weight as compared to others who had never been obese (Leibel et al., 1995, Johannsen et al., 2012).

In contrast, a negative energy balance (i.e., more expenditure than intake) enables weight loss. BAT can play a direct role in energy expenditure by stimulating thermogenesis and is a potential target for weight loss and new weight maintenance (Christiansen and Garby, 2002, Saito, 2013). In adults, it has been calculated that with the maximum activation of BAT, 4 kg of weight could be lost over one year (Carey and Kingwell, 2013). Furthermore, in humans and rodents, 40 -50 g of the maximum active BAT could contribute up to 20% of the daily energy expenditure (Rothwell and Stock, 1979b, Rothwell and Stock, 1983).

1.2.3.5 Interscapular BAT

BAT is located in several places, but these locations vary between species. In humans, the main BAT depot is the supraclavicular, while in rodents, is the interscapular region (i.e., between the shoulder blades) (Nedergaard et al., 2007, Fruhbeck et al., 2009). In a rat foetus, cell aggregation in the interscapular area appears around day 15 of intrauterine life, and by day 17, BAT appears to be rich in the vasculature (Nnodim & Lever, 1985). The TG surface area of the interscapular BAT increases 20 fold up to the time of birth (0.44 x 10^2 cm^2), increases again by 4 weeks of age (9.43 x 10^2 cm^2), and demonstrated another small increase by 6 months of age (11.67 x 10^2 cm^2) (Nnodim, 1988). Interscapular BAT developed in intrauterine life is to provide the foetus with protection from the cold external environment (Barnd et al., 1970).

In rodents, interscapular BAT contributes significantly to NST (Cannon and Nedergaard, 2004) as follows: the bilateral denervation or excision of this depot (Dulloo and Miller, 1984) can lead to a 20% reduction in its capacity for NST, to abnormal fat accumulation and to rapid weight gain that can occur without an increase in food intake (Connolly et al., 1982).

1.2.4 Genes expressed in BAT

There are a variety of genes expressed in BAT; however, the most important gene is UCP1, which is expressed uniquely in the inner mitochondrial membrane of BAT and is essential for NST (Cannon and Nedergaard, 2010, Cypess et al., 2013b). BAT thermogenesis is regulated by β_3-AR, which can be induced by β_3-AR agonist (Robidoux et al., 2004, Mund and Frishman, 2013). Moreover, transcription genes such as PPARγ and PGC1α play a critical role in regulating UCP1 expression (Puigserver et al., 1998, Villarroya et al., 2007).

1.2.4.1 Genes involved in BAT thermogenesis

The PKA activation step of the thermogenic cascade, responsible for activating lipolytic enzymes, is followed by the expression of UCP1, PPARγ and PGC1α. The UCP1 expression is controlled by the SNS, which activates the classical thermogenic pathway by promoting β-ARs activity (Klaus et al., 2001, Cannon and Nedergaard, 2004). Mice deficient in UCP1 showed weight gain, but those with an overexpression of UCP1 showed protection from obesity (Kopecky et al., 1995, Li et al., 2000). A loss of UCP1 in mice fed a HFD, which induced the whiting of BAT and glucose intolerance (Winn et al., 2017). Mice with knockout β-AR (i.e., all the three subtypes β_1, β_2 and β_3) exhibited cold intolerance and also showed obesity

although normophagia also, their interscapular BAT showed WAT phenotypical features (Bachman et al., 2002, Jimenez et al., 2002).

The expression of PGC1α increases in BAT with cold exposure through releasing NE by SNS and subsequently activating β_3-AR. Moreover, PGC1α transcription mediated by the cAMP signalling pathway (Puigserver et al., 1998, Gómez-Ambrosi et al., 2001). Moreover, PGC1α can activate another key component for thermogenesis: PPARγ (Barbera et al., 2001). In PGC1α-null mice, cold exposure does not induce UCP1 expression (Lin et al., 2004).

PPARγ plays several roles in BAT including, brown adipocyte differentiation (Nedergaard et al., 2005) and the enhancement of the expression of UCP1 (Nedergaard et al., 2001). UCP1 transcription by PPARγ is regulated during brown adipocyte differentiation and by thermogenesis (Villarroya et al., 2007). With cold exposure, PPARα induces lipolysis, and then FFAs release and coordinate UCP1 transcription (i.e., thermogenesis) by a lipid oxidation mechanism (Villarroya et al., 2007) (see Fig. 1.10). NE leads to a decrease in PPARγ mRNA (messenger ribonucleic acid) in brown adipocytes, yet, the expression returns to the baseline 24 hours after NE exposure (Lindgren et al., 2004). Mice lacking PPARγ in adipose tissue show reduced adiposity; however, null-PPARγ cells cannot differentiate into mature brown adipocytes (Rosen et al., 2000, He et al., 2003, Imai et al., 2004).

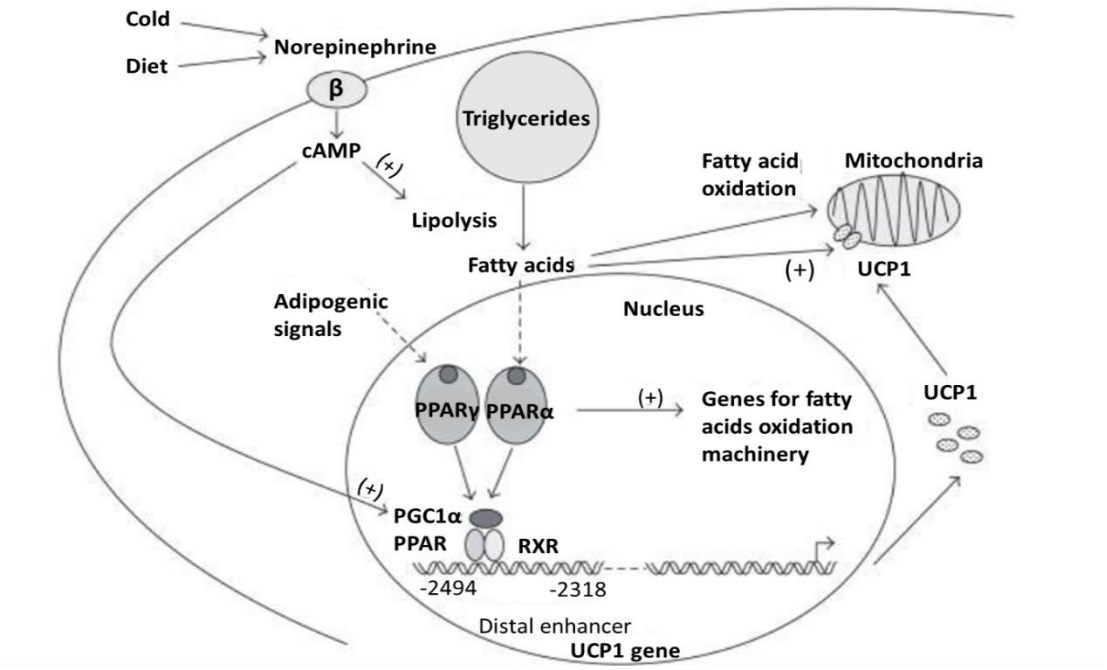


Figure 1.10: Scheme representing UCP1 regulation by PPARα, PPARγ and PGC1α.

During brown adipocyte differentiation, adipogenic signals tightly regulate the UCP1 gene via PPARγ and PGC1α. The role of PPARα is to activate lipolysis and FAs to coordinate UCP1 thermogenesis. Scheme adapted from (Villarroya et al., 2007).

TRPV1 channels are involved in temperature regulation and energy homeostasis (Christie et al., 2018). There is a variety of TRPV1 stimuli, such as a pH of < 5.9 (Cao et al., 2004, Dhaka et al., 2009) and certain food components. Such components include the capsaicin found in hot chillies (Caterina et al., 1997), the allicin and diallyl sulfides found in garlic (Iwasaki et al., 2006, Salazar et al., 2008) and the piperine found in black pepper (Okumura et al., 2010). TRPV1 has several roles in energy regulation, is mediated by the central nervous system (CNS) and enables NE release to bind to β-AR, increasing energy expenditure (Longhurst et al., 1984, Watanabe et al., 1988, Yoshioka et al., 1995, Matsumoto et al., 2000). TRPV1 may inhibit the differentiation of pre-adipocytes into mature brown

adipocytes and decrease their lipid content by increasing lipolysis (Zhang et al., 2007). This could explain the reduced lipid accumulation with capsaicin, and especially browning of the WAT and the increased thermogenesis (Baboota et al., 2014, Sun et al., 2017).

However, there are also endogenous TRPV1 agonists known as endovanilloids, which when released in sufficient amounts, stimulate a TRPV1-mediated response by direct binding and activating the channel.

1.2.4.2 Lipid transporter gene in BAT

Cold-induced β-AR signalling also induces the intracellular hydrolysis of stored TG to break down lipids into FFAs by ATGL and HSL (Zechner et al., 2012). Lipolysis is essential for NST in BAT because the released FFAs activate UCP1 and act as a primary fuel (Cannon and Nedergaard, 2004). ATGL knockout mice showed cold intolerance, their BAT changed to WAT-like tissue with impaired thermogenesis and they showed decreased UCP1 (Haemmerle et al., 2006, Ahmadian et al., 2011). The pharmacological inhibition of ATGL activity also impairs cellular respiration and UCP1 activity (Li et al., 2014). ATGL activity is crucial for the transcriptional activity of PPARα (Haemmerle et al., 2011).

1.2.4.3 Energy-sensing gene

Energy intake is regulated by a complex system involving the hormone leptin, which originates from WAT and can signal to the hypothalamus (Masuzaki et al., 1995). Leptin acts upon the leptin receptor that is widely expressed in the CNS (Campfield et al., 1996, Burguera et al., 2000, Hegyi et al., 2004) and in WAT (Frederich et al., 1995). There is no leptin expression in the BAT (Cinti et al., 1997) but, leptin expression may be

detected in BAT from contaminating white adipocytes that arise within BAT (Trayhurn et al., 1995). Leptin crosses the blood-brain barrier to provide information regarding energy status. This, in humans and rodents, can result in decreased energy intake and an increased expenditure (Pelleymounter et al., 1995, Halaas et al., 1995, Jorgensen et al., 1998, Farooqi et al., 2001, Jeon et al., 2003, Licinio et al., 2004). An increase circulating leptin can promote energy expenditure by increasing SNS activity, thereby stimulating BAT thermogenesis, as confirmed in rodents (Feldmann et al., 2009, Simonds et al., 2014). In addition, when rats were injected with leptin into the ventromedial hypothalamus (VMH), glucose uptake by BAT was increased, along with plasma catecholamines, and thermogenesis was enabled (Minokoshi et al., 1999). Leptin expression increases as the stored lipids and insulin levels increase (Frederich et al., 1995, Maffei et al., 1995, Wabitsch et al., 1996). However, starvation reduces leptin mRNA expression (Frederich et al., 1995, Boden et al., 1996). Previous studies on rat reported a rapid decline in circulating and mRNA level of leptin with cold exposure (MacDougald et al., 1995, Trayhurn et al., 1995).

1.2.4.4 An alternative thermogenic pathway was identified

An alternative thermogenic pathway was identified in brite adipocytes and termed UCP1-independent thermogenesis within sacro/endoplasmic reticulum calcium ATpase2b (SERCA2b) (Ikeda et al., 2017). In response to the cold, NE binds to α_1-AR and β_3-AR to increase calcium flux by activating SERCA2b and ryanodine receptor 2 (RyR2) in beige adipocytes. SERCA2b transports the calcium back to the endoplasmic reticulum (ER)

to be stored and to the mitochondria (Denton, 2009). Increased calcium activates pyruvate dehydrogenase phosphatase (PDP1c), which activates the enzyme pyruvate dehydrogenase (PDH) and ATP synthesis. In the absence of UCP1, brite adipocytes utilise glucose as a fuel for ATP synthesis by enhancing glycolysis, the citric acid cycle (TCA) metabolism and the electron transport chain (ETC) (Ikeda et al., 2017). Although BAT is rich with mitochondria, it expresses low amounts of ATP synthase and consequently ATP (Kramarova et al., 2008). Thus, ATP-dependent thermogenesis is less likely to compensate for the loss of UCP1 in BAT. However, brite adipocytes express high levels of ATP synthase, which produces ATP through glycolysis, TCA metabolism and mitochondrial ETC. Therefore, SERCA2b ATP dependent thermogenesis in brite adipocytes can compensate for UCP1 loss (Ikeda et al., 2017).

1.3 General physiology and physiological changes with gestation

The laboratory rat is an essential part of biochemical research. They substituted the human being in many experimental scientific studies (Sengupta, 2013). Rats are the most frequently used rodents in experimental research, which counts for 20% of the total number of mammals utilised for scientific purposes (Fagundes and Taha, 2004).

The average laboratory rat's lifespan is about 21 months and some continue to live to 3 years of age (Andreollo et al., 2012). Weaning is the first phase of rat life; the average age of weaning is 3 weeks of age (Sengupta, 2013). They reach the second phase of rat-life, which is puberty and sexual maturity by 6-7 weeks of age and then have about 12 months to breed (Adams and Boice, 1983, Sengupta, 2013). For both genders, the age at mating is 8-10 weeks. For female rats, each oestrus cycle (i.e., physiological changes that are induced by reproductive hormones in female mammals), lasts 4-5 days and they ovulate 8-11 hours after the onset of oestrus (Sengupta, 2013). The implantation occur by the 5^{th} day of the oestrus cycle and the average gestation length is 21-23 days (Sengupta, 2013).

Generally, rat gestations characterised by alteration of lipid metabolism, which could be labelled as an anabolic phase for the first two thirds and a catabolic phase for the last third (Herrera and Ortega-Senovilla, 2010). These changes occur to accommodate the increase metabolic needs of the foetus (Lain and Catalano, 2007). Pregnancy is characterized by

hyperlipidaemia (Warth et al., 1975). During the first 14 weeks of pregnancy in women the lipids, especially TGs concentrations decline (Butte, 2000, Herrera, 2002). Lipids are important for placental function and membrane formation and the lipids concentration through pregnancy adapts primarily to the changes in adipose tissue metabolism, endocrine adaptations and carbohydrate metabolism (Butte, 2000). A pervious study showed that during rat gestation, there is a progressive increase in the conversion of glucose to fatty acids and glycerol glycerides in adipose tissue until day 20 of rat gestation (Palacín et al., 1991). Moreover, LPL activity increases, which could promote fat deposition in rat pregnancy by hydrolysing both chylomicrons and very low-density lipoproteins (VLDLs) in order to release NEFA/glycerol to be utilised by adipose tissue (Alvarez et al., 1996). Early gestation anabolism is supported by increase intracellular utilisation of glycerol. Under normal conditions, the conversion of glycerol to glycerol-3-phosphate, which is an essential precursor for TG synthesis, is minimum because of the low activity of the enzyme glycerol kinase (Thenen and Mayer, 1975). As a result, decrease adipose tissue Lipolytic activity alongside increased capacity of maternal tissue to utilise glucose and intracellular glycerol for the production of glycerol-3-phosphate, result in increased TG accumulation (Thenen and Mayer, 1975).

At the last third of gestation, the metabolism switches to catabolic phase with an accelerated rate breakdown of fat deposits because of augmented adipose tissue Lipolytic activity. Previous studies in late pregnant rats showed increased mRNA expression of HSL in WAT (Martineau et al., 2015). Furthermore, it has been shown that LPL activity reduced in rat and

human late-gestation (Pujol et al., 2005), thus decreasing the deposit of lipids in maternal adipocytes. NEFA and glycerol are converted to acyl-CoA and glycerol-3-phate, respectively, by the liver; partial re-esterification is performed for TGs synthesis. The hepatic TGs are mobilised to native VLDL particles and then released into maternal circulation. Alternatively, glycerol could be used for glucose synthesis, while NEFA could be oxidized to acetyl-CoA to produce energy and ketone bodies synthesis. These changes are essential for the foetal development because during late-gestation, requirements for metabolic substrates are increased considerably. During maternal fasting periods, when essential gluconeogenic-substrates are sparse while delivery of newly formed glucose is vital for the foetus, at that time, the preferable use of glycerol for gluconeogenesis is greater important (Zorzano et al., 1986). Furthermore, studies have shown that under fed conditions in early pregnancy, plasma ketone body levels are lower in pregnant than in non-pregnant rats, which suggest an augmented utilization of this energy form (Ricciolini et al., 2001).

Glucose homeostasis is influenced by insulin secretion and sensitivity while both glucose and insulin levels are affected by protein and lipid metabolism (Nelson et al., 2010). During early gestation, plasma glucose level declines, to reflect maternal adaptation rather than changes in fetal utilisation (Mills et al., 1998), and is associated by slightly improved or normal glucose tolerance (Catalano et al., 1991, Catalano et al., 1992, Catalano et al., 1993).

The development of insulin resistance with pregnancy is a normal physiological process (Ryan et al., 1985). Progressive insulin resistance

with pregnancy, maternal adiposity and placental hormones can all contribute to the development of metabolic disorder known as gestational diabetes mellitus (GDM) (Buchanan and Xiang, 2005). The GDM diagnosis is made when the glucose intolerance first detected during gestation (Chu et al., 2007). This might lead to insulin resistance in some obese women while non-pregnant (Butte, 2000, Lain and Catalano, 2007).

1.4 Maternal obesity

Maternal weight gain during gestation is expected, as it occur to support the developing foetus (Nelson et al., 2010). Previous studies support the presence of association between maternal obesity and a greater risk of obesity for their offspring later in life (Whitaker, 2004, Koupil and Toivanen, 2008, Tequeanes et al., 2009, Stuebe et al., 2009). The extent of which maternal obesity influences offspring's weight and body composition depends on many factors, which include exposure time during gestation (i.e., early, mid or late gestation) or during lactation, diet and energy content (Nelson et al., 2010).

1.4.1 Obesity programming

Clinical and epidemiological studies found a great link between maternal dietary intake and composition with the risk of adulthood obesity in the offspring (Ravelli et al., 1998, Ravelli et al., 1999). Maternal obesity is a result of the imbalance energy homeostasis that can affect foetal adipose tissue differentiation and may contribute to the impairment in the offspring's adipose tissue function later in life (Lukaszewski et al., 2013). This effect might include other changes in cell size (i.e., hypertrophy, enlarged

adipocytes as a result of TG deposition), or increase cell number (i.e., hyperplasia, increase white adipocytes differentiation) (Lukaszewski et al., 2013).

A previous study fed the rats to either a control diet with a junk food diet during gestation and/or lactation and/or postnatally or to control diet throughout (Bayol et al., 2007). The aim of this study was to investigate whether maternal exposure to junk food can promote obesity development by affecting the offspring's feeding behaviour. Obese dams consumed more food during pregnancy with majority of nutrient derived from junk food as they preferred consuming fat, salt, carbohydrate-rich food. They were heavier by late gestation because of higher energy intake and reduced physical activity, however, by end of lactation their body weight was comparable to those fed the control diet (Bayol et al., 2007). This could be a result of investing more energy in milk production (Bayol et al., 2007), however, this study did not measure the milk composition. A previous study analysed milk composition in a cafeteria fed diet rats found that the milk was richer fat and energy content (Rolls et al., 1986). The offspring weaned on junk food and born to a mother was fed a junk food during gestation and lactation showed higher energy intake (mainly from junk food), as compared to those fed a control diet during gestation and lactation or fed junk food during gestation then switched to control diet during lactation (Bayol et al., 2007). These suggest that offspring preference for junk food was promoted while exposed to it during gestation and lactation or gestation only (Bayol et al., 2007).

Rats were switched to junk food at weaning showed hyperphagia as compared to those switched to control diet, however, offspring exposed to junk food during gestation and lactation then switched to chow diet at weaning showed reduction in food intake (Bayol et al., 2007). It is important to mention that palatability may play a role in appetite regulation and energy consumption in both dams and offspring, as they preferred the food rich in fat and sugar. The body weight of the offspring exposed to control diet during lactation period only was similar to those fed a control diet throughout the study; they also showed less energy intake as compared to those fed junk food throughout the study (Bayol et al., 2007). This suggests the importance of lactation on appetite regulation. It was summarised that a balanced diet with moderate energy content during pregnancy and lactation could counteract the adverse programming of the offspring feeding habits and prevent obesity later in life (Bayol et al., 2007).

Another previous study investigated whether the offspring's exposure to maternal obesity during gestation only would promote their ability to develop obesity later (Shankar et al., 2008). Dams fed high-fat diet (HFD) were heavier and exhibited a 98% more fat as compared to those fed a control diet. Neither offspring's birth weight nor intake was changed by the maternal HFD. This suggest that the mechanism of programming was not dependent on the intake by itself. Moreover, pups fed a control diet postnatally exhibited no difference in their body weight (Shankar et al., 2008). However, feeding HFD postnatally reinforced the effect of in-utero exposure to HFD on weight gain, suggesting a contribution of postnatal feeding in modifying the programming effect of maternal obesity. Moreover,

insulin level was higher in the offspring born to obese dams this response was reinforced when offspring fed HFD. Obesity programming during gestation appears to occur without influencing birth weight and maybe impact metabolism and endocrine function (Shankar et al., 2008).

Previous studies agreed that the maternal diet did not seem to affect the offspring's birth weight (Chen et al., 2008, Shankar et al., 2008), however, offspring born to dams fed HFD during gestation or lactation or lactation alone showed rapid weight gain, which continues postnatally depending on sex (Desai et al., 2014). The sex-dependent response was only recorded in this study for those exposed to HFD during lactation where males showed elevated cholesterol levels, the reason yet to be determined but might be due to the different effects of early overfeeding which differ depend on gender (Desai et al., 2014).

Although the main negative outcome of maternal obesity in women is the increased birth weight (Harpsoe et al., 2013), rodent studies showed no effect of maternal obesity on birth weight (Chen et al., 2008, Shankar et al., 2008, Desai et al., 2014), or exhibited a lower offspring weight as compared to controls (Bayol et al., 2007, Nivoit et al., 2009). These studies attributed the lower birth weight to restricted protein intake, diet exposure period or other experimental factors. The comparable birth weight of offspring born to dams fed HFD or dams fed control diet is suggested to occur by housing temperature, which represent a mild cold exposure. Cold is the most effective factor that is known to inducing BAT activity and it could be the explanation that reduced the impact of maternal obesity on birth weights.

Moreover, pregnancy outcomes such as birth weight could be programmed through changes in housing temperature.

To conclude, adiposity in offspring can be programmed at several developmental windows (Shankar et al., 2008). Maternal diet during gestation and lactation influence the offspring appetite later in life (Bayol et al., 2007), this effect is pronounced with feeding HFD post-weaning (Chen et al., 2008, Shankar et al., 2008). Consuming a well-balanced diet during gestation and lactation might protect the mothers and offspring from developing obesity and insulin resistance. Moreover, exposing maternal to mild cold might activate BAT and thus, protect against obesity and insulin resistance. This effect may be cover the offspring and protect them against developing obesity later in life, through maternal programming of their metabolism. However, studies on maternal obesity during gestation were not conducted yet on thermoneutrality, which is crucial to eliminate the ambient temperature effect as a factor that plays a role in reducing diet-induced obesity in dams and the programming effect on the offspring.

1.5 Rats as an experimental model

The use of animal models has played an essential role in biological and medical research (Barré-Sinoussi and Montagutelli, 2015). There are some similarities between human and animal evolution on many different levels including anatomical, behavioural, neurological and biochemical that justify their use as a model in scientific research (Perry, 2007). The use of animals as a model is not only based on shared similarities in terms of biology, but also because diseases that affect humans often affect other species (Barré-

Sinoussi and Montagutelli, 2015). Although there is no mammal that is able to mimic all human conditions, it is not ethically acceptable to experiment on humans because of the potential to produce adverse effects (Martin-Gronert and Ozanne, 2007, Barré-Sinoussi and Montagutelli, 2015).

Rats are widely used as a model for human disease as they are relatively inexpensive and easy to handle (Martins, 2003). They offer many advantages when compared to other animals, for example, rats have physiological conditions that correspond well to humans, and their smaller size makes them easier to handle and to perform surgical procedures. They also have cognition that is superior to that of other animals in terms of memory and learning (Iannaccone and Jacob, 2009). Rats are a good model for metabolic syndrome in humans (Aleixandre de Artinano and Miguel Castro, 2009, Hattori et al., 2011) and Spurge-Dawaly rat are considered to be a standard model for HFHS (Marques et al., 2016). Furthermore, in gestation, using rats is beneficial because they have a relatively short gestation period (21 - 23 days) making the observation of the dietary manipulation more practical (Symonds and Budge, 2009).

The disadvantages include the late postnatal maturation of the hypothalamic-pituitary axis (HPA) as compared to humans (in which the HPA matures in mid to late gestation) (Muhlhausler et al., 2004, Symonds, 2007). Moreover, rats are litter-bearing species, which may reduce offspring weight and the amount of the delivered in-utero nutrient (Ryan and Vandenbergh, 2002, Rodel et al., 2008).

Adipose tissue depot location is different between species, for example in human the main BAT depot is supraclavicular whereas in rodent the main is the interscapular (Nedergaard et al., 2007, Vosselman et al., 2013).

1.6 Study aims and hypothesis

This chapter reviewed the potential role of BAT in managing and preventing obesity by increasing energy expenditure and the effect of housing temperature on UCP1. As discussed, cold exposure is a known BAT activator, and my particular interest is in the effect of the standard housing temperature conditions on BAT thermogenic capacity.

The aim of this thesis is to determine whether a standard housing temperature applies a thermogenic challenge to rats, hence activating interscapular BAT (i.e., UCP1 abundance). Therefore, the weight and the biological functions (i.e., phenotype and genotype) were examined alongside the effect on plasma metabolites. The main hypothesis of this study is that the relative cool of a standard housing temperature can activate BAT, masking the adverse effect of the high-fat high sucrose diet. However, gestation can modulate BAT capacity. The next chapters were designated to test this hypothesis.

Chapter 2 presents the details of the method utilised in this thesis, this including tissue preparation, immunohistochemistry (IHC), enzyme-linked immunosorbent assay (ELISA) and gene expression procedure. Furthermore, chapter 2 presents the details of the statistical tests utilised in this thesis.

Chapter 3 presents the analysis of the total body weight, interscapular BAT and total WAT weights and plasma metabolites. The aim of chapter 3 is to test the effect of housing temperature and HFHS obesity on the macronutrient metabolism. This was achieved by analysing total body weight growth, body fat composition, organ weight and plasma metabolite concentration.

Chapter 4 investigates the effects of housing temperature conditions on the gene expression profile of genes related to BAT function and the mitochondrial UCP1 abundance. The aim of chapter 4 is to explore the effect of changes in housing temperature conditions upon BAT thermogenic capacity. This is achieved by analysing gene expression by a quantitative polymerase chain reaction and adipose tissue mitochondrial UCP1 abundance, using histological IHC.

Chapter 2 - Material and methods

In this chapter, a summary of the study design, experimental techniques and the material used to determine the results will be presented. The study protocol was designed by a Dr N Dellschaft and Professor ME Symonds. All the rat study experimentation (i.e., tissue dissection, processing, weights, plasma measurements and dissection of rat), were performed by Child Health Division staff members Dr Dellschaft and PhD students. Fasting plasma glucose, triglycerides and NEFA analysis were performed by Child Health staff members. Moreover, RNA extraction was performed by PhD students, Mrs Albustanji and Ms Perez. Reference genes were validated by Dr. Dellschaft and the primers were developed by Child Health Division laboratory technicians Dr Bloor, Mr Pope and Mrs Albustanji. Gene expression of SERCA2B and B3AR was performed by Mrs Albustanji.

2.1 Procedural and legal declaration

All rat experiments carried out in this study were conducted at the Bio Support Unit, Queen's Medical Centre at the University of Nottingham. Procedures in this study were performed in accordance with the UK Home Office and the UK Animals (Scientific Procedures) Act, 1986. Moreover, all experimental procedures were completed under the necessary licence and with ethical approval from the University of Nottingham. The evaluation and implementation of chemicals, reagents, antibodies and laboratory procedures used were in compliance with the UK Health and Safety Executive's Control of Substances Hazardous to Health (COSHH, SI No. 1657, 1988) and Risk Assessment guidelines.

All the protocols and lab-based techniques were conducted within the Department of Child Health, Obstetrics and Gynaecology, School of Medicine, Queen's Medical Centre, by methods that were either recommended by the manufacturers or optimised by myself or Child Health division staff members Dr Bloor, Dr Dellschaft, Mr Pope and Mrs. Pincott-Allen.

2.2 Study design

The presented work was carried out on existing tissue from a pre-existing animal study started in 2015. The study aimed to investigate the outcomes of dietary and housing temperature interventions in rats before and during pregnancy, with respect to effects on their brown adipose tissue (BAT).

1) A thermo-neutral temperature of 27°C, was compared to the standard temperature normally used in rat husbandry and breeding, (i.e., 20°C). They were exposed to this intervention from four-weeks of age until the dissection date.
2) A high-fat, high-sucrose diet (HFHS) was compared to a standard rat diet in order to induce obesity (Yang et al., 2012). This diet was started at four-weeks of age and continued until the end of the study.

A 2 x 2 factorial design was used, which yielded four intervention groups (20C, 27C, 20H, and 27H), (Figure 2.1). Intervention outcomes were studied at three-time points, i.e., unmated females, at 10-days gestation (mid-gestation) and at 19-days gestation (late gestation). Animal body weight was recorded twice a week.

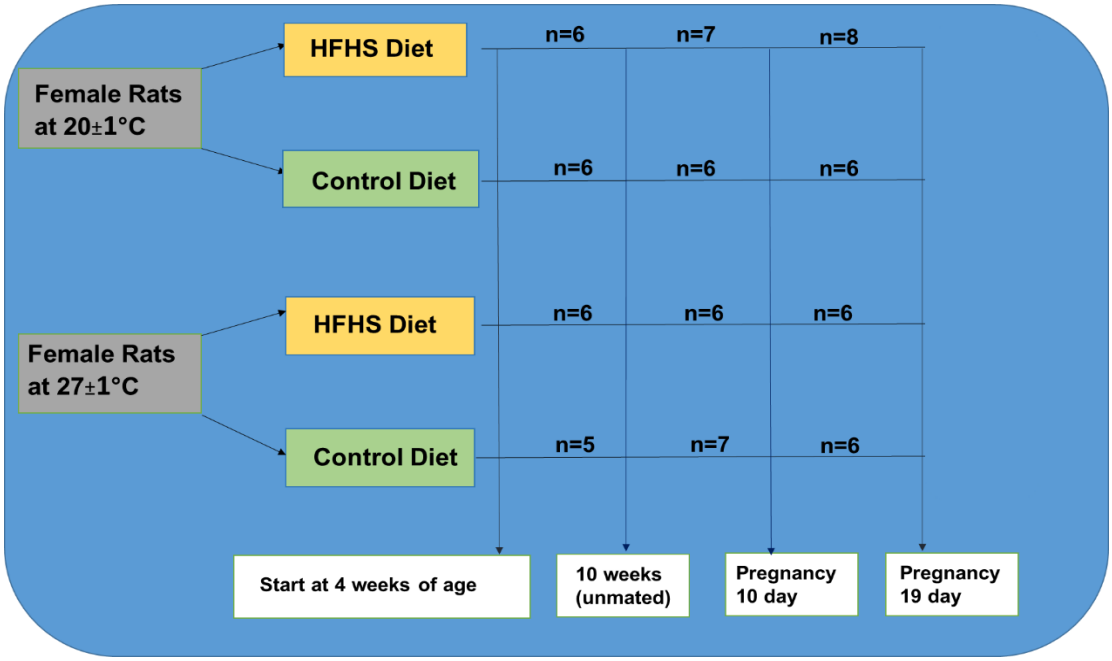


Figure 2.1: Schematic overview of the number of rodents involved in the study.

One animal from the unmated time point, was housed at thermoneutral temperature (27°C) condition and fed a control diet was omitted following dissection due to renal tumour, leaving 5 animals in this group.

2.2.1 Animals, diets and ambient temperature

Seventy-six female Sprague-Dawley rats (Charles River laboratory, Saffron Walden, UK) of similar body weights and ages were entered into this study. In addition, 16 male rats were used for mating and comparison purposes. Six animals supposed to be in each intervention subgroup, however, one was eliminated from 27C at the unmated time point because a renal tumour was found at dissection. Extra animals were added to the pregnancy sub-groups as the researchers believed it would not be easy to get them pregnant especially while consuming the HFHS diet and getting heavier. Moreover, One animal from the unmated time point, was housed at thermoneutral temperature (27°C) condition and fed a control diet was

omitted following dissection due to renal tumour, leaving 5 animals in this group.

Animals were brought to the Bio Support Unit a day before the intervention started and were kept under controlled conditions, i.e., light on from 0700h to 1900h and humidity 40-50% throughout the study. Animals were randomly assigned to the following intervention groups:

Thermal: Rodents were housed at either

- Standard housing temperature of 20 ± 1°C
- Thermoneutral temperature of 27 ± 1°C (Rosell et al., 2014).

Diet:

- Control diet that contained 18% fat (soybean oil), 24% protein and 58% carbohydrates of which 7% are mono and disaccharides; 3.1 kcal/g (Harlan Teklad Global 18% Protein Rodent Diet, Harlan Laboratories, Bicester, UK).
- High-fat, high sucrose diet (HFHS) which contained 39% fat (lard), 22 % protein, and 39% carbohydrates of which 44% sucrose; 4.6 kcal/g (Abbot Nutrition, Maidenhead, UK).

2.2.1.1 Animal mating

Each female was randomly housed with a male from the same intervention group and monitored each weekday in the morning. Females were considered pregnant (day 1) when operculum was found. Following conception, rats were returned to their original cages and their weight was monitored twice weekly until the end of the study.

2.2.2 Post-mortem analysis and plasma sampling

All animals were humanely euthanised at one of the three allocated time points between 9:00a.m-12:00p.m by CO_2 inhalation followed by cervical dislocation. The blood sample was withdrawn from a 8 hours fasted rats by cardiac puncture and collected into ethylenediaminetetraacetic acid (EDTA) tubes. Following blood collection, samples were rapidly centrifuged at 3,000 round per minute (RPM) for 10 minutes at 4°C to separate the plasma which was then stored at -80°C in a freezer for further analysis. Plasma was used to measure Plasma concentrations of glucose (GAGO-20, Sigma Aldrich, Gillingham, UK), triglycerides (GPO DAOS method, Wako, Neuss, Germany), non-esterified fatty acids (NEFA-HR(2), Wako, Neuss, Germany).

BAT, white adipose tissue (WAT), major organs and all other depots were weighed. Random sections of BAT were sampled for histology and fixed in 10% formalin. All remaining tissues were frozen by liquid nitrogen and stored in a -80°C freezer.

2.2.3 Tissue analysis

Prior to the experimental work, benches and instruments were sterilised using RNAsezap (Ambion, Foster City, California, USA), or 1% Virkon disinfectant (Antec International, Sudbury, Suffolk, UK) and 70% denatured ethanol (ethanol (Ecolabs, Sutton, Surrey, UK). All equipment used was autoclaved and sterile pipette tips were used to minimise contamination and preserve the integrity of the samples throughout the study. Sterile nuclease-free water (Ambion, Inc, UK) was used for all gene expression dilutions and reagent preparations. The desired tissue was removed from -80°C storage

and transferred on dry ice prior to processing. All samples were returned to a -80°C freezer until needed for further analysis.

2.3 Histology

2.3.1 The principle of the technique

Histology is the study of a microscopic structure sectioned in a thin layer to enable the visualising and distinguishing of details of the biological structures and cellular components, following staining with an appropriate histological stain. Prior to tissue staining, all tissues were fixed in formaldehyde to prevent tissue degradation, which irreversibly binds to amino acids to maintain cellular structures and preserve tissue from protein degradation (Werner et al., 2000). It is necessary following fixation to embed each sample in a holding matrix, for instance, paraffin wax, to ensure sample structural integrity while sectioning for microscopic analysis. Paraffin wax is a commonly used matrix for light microscopy. However, it is essential to dehydrate the tissue by immersion in ethanol and xylene, before embedding in the wax, as it is immiscible with water. Once paraffin blocks are solidified, tissues can then be sliced using the microtome.

2.3.2 Histological tissue processing

Random sections of BAT were taken from paraformaldehyde fixed tissue from each group (10% v/v formaldehyde in 0.9% w/v sodium chloride/ distilled water (Fisher Scientific, Loughborough, Leicestershire, UK) saline solution). Each sample segment was placed into a Histosette II (Simport, Quebec, Canada) 30mm x 27mm x 5mm cassette and processed by increasing ethanol concentration to dehydrate the tissue (six stages). The ethanol was then cleared by xylene in three stages (Fisher Scientific).

Samples were submerged in the paraffin wax in three stages using a Shandon Excelsior™, an advanced tissue wax processor (Thermo Fisher Scientific, Runcorn, Cheshire, UK) at 60°C. Overnight solidification was then allowed for approximately ~18h (see Table 2.1).

Table 2.1 Summary of the processing programme used for BAT.

Solution	Number of baths	Temp.	Time (min)/bath
Alcohol	6	15°C	60
Xylene	3	15°C	45
Wax	3	60°C	45

Tissue embedded in paraffin wax was sectioned into 5µm slice, using a sledge microtome (Anglia Scientific, Cambridge, UK). Prior to mounting the section, all slides were rinsed in 70% alcohol and transferred to a warm floating bath (~45ºC) filled with distilled water, to allow sections to de-wrinkle and stick to the Superfrost Plus slides (Menzel-Gläser Inc., Braunschweig, Germany) See Figure 2.2. The slides were dried on heat racks for approximately 20 minutes before oven incubation. All slides should be incubated in an oven at 37◦C overnight 24 hours prior to any histological treatment.

In total, five slides per animal were prepared (76 animal sample x 5 slides= 380 total number of slides) for this assay and subsequent procedures that were conducted in this study.

2.3.2 Immunohistochemistry

2.3.2.1 The principle of the technique

Immunohistochemistry (IHC) is a histological method that mixes immunological, anatomical and biochemical techniques used to determine and localise a specific antigen, for instance, a target protein, in a histological section. Upon antibody target antigen interaction, a signal will be produced and visualisation can be achieved using a conjugate signalling marker by a direct or indirect method of staining, which involves enzymes and a fluorescent dye (Figure 2.2) (Mason and Sammons, 1978, Ramos-Vara, 2005). In the direct staining, the primary antibody conjugate is used to bind with the target antigen, resulting in signal production. In indirect staining, a primary and secondary antibody conjugate complex is used and it is more specific than direct staining (Ramos-Vara, 2005).

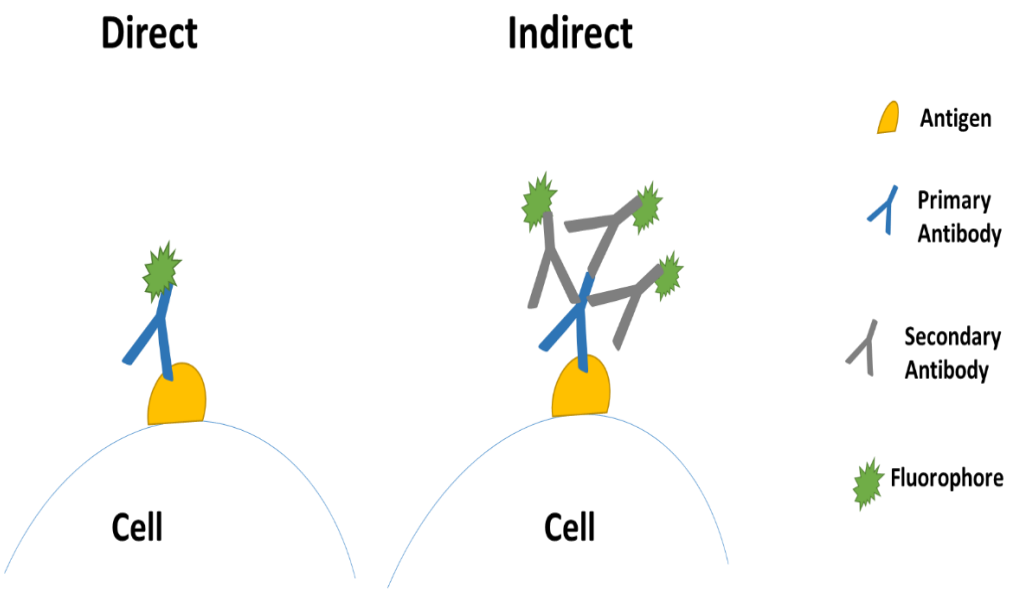


Figure 2.2: Direct and indirect immunostaining methods.

In the direct and method of IHC, specific conjugations for the primary antibody were added to bind the target antigen, whereas, in indirect IHC, secondary antibody to form an antigen-antibody complex. With either method, signals (e.g. colour development) are produced for measurement.

In this study, I used the indirect method of IHC, the most common enzyme used being horseradish peroxidase (HRP). In the presence of a chromogenic substance known as 3'-3'-diaminobenzidine (DAB), HRP develops a brown precipitate (Graham and Karnovsky, 1966). Before exposing the tissue sections to an antibody, it should be dewaxed and rehydrate to allow the reagent to reach the tissue. As tissues were initially formalin fixed, this resulted in cross-linking of proteins and consequently many antigenic sites could be masked. Therefore, all these protein cross-linked need to be broken to unmask hidden antigen sites b treating with

heat-induced epitope retrieval (HIER) steps (Shi et al., 1991), which involves warming with a citrate buffer.

2.3.2.2 IHC staining procedure

IHC was performed to determine the level of brown deposition in the interscapular BAT (Morroni et al., 1995). The rabbit anti-UCP1 antibody was used at a dilution factor of 1:3000 (ab10983, Abcam, Cambridge, UK), after experimenting with a range of dilutions based on the literatures (Kooijman et al., 2015, Rong et al., 2007, Novoselova et al., 2016).

A positive control and a negative control were used in each IHC run (Figure 2.3). A positive control is a sample from rat interscapular BAT, which contains the target protein (i.e., UCP1) and process as the sample, whereas a negative control is a sample with either no target protein (i.e., rat WAT) or with the target protein (i.e., interscapular BAT) but not being subjected to the antibody.

Slides were labelled with a random identifier created by the software, placed on a slide rack, and then loaded into Lecia BOND-MAX™ IHC slide processor (Leica Microsystems, Newcastle, UK), which runs 30 slides each time. Slides were then run on an automated software program (Vision Biosystems Bond version 3.4A), using Bond Polymer Refine Detection reagent (Leica).

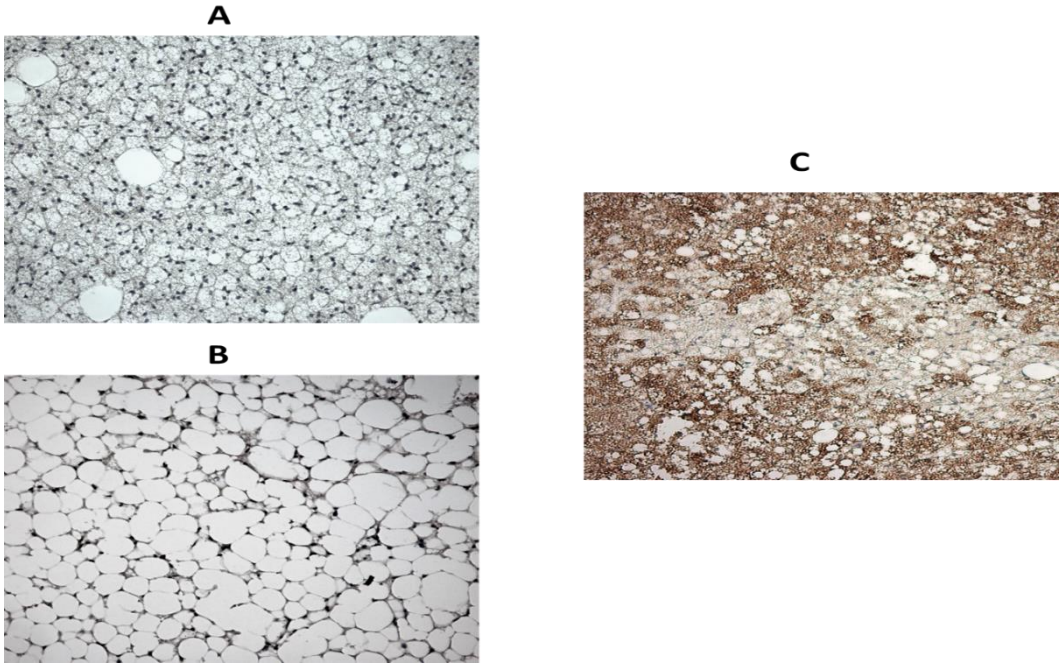


Figure 2.3: Example of (A, B) a negative and (C) a positive controls.

Positive and negative control were included in each BOND-MAX run. The negative control (A) is a rat interscapular BAT and process the sample as the sample except for not being exposed to the antibody to ensure that the BondMax settings are accurate. The negative control (B) is a rat WAT processed as the latter negative control and used to ensure that the antibody used is accurate and specific for the target protein. The positive (C) is a rat interscapular BAT were processed as the sample.

Slides were first washed with xylene and ethanol for 1 minute each and then incubated at 95°C with a citrate buffer for 15 minutes. They were treated with peroxide block for 5 minutes at room temperature and then all samples (apart from the negative control) were exposed to the primary anti-UCP1 antibody. The slides were washed twice with Bond Wash solution and distilled water and then exposed to 150 µl of HRP conjugated secondary antibody for 8 minutes before being rewashed. After that, the slides were exposed to 3,3'-DAB for 10 minutes (until a brown precipitate had developed), followed by nuclear staining with Harris' haematoxylin for

5 minutes and then washed for the final time. Thereafter, the slides were dehydrated by ethanol in two steps for 2 minutes each, then cleared in xylene in two steps for 5 minutes in total, before they were mounted with glass coverslips (VWR), using DPX mounting medium (Fisher Scientific, Loughborough, Leicestershire, UK) and left to dry overnight.

Blinded tissue sections were visualised using Leica DM RB and Nikon Eclipse 90i microscope (Nikon UK, Kingston upon Thames, Surrey, UK) at 10x magnification. Then images were captured with (Hamamatsu ORCA-ER camera, Hamamatsu city, Japan), at 10 random areas, that were cropped and treated as an individual image (Figure 2.5), using velocity quantification software (v6.1.1, Improvision Ltd, Coventry, UK) (Sharkey et al., 2009). Five images per sample were analysed using The ImageJ software that is free and has an open access. Quantification of adipocytes size and number using ImageJ was as the following, Image was first calibrated to the programme to allow recognition of sample size based on number of pixels and the microscopic magnification, this was achieved by ‘set scale’ option. This setting was applied on all the following images to ensure calibration. The image background was removed by selecting ‘Subtract background’ option. The total volume area of adipocytes in field for each image was measured by ImageJ and exported to Excel spreadsheet. Adipocytes counting was achieved by enhancing each cell membrane using ‘Dilate’ option. The number of the cells per field was then counted manually using a tool that counts cell number and display it on each cell centre. Then the values was exported to excel spreadsheet to be used in statistical analysis.

Following this, the quantification of UCP1 was achieved by first, converting the image to an 8-bit grayscale by selecting image-Tybe-8-bit. This controls assessing of the stained area and unable assessment manipulation. To enable stained cells counting, positive and negative stained areas were made distinguished by different colours as a marker. The total dark areas including cell membranes was measured by the software and recorded as a value. To asses positive UCP1-staining, the threshold setting was manually chosen by selecting Image-adjust-threshold tool. The hue threshold was set to (start: 202, end: 255), which is the appropriate intensity of brown stain to enable accurate measurement of the stained UCP1. ‘Limit to threshold’ option allowed for measuring only the grey area rather than the whole image. For each image, the software calculated and recorded the total UCP1 stained area. The relative total percent of UCP1 staining was calculated by dividing the total dark area by the total UCP1-stained area. An arbitrary unit was chosen as a measurement unit. To avoid investigator bias, during data analysis (see figure 2.4 for area selection), UCP1 stain slide was a blinded procedure by a labelled treatment code.

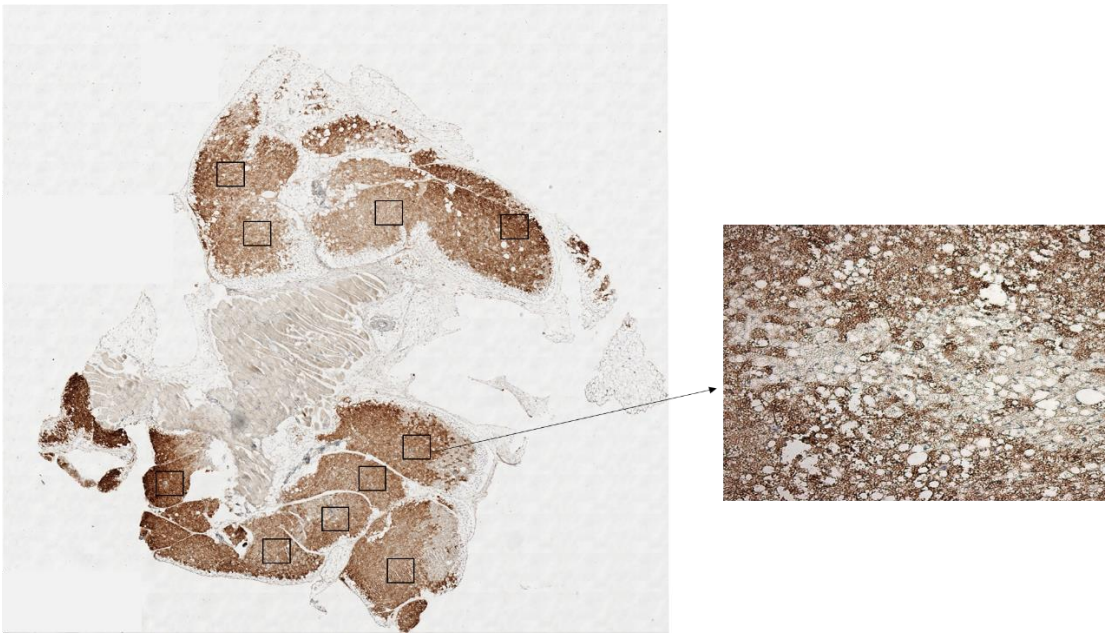


Figure 2.4: Illustration of selection areas for IHC analysis.

Ten random areas measured 0.1 mm^2, were randomly distributed across the tissue, selection criteria includes avoiding edges and tear sites.

2.4 Insulin assay

2.4.1 Sandwich Enzyme-Linked Immuno-Sorbent Assay (ELISA) principle

ELISA is a sensitive immunoassay employed to quantify the level of a protein in plasma using a specific antibody. The sandwich ELISA, the type used in this study to measure insulin, involves quantifying the amount of the antigen within two layers of antibody (i.e. capture and detection antibody). The principle of sandwich ELISA is as follows. A 96 well micro-plate with blocked non-specific binding sites and is coated with a specific antibody. As the antigen contained in the sample is added, it binds to the captivating antibody and then to the detecting antibody. Which is added to detect the antigen and binds to it. When the detection antibody is conjugated with biotin, they form a strong, non-covalent bond by the interaction with

streptavidin. HRP, a known detection enzyme, is bound in the same proportion as the antigen level in plasma. Lastly, a substrate is added and converted by the enzyme, to then be detected quantitatively. All non-bound reagents and remaining detection antibody and enzyme are washed off the wells in order to decrease the background signal, thereby increasing the signal noise ratio. Tetramethylbenzidine (TMB) is added to the wells as a common substrate used for HRP, and yields a blue colour, which is measured by a micro-plate reader. Results should be read within 30 minutes of adding the stop solution, which will stop the reaction by producing a yellow colour as the substrate acidifies. Sandwich ELISA principle is illustrated in Figure 2.5.

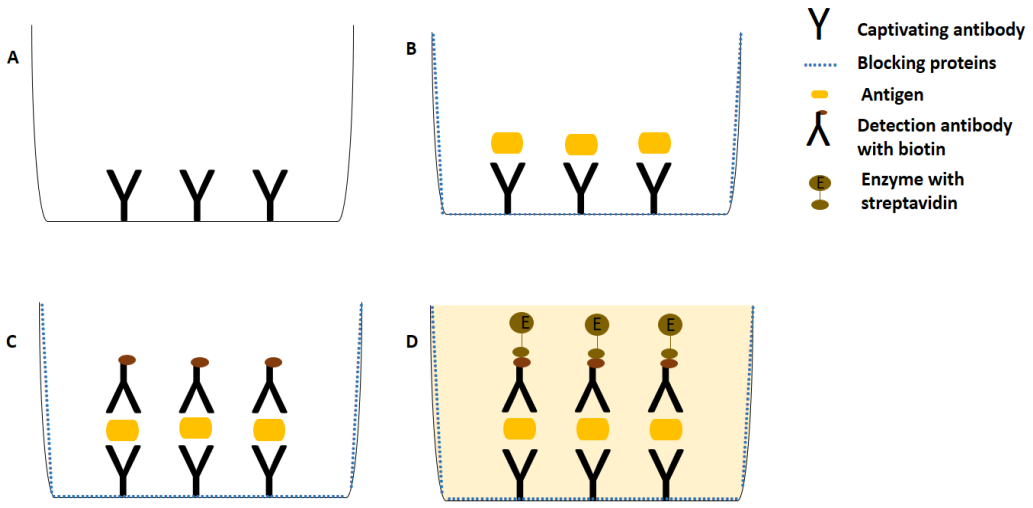


Figure 2.5: Schematic design of sandwich ELISA principle.

A: wells are coated with captivating antibodies and it specific for insulin antigen. B: wells wall are blocked with non-specific proteins and samples containing Ag were added. C: the detection antibody binds to the antigen. D: HPR bind to the detection antibody by the interaction of biotin and streptavidin and the substrate turns a yellow colour as it acidifies.

2.4.2 Sandwich ELISA procedure steps

To assess the plasma insulin concentration, the insulin rat Ultrasensitive ELISA Kit (80-INSRT-E01; ALPCO Diagnostics, Inc.; Salem, NH, USA) was used according to the manufacturer's instructions. Each plate includes six standards created by the manufacturer to compare against the study plasma sample, with concentrations ranging from 0.15 to 5.5 ng/ml. Two controls were included, which allowed variance correction between plates. Figure 2.6 shows the standard curve.

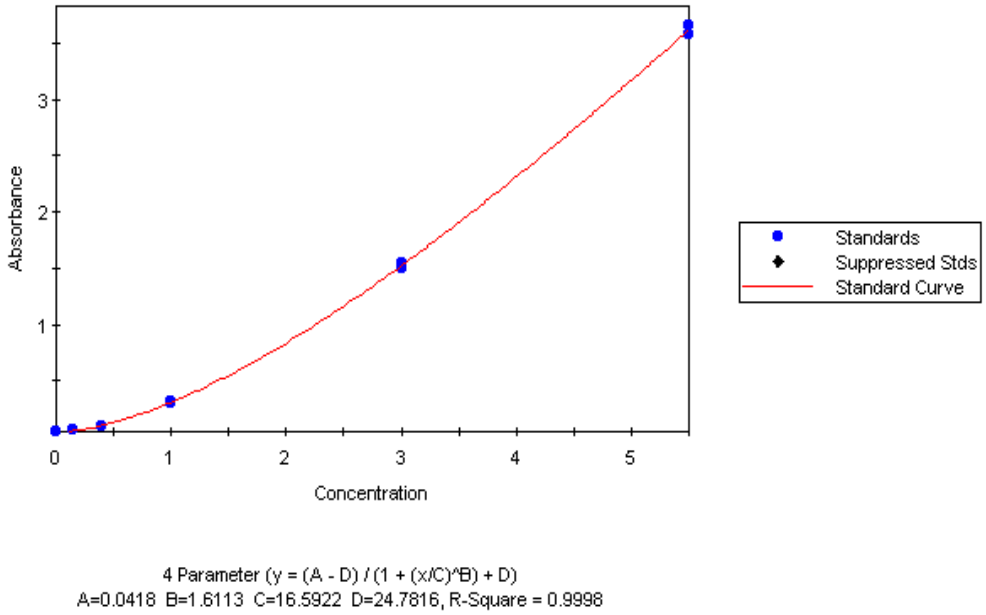


Figure 2.6: Insulin ELISA standard curve.

Prior to use, all reagents, micro-plate and stripes should be brought to room temperature, approximately 25°C, and gently mixed. In each well, 10 µL of each of the standards, controls and samples was pipetted in duplicate in its designated wells. A streptavidin HRP conjugate was pipetted, sealed and incubated in a micro-plate shaker at 700-900 RPM at room temperature for 2 hours. Wells were then decanted and washed with 350 µl wash buffer six

times using the micro-plate washer (BioTek Instruments Inc., Winooski, VY, USA). Then, the micro-plate was tapped firmly on absorbent towels to remove any remaining buffer, fluids or bubbles that might affect the reading. 100 µl of TMB substrate was pipetted into each well and the micro-plate was sealed and incubated for 15 minutes in the micro-plate shaker at 700-900 RPM at room temperature. To stop the reaction, 100 µL of stop solution was added; within 30 minutes of adding the stop solution, the micro-plate should be loaded in the micro-plate reader (µQuant, BioTek) and read at 450nm wavelength. The insulin concentration was calculated by the microplate software with duplication of the sample enabling an estimation of coefficient variability (inter-plate variability).

At 10-day gestation, two animals (from the 20H group) and one animal each from the 27C and 27H groups were omitted from the statistical analysis, owing to an extremely low or high reading of plasma insulin (~15 fold). At gestation, day 19, one animal from the 20H group and another one from the 27C were removed from the insulin results, as they showed an abnormally high result (15 fold) or insufficient serum, respectively. Unfortunately, there was insufficient remaining plasma to repeat the test. Omission of samples may reduce the test's reliability, therefore, potentially reducing the statistical significance of the analysis obtained.

2.5 Ribonucleic acid extraction

Ribonucleic acid extraction (RNA) was performed by PhD students in the Child Health division using a modified version of the single acidified phenol chloroform homogenisation method (Chomczynski and Sacchi, 1987), in addition to extraction kits and instruments. RNA extraction is achieved by

lysing and homogenising the samples in phenol and guanidine thiocyanate mono-phase solution; with this step denatures all of the proteins and inhibits RNAase activity (Chomczynski, 1993). Chloroform addition results in the formation of three separate phases (i.e. layers); the protein will be dissolved in the lowest layer, deoxyribonucleic acid (DNA) dissolved in the middle layer (i.e. interphase) and RNA dissolved in the top phase, also known as the aqueous phase (Chomczynski and Sacchi, 1987, Chomczynski, 1993). Following the separating of each phase, the uppermost phase (the aqueous RNA layer) is treated with alcohol in order to allow appropriate binding conditions and then purified by a RNA centrifuge column, which RNA ≥100µg binds to the membrane. This is followed by several steps of washing with ethanol and a guanidium salt-based buffer, to ensure contamination-free working material, before eluting the RNA with nuclease-free water. RNA extraction produces an unknown content, which could be consist of protein or protein-like products. The following step is designed to detect whether the extracted RNA is well concentrated and pure enough to be analysed further. This is achieved using spectrophotometry. The nucleic acids absorb ultraviolet (UV) lights at wavelength 260nm; therefore, RNA concentration can be determined by estimating the relative wavelength. Proteins usually absorb light at wavelength 280 nm and pure uncontaminated RNA preparation is expected to be A260/A280 wavelength (Glasel, 1995); the intended absorbance ratio is between 1.8 and 2.0 (Wilson and Walker, 2010).

2.5.1 RNA extraction procedures

All BAT samples were identified by animal ID and transferred into dry ice box. In each Dispomix tube (Medic Tools, Zurich, Switzerland), ~100 mg of BAT was chopped and 500 µl of TRI® reagent was added (Sigma Chemical Company, Poole, UK). Samples were homogenised using a Dispomix homogeniser (Medic Tools, Zurich, Switzweland) at 3,000 RPM for 40 seconds. Prior to vortexing the homogenate, the tubes were floated in a 37 °C water bath for 2 minutes, to break down the lipid content. The homogenate was mixed by the vortex 5 times over 30 seconds and centrifuged at 3,000 RPM for one minute at room temperature. Afterwards, the supernatant was carefully aspirated into a labelled sterile 1.5 ml Eppendorf tube; then, 100 µl of analytic grade chloroform (Fisher Scientific, Leicestershire, UK) was added, mixed by vortex and incubated for 10 minutes at room temperature in order for each phase to separate.

Following phase separation, samples were centrifuged at 12,000 RPM for 15 minutes at 4 °C. Of the uppermost (i.e., aqueous) layer, ~100 µl was carefully aspirated into a labelled genomic deoxyribonucleic acid (gDNA) eliminator column and centrifuged at 8,000 RPM for 1 minute at room temperature to eliminate any gDNA contamination. An equal volume of 70% ethanol was added to each sample and mixed by inversion vortex.

RNA purification was performed using the RNeasy Plus Mini extraction kit (Qiagen, Crawley, West Sussex, UK). RNeasy spin columns were prepared for each sample and 700µl of each sample was pipetted into the column. The columns were centrifuged at 8,000 RPM for 15 seconds, after which the flow through was then disposed of. The step in which the aqueous

phase was aspirated, as described was repeated until the total sample volume had passed through the column.

The following steps were performed on an RNase-free bench with 700µl of RW1 buffer added to each RNeasy spin column and centrifuged at 8,000 RPM for 15 seconds at room temperature, after which the flow-through was disposed of. Next, 500µl of a mild washing buffer (RPE buffer) was added to the RNeasy spin column and centrifuged at 8,000 RPM for 15 seconds and the flow-through was discarded. Another, 500µl of RPE buffer was added to the RNeasy spin column and centrifuged at 8,000 RPM for 2 minutes at room temperature and the flow-through was disposed of. The mini spin RNeasy column was then transferred into a sterile 2ml collection tube and loaded into the centrifuge at 8000g RPM for 1 minute at room temperature, to remove any possible carry-over of RPE. In all previous steps, RNeasy was always removed carefully, so that that it was never exposed to the flow-through and the collection tube was always unloaded completely. The collection tube was then discarded, the RNeasy column placed in a sterile, labelled 1.5ml Eppendorf tube to which 50µl of RNAse-free water was added and centrifuged at 8,000 RPM for 1 minute at room temperature. The eluted sample was re-pipetted back to the column and the centrifugation was repeated to increase the concentration of RNA obtained.

To detect the RNA concentration and assess its purity, the NanoDrop® ND-1000 (NanoDrop Technologies, Wilmington, DE, USA) spectrophotometer was used.

2.5.2 Polymerase chain reaction

The polymerase chain reaction (PCR) concept is based on amplification of a specific DNA, in the presence of only trace amounts. To run a PCR assay, it is necessary to have a template DNA, nucleotides, primers or probes, and DNA polymerase. Primers are a small DNA segment that's forms the reaction specifier, directing the PCR to the correct DNA product to amplify, using a sequence complementary to the target DNA. The PCR reaction is initiated by heating the reaction mixture above its melting point to denature complementary DNA. The temperature is then decreased to allow annealing of the primers. The reaction is heated again to allow DNA polymerase to extend (Garibyan and Avashia, 2013). Following each cycle the amount of DNA is doubled leading to a fast increase in target DNA (Saiki et al., 1988).

Primer design is a critical aspect of working with PCR analysis, and poorly designed primers decrease the yield product by interacting with one another and forming dimers or through different annealing and melting temperatures. Table 2.2 is showing the general criteria of optimal PCR primer design (Butler, 2005).

Table 2.02. General criteria for optimal PCR primer design.

Parameter	Optimal Values
Primer length	18-30 bases
Guanine/cytosine (GC) content	40-60%
Melting temperature	60 °C ± 5 °C
Temp. difference between forward & reverse primer	2-3 °C or ≤ 5 °C
No G/C and AT residues	< 3 consecutive bases
No complementarity to other primer (dimers)	≤ 3 continuous bases
Distance between primers on target sequence	2000 bases apart
No long run with the same base	<4 continuous bases

Samples produced by newly designed primers are sent for DNA sequencing at the University of Nottingham, Centre of Genetics and Genomics located at Queen's Medical Centre and cross-referenced with the National Centre for Biotechnology Information (NCBI) database.

2.5.3 Reverse transcription polymerase chain reaction

2.5.3.1 Principle of RT-PCR

As the PCR function is based on amplification of double-stranded molecules, such as DNA, single-stranded RNA should be converted by transcription into a double-stranded complementary DNA (cDNA) by a process known as reserve transcription polymerase chain reaction (RT-

PCR), and includes the use of a DNA primer and a reverse transcriptase enzyme.

Template mRNA is required to anneal a DNA primer sequence to its complementary mRNA form. Elongation and transcription occur by means of the enzymatic reaction, thereby, creating cDNA ready for PCR to be transcribed to a double-stranded molecule and further amplification is applied. Figure 2.7 illustrate the RT-PCR principle.

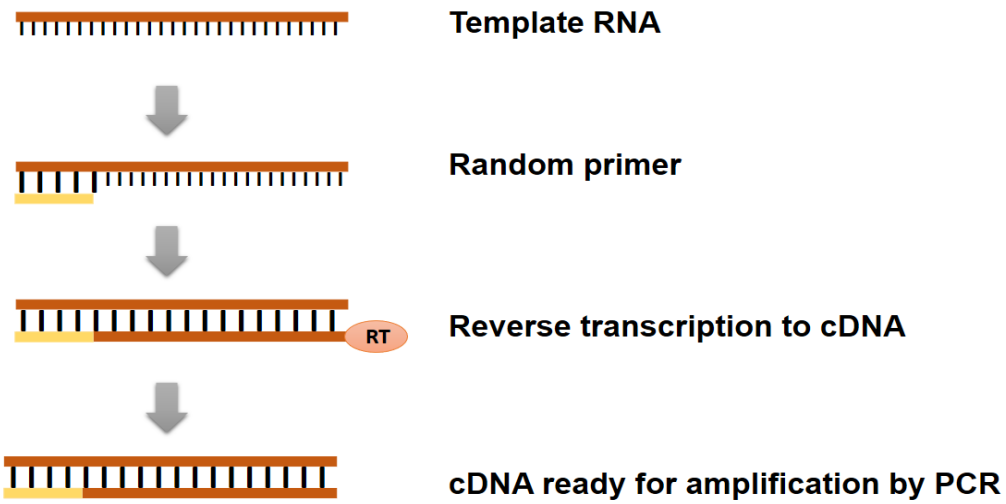


Figure 2.7: Reverse transcription of polymerase chain reaction.

The primer binds to the template mRNA, resulting in a sequence elongation by cDNA. The template of cDNA is then ready for amplification by PCR.

2.5.4 Quantitative polymerase chain reaction

2.5.4.1 The principle of the Q-PCR technique

Thanks to the development of PCR technology, analysis including detection and quantification of DNA or mRNA can be performed in real-time without added steps such as northern blotting or gel electrophoresis, thereby reducing time, expense and the possibility of contamination (Reischl and

Kochanowski, 1999). The use of Q-PCR eliminates the need to use hazardous fluorescence, for example, ethidium bromide. The intensity of the fluorescent signal is correlated with the amount of DNA bound to a fluorescent tag, i.e., a greater fluorescence signal is related to a higher amount of DNA present. The SYBR Green technique involves its adherence to minor grooves on the DNA, which produce fluorescence (Denman and McSweeney, 2005). TaqMan is a highly specific assay for PCR, developed for the detection of single nucleotide polymorphisms, the principle being based on nuclease activity and fluorophore-based detection.

The PCR instrument is programmed to a calculated baseline, which is the number of PCR cycles that a reporter fluorescent signal is accumulating below the level of detection; the software then determines the baseline based on an arbitrary threshold. The baseline determines the cycle threshold (Ct), defined as the detection of fluorescent signals after a certain level of background fluorescein has been crossed, known also as the crossing point (C_p) (Arya et al., 2005). The cycle threshold is the measurement used to assess for quantification and correlation with the initial amount of target template.

Q-PCR allows quantification of cDNA concentration by plotting the log of known standard serial dilutions versus C_t on a straight line. The efficiency (E) and correlation coefficient (R^2) which are verification tests for the experiment, are both determined by plotting the known dilution series on a graph versus the cycle number when threshold is reached on a graph. The efficiency formula is calculated: Efficiency of PCR reaction = $10^{(-1/\text{gradient})}$ -1 (Pfaffl, 2001). Figure 2.8 shows the standard curve of PCR.

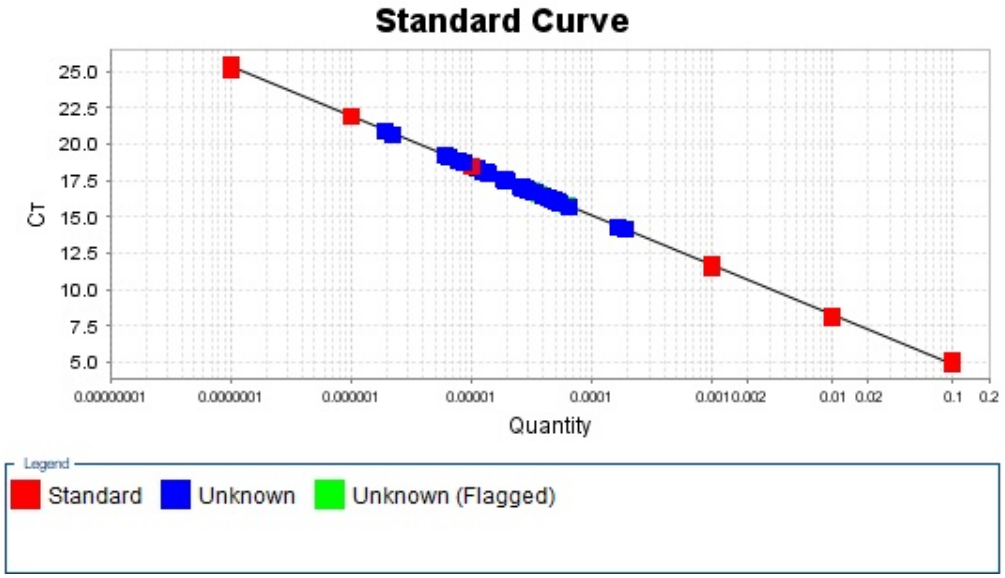


Figure 2.8: Standard curve generated by Q-PCR's software.

A linear graph of the polymerase chain reaction was created by plotting the cycle number versus unknown and known dilution series.

Prior to quantifying the gene expression, it is essential to normalise the samples for the amount of intrinsic variation by analysing the expression of a gene known as the housekeeping gene. It is usually expressed in relatively high amounts by all cells. Using a mathematical equation known as the comparative threshold ($2^{-\Delta Ct}$), relative quantification of gene expression can be determined (Livak and Schmittgen, 2001), where ΔC_t = [average Ct of target gene – average Ct of housekeeping gene (of the same sample)]. This mathematical model assumes PCR efficiency is 100%, i.e., the whole cDNA strands were replicated, hence 2^. However, TaqMan is unlike SYBR Green, in which the efficacy is always assumed to be 2. The accepted efficiency of the housekeeping gene and target gene should be approximately equal to each other and ~90-105% (Arya et al., 2005).

It is important that the fluorescent dye SYBR Green, for example, binds to the target double-stranded DNA, and it may also bind to any non-specific

dye-DNA complex such as a primer dimer. Therefore, it is essential to analyse PCR to ensure the product quality. This quality measurement is verified by producing the melt curve, which records the temperature changes through the PCR assay by measuring a decrease in the fluorescent signal. A single peak, also known as (single amplicon) reflects a very specific product (Figure 2.9). The presence of any nonspecific products will produce broader peaks following the analysis.

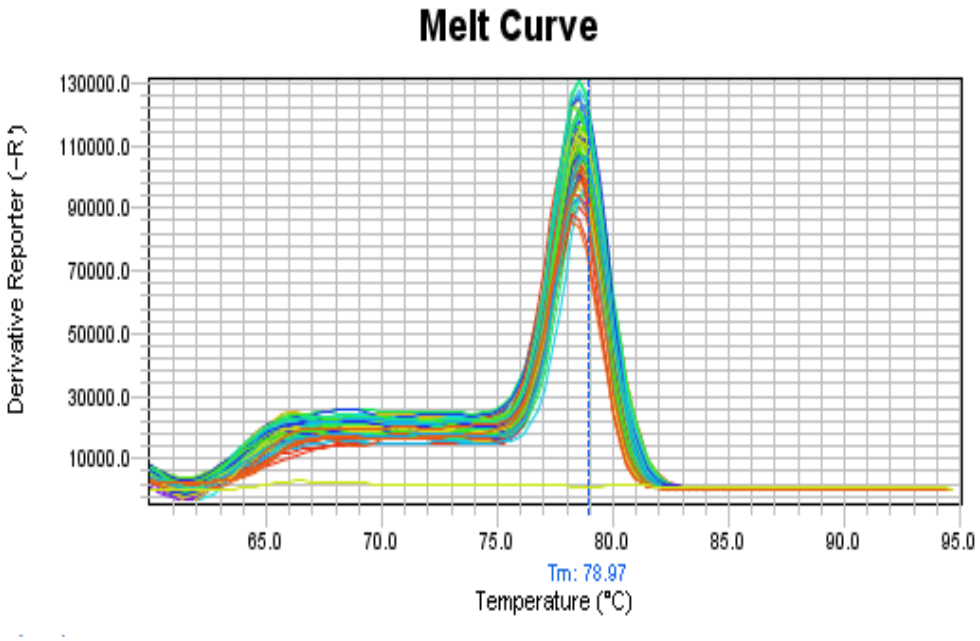


Figure 2.9: The melt curve generated by Q-PCR software.

The single peak indicates a high specificity of all the cDNA samples. The melting temperature is 80°C. Neither contamination products, nor DNA dimer were produced, as they would show up as an additional peak. The yellow coloured lines represent the negative controls.

2.5.4.2 Development of oligonucleotide primers for Q-PCR

Primers used in this study were designed using Beacon Designer 4.0 software (Premier Biosoft, Palo Alto, CA, USA) with the rodent genome sequence from the NCBI database, ensuring higher amplification specificity

of the target gene. The software designed the primers flanking exon boundaries in the intron sequence, and primers at similar optimum annealing temperature; a guanine-cytosine base pair content and length were chosen in order to achieve suitable reaction conditions (Ye et al., 2012). All the designed primers were examined using the NCBI nucleotide Basic Local Alignment Search Tool (BLAST) to ensure the amplification of the correct sequence. All primers were stored in nuclease-free water at a concentration of 100 µmol/l. Table 2.3 presents details of primer sequences and Table 2.4 and 2.5 for primer used in this study.

Table 0.3. Reference genes primer sequences for mRNA quantification.

Reference Gene	Oligonucleotide Sequence (5´-3´)	Publication
TATA box binding protein (TBP)	Forward 5'-TGGGATTGTACCACAGCTCCA-3' Reverse 5'-CTCATGATGACTGCAGCAAACC-3'	(Langnaese et al., 2008)
Tyrosine 3-monooxygenase tryptophan (YWHAZ)	Forward 5'-GATGAAGCCATTGCTGAACTTG-3' Reverse 5'-GTCTCCTTGGGTATCCGATGTC-3'	(Langnaese et al., 2008)

Table 2.4. Target genes sequences for SYBR Green mRNA quantification.

Target Gene	Oligonucleotide Sequence (5´-3´)	Publication
Uncoupling protein-1 (UCP1)	Forward GCCTAGCAGACATCATCACCT Reverse GTTTCGGCAATCCTTCTGTC	(Dixen et al., 2013)
Peroxisome proliferator-activated receptor gamma (PPARγ)	Forward CCCAATGGTTGCTGATTACA Reverse GGACGCAGGCTCTACTTTGA	Developed in-house
Leptin (Ob)	Forward TTCACACACGCAGTCGGTAT Reverse AGGTCTCGCAGGTTCTCCAG	Developed in-house

Table 2.4. Target genes probes for TaqMan.

Target gene	Gene Symbol	Organism	Gene Aliases	Unique Assay ID	Amplicon Length (bp)	Assay Design
Peroxisome proliferator-activated receptor gamma coactivator 1-alpha	PGC1α	Rat	Not Available	qRboCIP0022855	102	Intron-spanning
Tumour necrosis factor, membrane from intracellular domain 1 intracellular domain 2 C-domain 2 Tumour necrosis factor, soluble form	TNF	Rat	Not Available	qRnoCEP0030948	112	Exonic
Patatin-like phospholipase domain-containing protein 2	Pnpla2	Rat	Not Available	qRnoCEP0023736	101	Exonic
Transient receptor potential cation channel subfamily V member 1	TRPV1	Rat	Not Available	qRnoCIP0024978	86	Intron-spanning

2.5.4.3 RT-PCR technique

This technique was completed using Real-Time PCR Reagents and Kits (Applied BioSystems, Warrington, Cheshire, UK). Samples were thawed at 4 °C. Two sterile 0.2 ml nuclease-free Eppendorf tubes were labelled for each sample, including the no template control (NTC) and the no reverse transcriptase control (NRTC). In each tube, 2 µl of sample RNA were added to 9 µl of nuclease-free water. Samples were then vortexed for 30 seconds. The Master Mix was prepared: 10 µl of 2X reverse transcription (RT) buffer, multiplied by the number of the samples and NTC, and 11 µl of Master Mix was added to all samples and NTC, but none for NRTC, as it was a control. Next, 10 µl of 2X RT buffer and 1 ml of nuclease-free water were added to the NRTC. Tubes were then centrifuged for 1 minute at 4,000 RPM and incubated in a thermal cycler (TechEn Inc., Milford, MA, USA) for 60 minutes at 37 °C. The reaction mix is heated to 95 °C for 5 minutes and then held at 4 °C for primer hybridisation and elongation. The prepared cDNA was stored at -20 °C.

2.5.4.4 Selection of housekeeping genes in Q-PCR

To enhance an experiment's reliability, housekeeping genes are used as an endogenous variant control to correct sample-to-sample variation and RNA quantification error; thus, it is essential that the selected housekeeping gene is validated (Bustin et al., 2009). A good housekeeping gene selection criterion is that it must have very little variation across the samples and be expressed relatively higher than the genes of interest (Silver et al., 2006). Previous studies suggest performing an accurate measurement of the mRNA expression level and the genomic mean of several housekeeping

genes (Vandesompele et al., 2002, Bustin et al., 2009), yet it is still critical to follow the criteria of good gene housekeeping selection. The housekeeping genes, selected TATA box binding protein (TBP) and tyrosine 3-monooxygenase/ tryptophan 5-monooxygenase activation protein zeta (YWHAZ) have previously been validated in BAT (Vandesompele et al., 2002, Turabelidze et al., 2010). They are expressed in acceptable amounts to account for sample-to-sample variation, and in the present study were processed through geNorm software v3.5 (Primer Design Ltd, Southampton, Hampshire, UK). The software uses an algorithm to calculate the geometric mean and pairwise variation of each reference gene against all genes in order to calculate stability. Using M values was calculated as the mean standard deviation of the log-transformed expression ratios across samples for certain relative gene to other housekeeping genes (Vandesompele et al., 2002), a lower M value confirms higher stability. Following these steps, TBP and YWHAS were selected as references gene for this study.

2.5.4.5 Quantitative polymerase chain reaction procedure

For each target gene analysed, a series of dilutions were prepared in the ratio of 1:10 dilution were prepared from the 1 ng/µl cDNA obtained from the RT-PCR with unknown samples, to confirm test efficacy. All unknown samples were measured with reference genes TBP and YWHAZ to normalise the cDNA samples.

Samples, standards, negative control, nuclease-free water, NCT and NRCT were run in a 96 well Q-PCR plate (Abgene, Thermo Fisher Scientific Inc., Waltham, MA, USA) in 10 µl aliquots. See Table 2.6 for the reaction mix

and Table 2.7 for the Master Mix. The sample was duplicated to calculate the coefficient variance of the experiment.

Table 0.5. Q-PCR reaction mix for SYBER green.

Reagent	Volume per reaction
cDNA	3µl
Master Mix	7µl
Nuclease-free water	1µl

Table 0.6. Master Mix reaction mixture for SYBR Green.

Reagent	Volume per reaction
SYBER green	5µl
Forward primer (diluted 1:40µl)	1µl
Reverse primer (diluted 1:40µl)	1µl

SYBER green Master Mix kit (Applied BioSystems, Warrington, Cheshire, UK) contains Taq DNA polymerase, magnesium chloride, dNTP mix optimised buffer. It was used for UCP1, PPARγ and leptin gene. The amount in this table is sufficient for one well only.

TaqMan method of Q-PCR does not require standards, since the probes are previously standardised by the manufacturer (BioRad, Watford, UK). However, using SybrGreen requires standards. SybrGreen standards are produced by concentrating the DNA of the primer to 1000 ng, to be used then as a zero standard. Then serial dilutions are made using one part of the zero standard and 9 parts of tRNA to produced -1 to -8 standards. Samples, NRTC, nuclease-free water were run in a 96 well Q-PCR plate (Abgene) in 10µl aliquots (Table 2.8). Duplication was performed in order to calculate the coefficient variance of the experiment.

Table 0.7. Q-PCR reaction mix for TaqMan.

Reagent	Volume per reaction
cDNA	3µl
Master Mix	7µl
Nuclease-free water diluted	1µl

The following formula should be used to calculate the required TaqMan Master Mix volume for each target gene, ATGL for instance, [n x 5µl iTaq Super Mix] + [n x 2.5µl nuclease-free water] + [n x 0.5µl probe], multiplied by 2, as samples are in duplicate. The required amount of the Master Mix, stored after preparation in -20 °C (Table 2.9). TaqMan iTaq is a ready-to-use universal probe containing an advanced buffer for an optimal probe-based Q-PCR, antibodies to mediate hot-start iTaq DNA polymerase and a blend of passive reference dyes.

Table 0.8. TaqMan Master Mix used for ATGL, PGC1α, TNFα and TRPV1α gene.

Reagent	Volume per reaction
iTaq	5µl
Nuclease-free water	2.5
Probe	0.5µl

Once the Q-PCR plate had been prepared, it was sealed using an Abgene thermal plate sealer (Abgene) and loaded into StepOne Plus Real-Time PCR system (Applied Biosystems). See Tables 2.10 and 2.11 illustrate the steps in the for Q-PCR programme.

Table 0.9. Q-PCR programme for SYBR Green.

Process	Temperature	Duration
1-intial denature of cDNA standard	95°C	15 minutes
2-denaturing cDNA standard	95°C	15 seconds
3-primers annealed*	60°C ± 2°C	30 seconds
5-producing melt curve**	65 -95°C in 1C increments	15 minutes
6-hold		10 minutes

The total time required for each run is 1 hour and 20 minutes.*step 1-3 was repeated for 45 cycles, ** repeated for 31 cycles.

Table 0.10. TaqMan Q-PCR programme required 40 minutes only for each plate.

Process	Temperature	Duration
1-Initial denaturing of cDNA standard	50°C	2 minutes
2- iTaq polymerase activation	95°C	20 Seconds
3- Melt curve for analysis*	95°C	1 second
4- Anneal /Extend	60°C	20 seconds

QPCR analysis results were measured using StepOne v2.2 (Applied Biosystems) software packages and gene expression data. TNFα was not expressed thus no results were produced for this gene.

2.6 Statistical analysis

Prior to any statistical analysis, the coefficient of variance (CV%) of all samples run in duplicate was calculated using Microsoft Office Excel software 2010 (Microsoft Corporation, Reading, Berkshire, UK). A CV of ≤ 5% was indicative of a low variance between the duplicates. Statistical analysis was performed using IBM SPSS v.24.0 statistical software for Windows package (IBM Corporation, NY, USA). All data were subjected to the Shapiro-Wilk normality test (i.e., for each sub-group individually) to determine if their distribution was parametric or non-parametric, $p \geq 0.05$ determining normality. Shapiro-wilk test is the most powerful for smaller sample size <50 (Ghasemi and Zahediasl, 2012). Normality test was performed for each of the comparable groups. Moreover, two-way analysis

of variance (ANOVA) was used for normally distributed data or the Mann-Whitney test for non-parametric data with fisher LSD post-hoc comparison (20C v 20H, 27C v 27H, 20C v 27C, 20H v 27H) within each of the three time points (0, 10, and 19 d/g) to test for changes due to the interventions. Correlation of BAT weight with, for instance total body weight was calculated using Pearson's correlation if samples had a parametric distribution or Spearman's rank correlation if samples had a non-parametric distribution. Statistical graphs were produced by GraphPad Prism v7.00 software (GraphPad Software, LA Jolla, CA, USA), and all data presented as a mean ± standard error of the mean (SEM).

In order to reduce the probability of types one and type two errors, type one error is the rejection the true null hypothesis, while type two is failing to reject false null hypothesis, which means the rejecting or accepting of the null hypothesis, respectively.

2.6.1 Power calculation

This study was only powered to demonstrate likely changes in UCP1. Other researcher performed this study power calculation before I joined the study. The power of the study was calculated using Minitab v16 statistical software (Minitab Ltd, Coventry, Warwickshire, UK). Using previously published data on the effect of acute cold exposure of UCP1 expression in a rodent model. The recommended sample size to detect a 35% difference between groups with a 10% standard deviation was 6 samples per group with a statistical power of 85% to yield a significant result of $p<0.05$.

Chapter 3 - The effect of different housing temperature condition and dietary intervention on body composition and plasma metabolites

3.1 Introduction and aims

The impact of changes in body composition that accompanies the development and progression of weight growth have an impact on metabolism, insulin sensitivity (Duren et al., 2008, Esser et al., 2014, Han and Lean, 2016), and several other plasma metabolites (Guilherme et al., 2008). Rats exposed to HFHS, before or during gestation, promotes obesity, insulin resistance and glucose impairment (Saldana et al., 2004, Radesky et al., 2008). Obesity is linked to impaired adipose tissue metabolism. Magnitude of that can vary among depot locations (Sam and Mazzone, 2014). An increase in brown adipose tissue (BAT) activity reduces glucose and lipid levels (Bartelt et al., 2011). Cold exposure accelerates the clearance of plasma triglycerides (TGs) in BAT, corrects dyslipidaemia and decreases their adverse effects of insulin resistance (Bartelt et al., 2011). The risk of metabolic syndrome is reduced by activating BAT and subsequently energy expenditure (Ravussin et al., 2014). BAT is activated subsequent to standard housing temperature (20°C). With cold exposure, BAT activity participates substantially in small mammals' metabolism, as a result of utilising lipids and glucose to produce heat, that counts for one-half (50%) of their metabolism (Cannon and Nedergaard, 2004). White adipose tissue (WAT) behaves differently with cold exposure, in inducing browning of adipose tissue with acute cold

exposure (Gao et al., 2017, Greenhill, 2013). Although BAT is one of the smallest fat depots in the body, it has a potential to generate large amount of heat thereby, influencing both energy balance, lipids and glucose homeostasis (Cannon and Nedergaard, 2011, Symonds, 2013).

This chapter investigates whether exposure of rats to standard housing temperature condition and thermoneutral temperature conditions modulate BAT metabolism by hidding the adverse effects of HFHS of a high-fat high sucrose (HFHS) diet on plasma metabolites, WAT, and BAT weights.

It was hypothesised that adult female rats exposed to standard housing temperature have a lower adverse effect i.e., glucose impairment, TGs, insulin insensitivity. The HFHS would increase total body weight, BAT and WAT that would continued through gestational period.

3.2 Material and methods

The current study was undertaken at the University of Nottingham, division of academic child health. A detailed discerption of the methods and statistical analysis can be found in Chapter 2**.** Briefly**,** ELISA was performed for insulin assay. Statistical analysis used in this chapter are normality test and two way ANOVA between the comparable groups. Furthermore, Pearson correlation was performed to determine the relation between total body weight and BAT weight.

3.3 Results

3.3.1 The effect of the HFHS diet and standard housing temperature and their contribution to whole body weight and fat deposition

All animals had free access to food and water throughout, and then they were fasted for 8 hours before euthanasia. As mentioned earlier the study intervention commenced at four-weeks of age. The effect of the intervention on differences in body weight are illustrated in Figures 3.1, 3.2 and 3.3. At 10-days of gestation, there was a trend towards increase in weight in those fed the HFHS diet and housed at the thermoneutral conditions. Animals fed the HFHS and housed under standard housing temperature conditions exhibited a trend towards increased weight gain in the late gestation period. Pre-gestation, weight gain of those fed the HFHS and housed under the standard housing temperature conditions higher among the groups, although this findings was not statistically significant.

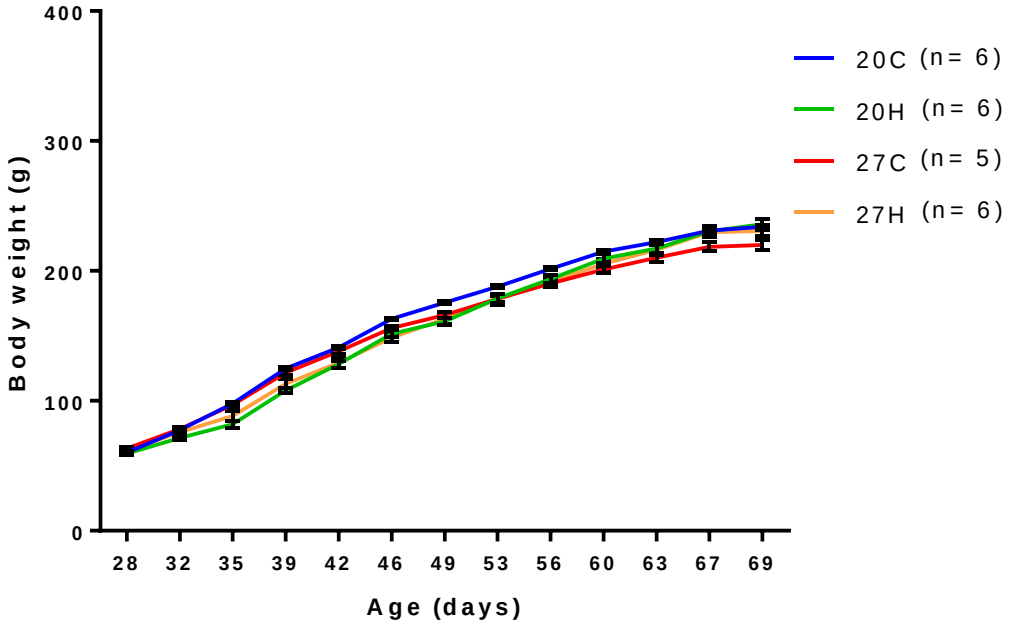


Figure 3.1: Cumulative body weight prior to gestation.

Weight was measured twice weekly. The numbers 20 and 27 indicate the housing temperature in degrees Celsius. C: control diet, H: HFHS, high-fat and high-sucrose diet. The data are presented as mean ± standard error of mean. The statistical analysis performed for the cumulative weight measurement was 2-way ANOVA with LSD post-hoc comparison for each day of weight measurement and revealed no statistical significance between the comparable groups.

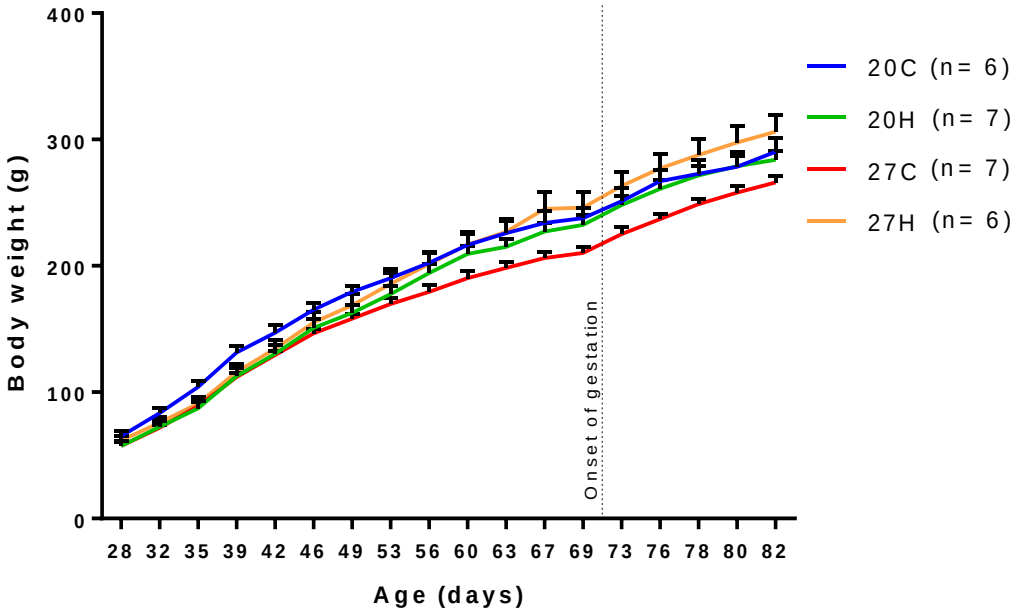


Figure 3.2: 10-days gestation cumulative body weight showing a trend towards increased weight gain in the animals fed HFHS diet.

The broken line indicates the period of beginning of gestation. Weight was measurements twice weekly. In the figure, the numbers 20 and 27 indicate housing temperature in Celsius. C: control diet, H: HFHS, high-fat and high-sucrose diet. The data are presented as mean ± standard error of mean. The statistical analysis performed for the cumulative weight measurement was 2-way ANOVA with LSD post-hoc comparison for each day of weight measurement revealed increased weight gain in the animals fed HFHS and housed under thermoneutrality (27°C) as compared to those fed the control diet.

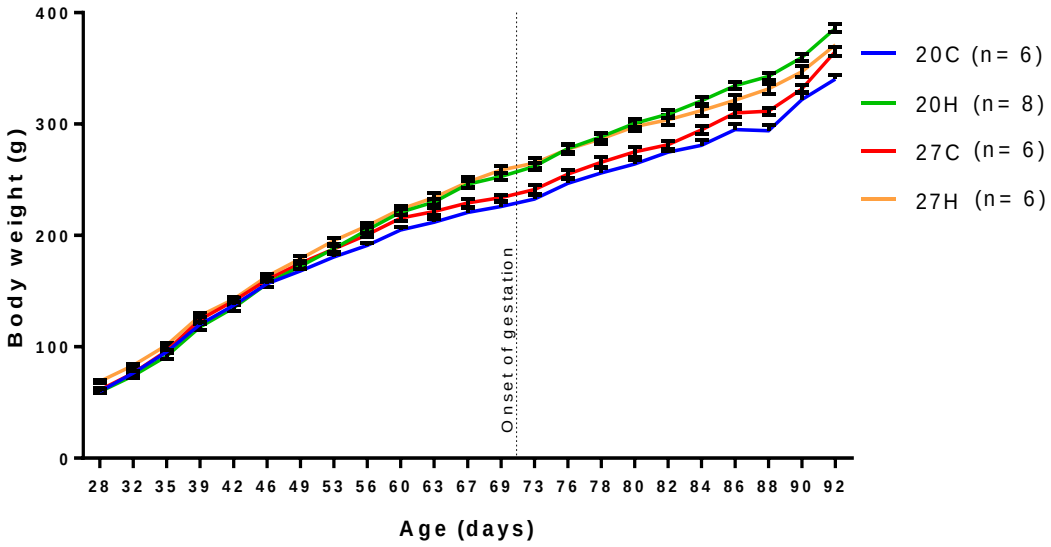


Figure 3.3: 19-days gestation cumulative body weight showing a trend towards increased weight gain in the animals fed HFHS diet.

The broken line indicates the period of beginning of gestation. Weight was measurements twice weekly. In the figure, the numbers 20 and 27 indicate housing temperature in Celsius. C: control diet, H: HFHS, high-fat high-sucrose diet. The data are presented as mean ± standard error of mean. The statistical analysis performed for the cumulative weight measurement was 2-way ANOVA with LSD post-hoc comparison for each day of weight measurement revealed increased weight gain in the animals fed HFHS and housed under standard housing temperature (20°C) as compared to those fed the control diet

3.3.1.1 Characteristics of BAT and WAT depots and the weights of major organs

Table 3.1 provides information on the characteristics of WAT and BAT at each time point. Pre-gestation, the WAT weight was increased in the animals fed HFHS diet, regardless of the housing temperature conditions. 10-days of gestation, the WAT weight showed a trend towards increase in the animals fed HFHS diet and housed under thermoneutral temperature conditions. At 19-days of gestation, the WAT weight was increased in the animals fed HFHS diet, and housed under standard housing temperature conditions.

The BAT weight exhibited an increase at both time points of gestation, at 10 and 19-days, in the rats fed the HFHS diet and in those housed under standard housing temperature conditions.

As expected, the HFHS diet was associated with increased kidney weight across the three-time points, before gestation, 10 and 19-days of gestation. At 10-day of gestation, kidneys weight was increased in the animals housed under standard housing temperature conditions and fed the control diet. In contrast, the liver weights of the animals fed the HFHS diet and housed under thermoneutral temperature conditions, as well as, the liver weight of those housed under standard housing temperature conditions and fed the control diet increased at 10 days of gestation. The heart weights of the animals fed the HFHS diet and housed under thermoneutral temperature conditions increased at 10-days of gestation (Table 3.2).

Table 0.1. The effect of housing temperature and diet on WAT and BAT relative weight to body weight.

	Group	20C	20H	27C	27H
Total WAT %	Unmated	1.853 ± 0.184[a]	2.64 ± 0.165[a**]	2.177 ± 0.191[b]	2.854 ± 0.281[b*]
	10 days	2.98 ± 0.118	2.99 ± 0.262[c]	2.934 ± 0.252[c*,d]	3.71 ± 0.2605[d*]
	19 days	2.838 ± 0.123[e]	3.359 ± 0.277[e*]	2.734 ± 0.280	3.388 ± 0.2696
Interscapular BAT%	Unmated	0.099 ± 0.005	0.150 ± 0.018	0.138 ± 0.027	0.142 ± 0.020
	10 days	0.117 ± 0.002	0.145 ± 0.014[f*]	0.103 ± 0.007	0.107 ± 0.005[f]
	19 days	0.117 ± 0.009[g]	0.152 ± 0.009[g*,h*]	0.091 ± 0.009	0.114 ± 0.007[h]

In the table, WAT, white adipose tissue; BAT, brown adipose tissue; HFHS, high fat high sucrose, the numbers 20 and 27 indicate housing temperature in Celsius. C: control diet, H: HFHS, high fat high sucrose diet. Data are presented as mean ± standard error of means. * = $p < 0.05$, ** = $p < 0.01$. The statistical analysis: Two-way ANOVA test was used for normally distributed data and the Mann-Whitney test was used for the non-parametric data to with fisher LSD post-hoc comparison (20C v 20H, 27C v 27H, 20C v 27C, 20H v 27H) within each of the three time points. Similar superscription indicate statistical significance (e.g., a vs a, b vs b, c vs c, d vs d, e vs e, f vs f, g vs g, h vs h).

Table 0.2. The effect of housing temperature and diet on organ weight.

	Group	20C	20H	27C	27H
Brain weight (g)	Unmated	0.778 ± 0.018	0.770 ± 0.208	0.893 ± 0.063	0.801 ± 0.034
	10 days	0.662 ± 0.022	0.629 ± 0.015	0.691 ± 0.019	0.579 ± 0.034
	19 days	0.539 ± 0.019	0.510 ± 0.016	0.545 ± 0.008	0.525 ± 0.013
Heart weight (g)	Unmated	0.4366 ± 0.020	0.4373 ± 0.035	0.4744 ± 0.028	0.3935 ± 0.017
	10 days	0.3562 ± 0.018	0.3783 ± 0.009	0.363 ±0.013^{a**}	0.3879 ± 0.019^{a}
	19 days	0.3314 ± 0.018	0.359 ± 0.0216	0.344 ± 0.0263	0.3059 ± 0.010
Kidney weight (g)	Unmated	0.8213 ± 0.012^{b}	0.935 ±0.059^{b,c*}	0.8314 ± 0.030	0.7947 ± 0.030^{c}
	10 days	0.735 ± 0.024^{d*}	0.7758 ± 0.027	0.709 ±0.023^{d,e}	0.7499 ±0.026^{e*}
	19 days	0.615 ± 0.0166^{f}	0.686 ± 0.026^{f**}	0.540 ± 0.0124	0.628 ± 0.0213
Liver weight (g)	Unmated	4.194 ± 0.1417	4.976 ± 0.1296	3.995 ± 0.1417	4.405 ± 0.2297
	10 days	4.638 ± 0.168^{g*}	4.764 ± 0.0908	4.39 ± 0.0673^{g,h}	4.653 ± 0.125^{h*}
	19 days	4.45 ± 0.1549	4.69 ± 0.0717	4.062 ± 0.2629	4.13 ± 0.1466

In the figure, WAT, white adipose tissue; BAT, brown adipose tissue; HFHS, high fat high sucrose. The numbers 20 and 27 indicate housing temperature in Celsius. C: control diet, H: HFHS, high fat high sucrose diet. Data are presented as mean ± standard error of means. * = p <0.05, ** =p <0.01. Statistical analysis: Two way ANOVA test for normally distributed data and Mann- Whitney test for non-parametric data with fisher LSD post-hoc comparison (20C v 20H, 27C v 27H, 20C v 27C, 20H v 27H) within each of the three each time points. Similar superscription indicate statistical significance (e.g., a vs a, b vs b, c vs c, d vs d, e vs e, f vs f, g vs g, h vs h).

3.3.1.2 The relationship between total body weights and BAT weights

There was no correlation between the total body weight (TBW) and BAT prior to gestation (Fig 3.4). However, in the 10 and 19-days of gestation groups, positive correlations between the TBW and BAT weights were determined by Person's correlation coefficients in the rats fed the control diet and housed under standard housing temperature conditions (20°C) (Fig. 3.5 and 3.6).

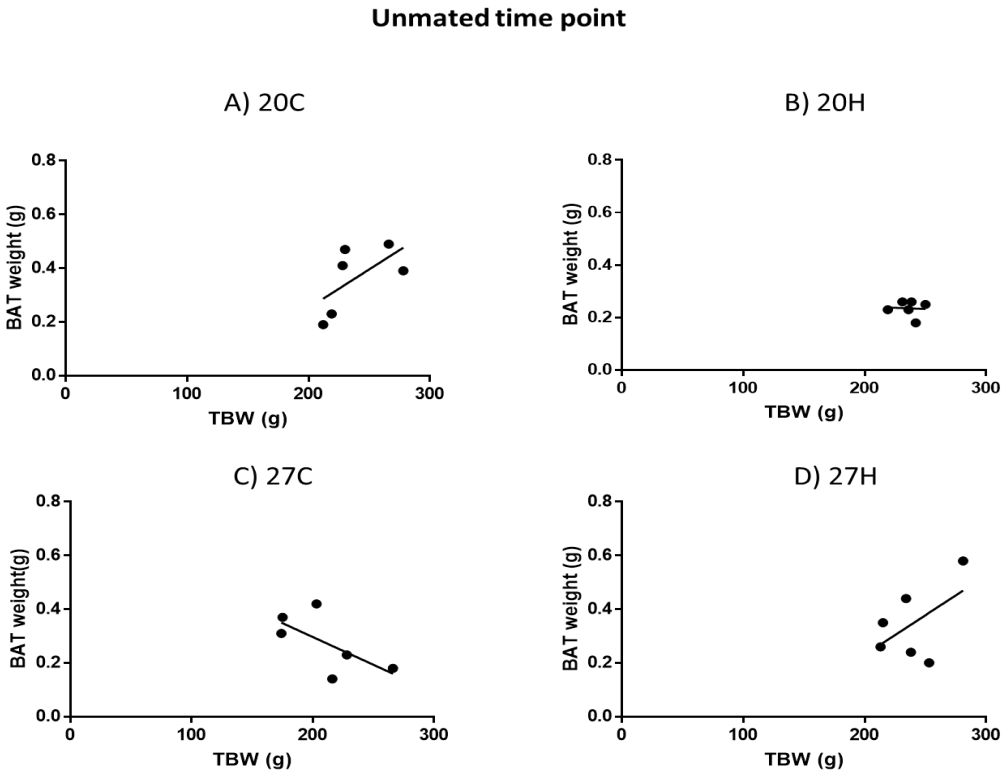


Figure 3.4: Absence of correlation between TBWs and BAT weight before gestation.

In figure, BAT, brown adipose tissue; HFHS, high-fat and high-sucrose; TBW, total body weight. A, rats fed the control diet and housed at 20°C (standard temperature). B, fed the HFHS diet and housed at 20°C. C, fed the control diet and housed at 27°C (thermoneutral temperature), and D, fed the HFHS diet and housed at 27°C. The statistical analysis used was Pearson's correlation for a parametric distribution or Spearman's rank correlation if samples had a non-parametric distribution.

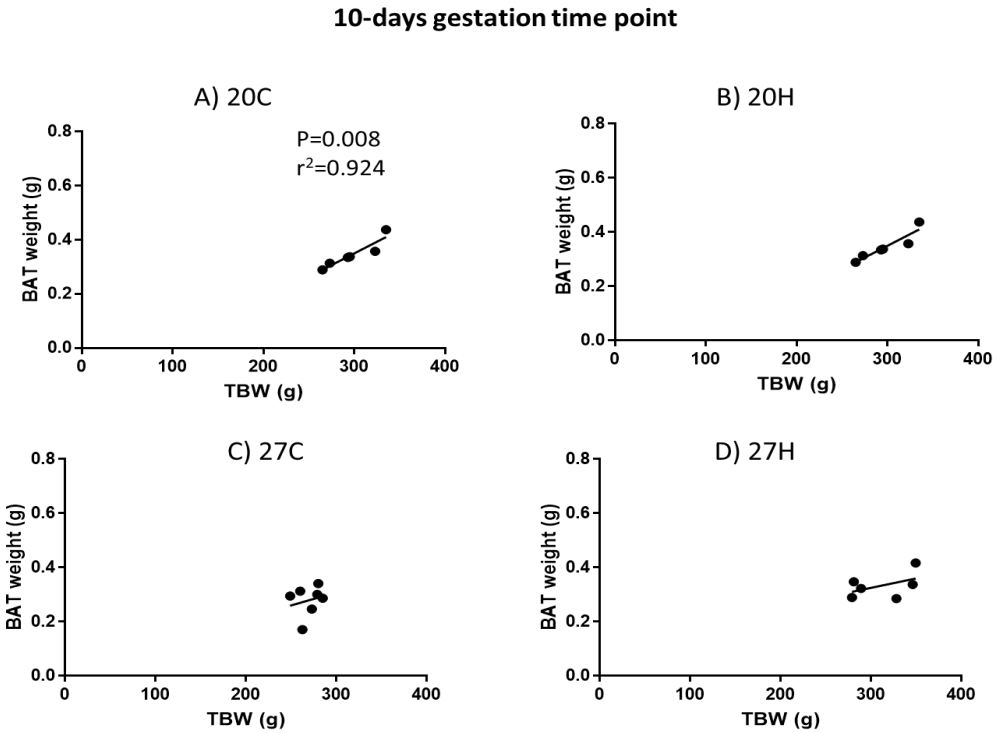


Figure 3.5: There was a correlation between TBW and BAT weight at 10 days of gestation in the animals fed the control diet and housed under standard housing temperature.

In the figure, BAT, brown adipose tissue; HFHS, high fat high sucrose; TBW, total body weight. A and E, rats fed the control diet and housed at 20°C (standard temperature) showing the finding at 10 days ($p=0.008$, $r^2= 0.924$). B, rats fed the HFHS diet and housed at 20°C, showing no correlation. C, rats fed the control diet and housed at 27°C (thermoneutral temperature), showing no correlation. D, rats fed a HFHS diet and housed at 27°C. The statistical analysis used was Pearson's correlation for a parametric distribution or Spearman's rank correlation if samples had a non-parametric distribution.

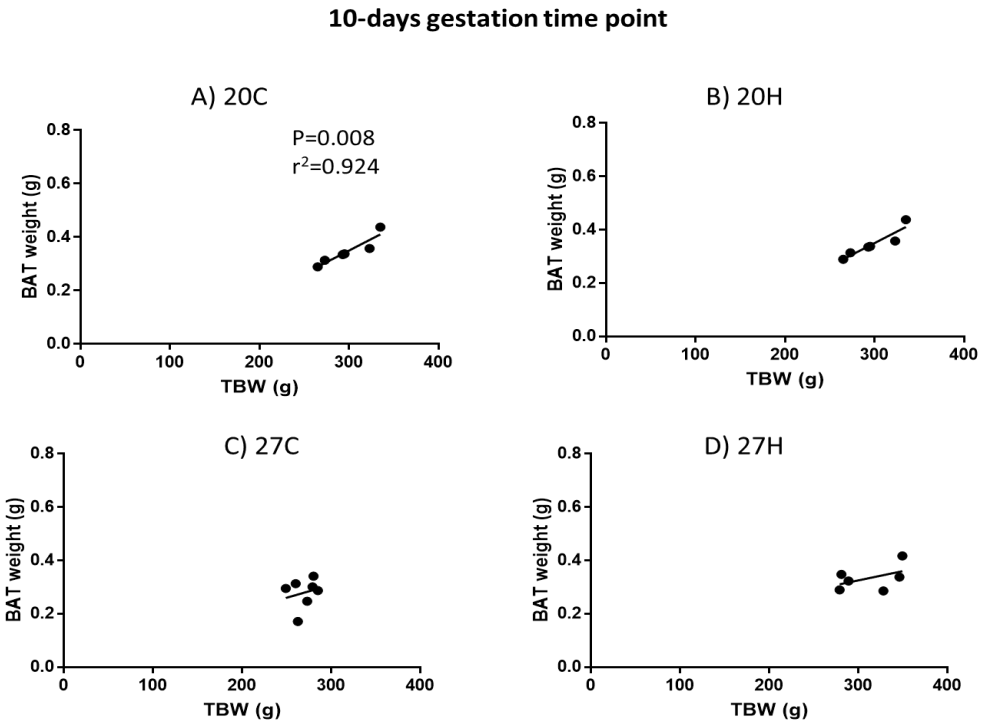


Figure 3.6: Correlation between TBW and BAT weight in 19 days of gestation in the animals fed the control diet and housed under standard housing temperature.

In the figure, BAT, brown adipose tissue; HFHS, high fat high sucrose; TBW, total body weight. A and E, rats fed the control diet and housed at 20°C (standard temperature) showing the finding at 10 days ($p=0.008$, $r^2= 0.924$). B, rats fed the HFHS diet and housed at 20°C, showing no correlation. C, rats fed the control diet and housed at 27°C (thermoneutral temperature), showing no correlation. D, rats fed a HFHS diet and housed at 27°C. The statistical analysis used was Pearson's correlation for a parametric distribution or Spearman's rank correlation if samples had a non-parametric distribution.

3.2.2 The effect of the housing temperature and diet on plasma metabolites

Fasting plasma insulin showed no statistical significance between the comparable groups at any of the time points (Fig. 3.7).

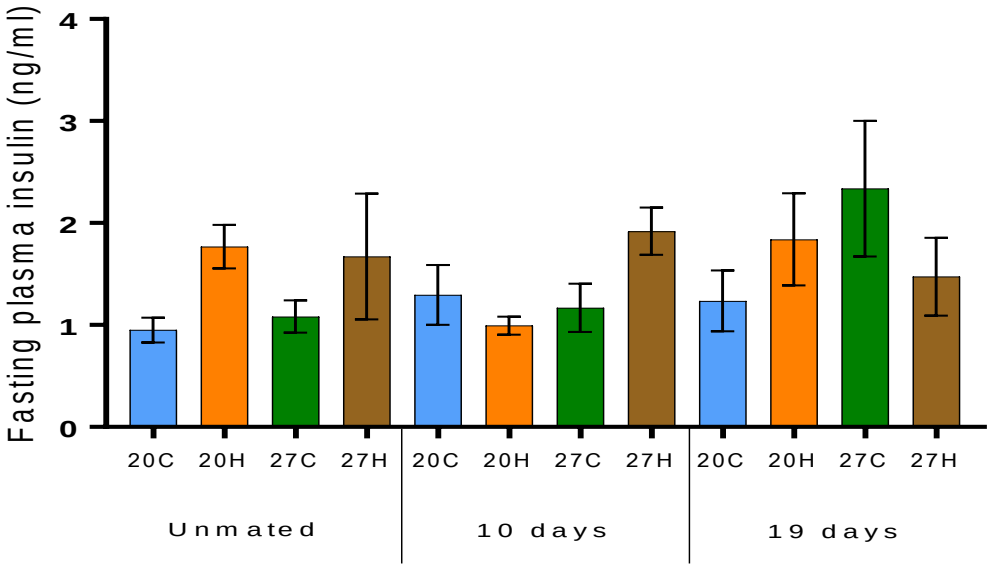


Figure 3.7: The effect of housing temperature and diet on fasting plasma insulin (ng/ml).

Days: number of days of gestation. The number 20 and 27 denote the temperature in degrees Celsius. H: HFHS diet and C: control diet. In the unmated group 20C, 20H, and 20C (*n* = 6), 27C (*n* = 5). In the 10-day gestation 20C and 27H (*n* = 6), and 20H and 27C (*n* = 7) and 20H (*n* = 5). In the 19-day gestation group, 20C and 27H (*n* = 6), 20H (*n* = 7) and 27C (*n* = 5). The values are mean ± standard error of mean. For statistical analysis: Two-way ANOVA test was conducted for normally distributed data and the Mann-Whitney test was used for the non-parametric data with fisher LSD post-hoc comparison (20C v 20H, 27C v 27H, 20C v 27C, 20H v 27H) within each of the three time points.

There were no differences in fasting plasma insulin, and fasting plasma glucose (Fig. 3.8) was elevated only in the animals housed under thermoneutral temperature conditions and fed the control diet prior to gestation. Fasting plasma TG levels were unaffected by housing temperature and diet, however TG level showed an insignificant increase

at late gestation (Fig. 3.9). Fasting plasma non-esterified fatty acids (NEFA) (Fig. 3.10) increased only in the late gestational period in the dams (i.e., pregnant female rat) fed the HFHS diet and housed under standard housing temperature conditions.

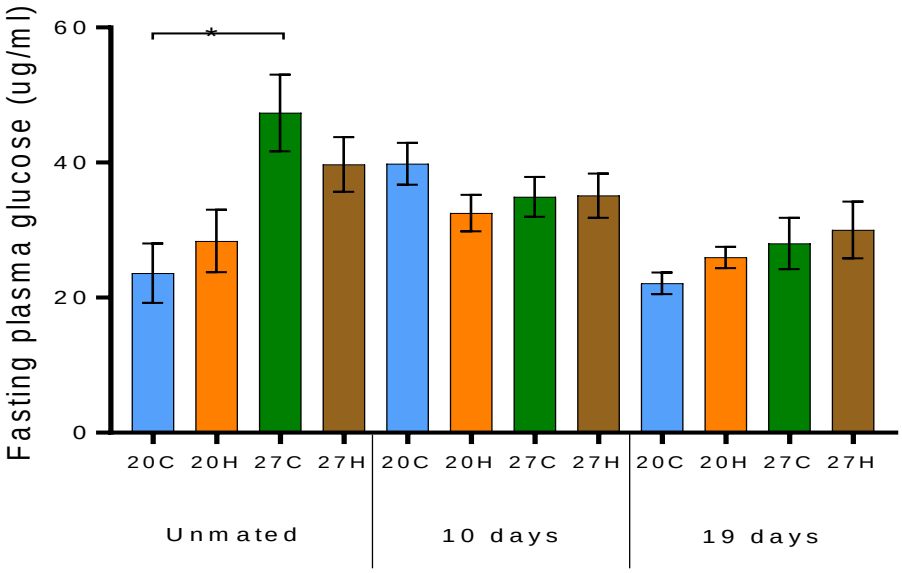


Figure 3.8: The effect of housing temperature and diet on fasting plasma glucose (µg/ml) at the three time points.

Days: number of days of gestation. The number 20 and 27 denote the temperature in degrees Celsius. H: HFHS diet and C: control diet. In the unmated group 20C, 20H, and 20C (*n* = 6), 27C (*n* = 5). In the 10-day gestation 20C (*n* = 6) and 27H, 20H, 27C and 20H (*n* = 7). In the 19-day gestation group, 20C, 27C and 27H (*n* = 6) and 20H (*n* = 8). The values are mean ± standard error of mean. The superscripts * indicate statistical significance ($p < 0.05$). For statistical analysis: Two-way ANOVA test was conducted for normally distributed data and the Mann-Whitney test was used for the non-parametric data with fisher LSD post-hoc comparison (20C v 20H, 27C v 27H, 20C v 27C, 20H v 27H) within each of the three time points.

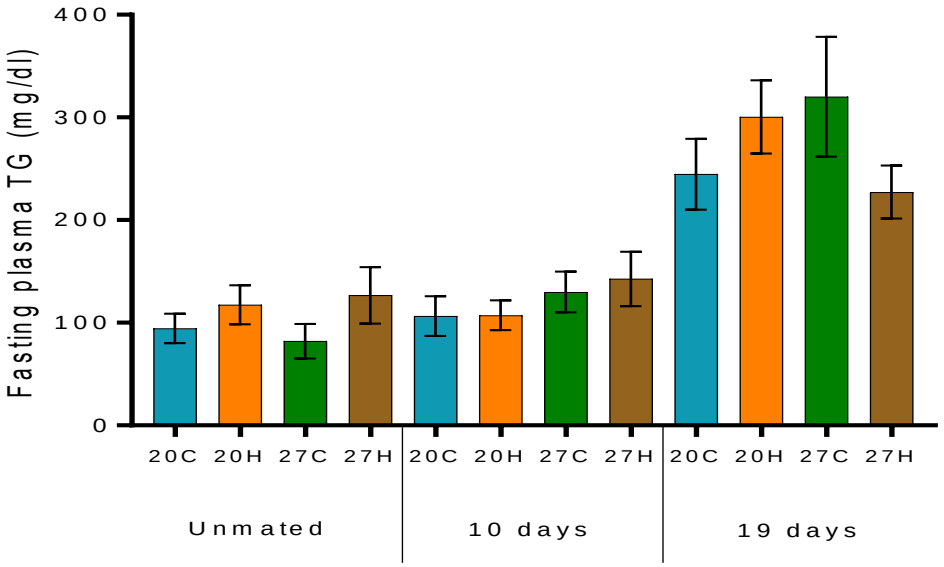


Figure 3.9: The effect of housing temperature and diet on fasting plasma triglycerides (mg/dl).

Days: number of days of gestation. The number 20 and 27 denote the temperature in degrees Celsius. H: HFHS diet and C: control diet. In the unmated group 20C, 20H, and 20C (*n* = 6), 27C (*n* = 5). In the 10-day gestation 20C (*n* = 6) and 27H, 20H, 27C and 20H (*n* = 7). In the 19-day gestation group, 20C, 27C and 27H (*n* = 6) and 20H (*n* = 8). The values are mean ± standard error of mean. For statistical analysis: Two-way ANOVA test was conducted for normally distributed data and the Mann-Whitney test was used for the non-parametric data with fisher LSD post-hoc comparison (20C v 20H, 27C v 27H, 20C v 27C, 20H v 27H) within each of the three the three time points.

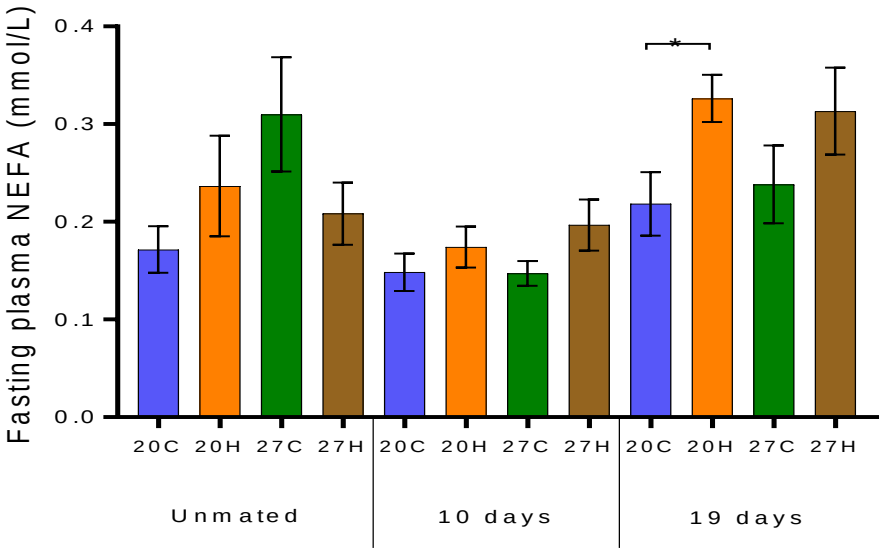


Figure 3.10: The effect of housing temperature and diet on fasting plasma NEFA (mmol/L).

Days: number of days of gestation. The number 20 and 27 denote the temperature in degrees Celsius. H: HFHS diet and C: control diet. In the unmated group 20C, 20H, and 20C (*n* = 6), 27C (*n* = 5). In the 10-day gestation 20C (*n* = 6) and 27H, 20H, 27C and 20H (*n* = 7). In the 19-day gestation group, 20C, 27C and 27H (*n* = 6) and 20H (*n* = 8). The values are mean ± standard error of mean. The superscripts * indicate statistical significance ($p < 0.05$) For statistical analysis: Two-way ANOVA test was conducted for normally distributed data and the Mann-Whitney test was used for the non-parametric data with fisher LSD post-hoc comparison (20C v 20H, 27C v 27H, 20C v 27C, 20H v 27H) within each of the three the three time points.

3.3 Discussion

3.3.1 The impact of standard housing temperature and a HFHS diet on the body composition of female rodents

In this study, of the two intervention (i.e., HFHS diet and standard housing temperature), the dietary intervention has the greatest effect on body weight gain and WAT weight. Increased weight gain during pregnancy has been attributed mainly to hyperphagia, foetal and placental growth, maternal fat deposition and reduced thermogenesis (Abelenda and Puerta, 1987, Schneider and Wade, 1987, Munilla and Herrera, 2000). In rats, a pervious study reported that weight gain started at first week of gestation whereas hyperphagia began later in pregnancy (Rocha et al., 2003). Hyperphagia support the weight gain as increased energy intake produces positive energy balance in order to face the gestational metabolic demands (Rocha et al., 2003). Leptin is an appetite suppressor hormone yet; previous studies reported increased levels with preexisting hyperphagia in gestation, which could be a physiological leptin resistance in hypothalamus (Rocha et al., 2003, Garcia et al., 2000, Ahima and Flier, 2000, Amico et al., 1998). Most of the maternal weight gain in the first two-thirds of gestation are due to maternal tissue expansion (blood volume, uterine expansion, mammary glands and stored fat) (Abrams and Selvin, 1995), at the last third of gestation, the dams weight gain attributed mainly to the maximum foetal and placental growth. This is regulated by progesterone during the third part of gestation in rat, which is the rapid fetal growth period. A previous study tested the progesterone role by performing ovariectomy with partial

progesterone replacement, which caused fetal and placental growth restriction (Mark et al., 2006). A previous study suggested that gestation inhibits thermogenesis by reducing BAT mitochondrial content, reduced beta 3 adrenergic receptor (β3-AR) expression, and increases leptin mRNA expression (Frontera et al., 2005), thereby these physiological changes occured to reserve energy for reproduction demands. Furthermore, as the duration of the study is longer for the pregnancy groups, the effect of the HFHS diet become more apparent on weight gain but may also be dependent on the animals being pregnant. The significant effect of the HFHS diet on the weight gain started at approximately the first day of gestation among the 10-days pregnancy group and lasted until animals were sacrificed. Whereas the 19 days of gestation, the dietary intervention effect on the weight gain started approximately at the 39th day of beginning of the intervention (i.e., few days before the mating and onset of gestation) and lasted throughout the intervention period. The effect of dietary intervention vary between to 10-days and 19-days, as it was pronounced under thermoneutral temperature condition at mid gestation (10-days), and under standard housing temperature at late gestation (19-days). These findings are in agreement with earlier publications (Murase et al., 2001, Sato et al., 2010, Yang et al., 2012, Cuthbert et al., 2017).

In the present study, as expected, the total WAT mass was increased in the animals fed the HFHS diet, these findings are in accordance with these of an earlier study (Romero Mdel et al., 2014). As reported earlier, HFHS diet alters lipid metabolism, which leads to increased adiposity (Samuel et al., 2010, Yang et al., 2012). In the late-pregnancy period, the WAT mass

increased, the latter is attributable to active lipid deposition, which is necessary to enable rapid foetal growth and prepare for lactation (Herrera, 2000, Herrera, 2002). Energy is stored in WAT at times of energy abundance, and this energy is then released at times of energy shortages (Herrera, 2000, Herrera, 2002).

In this study, interscapular BAT mass increased with both standard housing temperature and HFHS in gestation. In addition, there was a positive correlation between the BAT mass and TBW during gestation in the animals housed under standard housing temperature conditions and fed the control diet. Other studies reported BAT mass increases with mild cold exposure (Chondronikola et al., 2016) and HFHS induced by high-carbohydrate (Kanarek and Orthen-Gambill, 1982), high-fat diets (Saxton and Eisen, 1984) and cafeteria diet (Romero Mdel et al., 2014). Below thermoneutrality (28 ± 1 °C) as in standard housing temperature (21 ± 1 °C), norepinephrine (NE) released and enhances both BAT hyperplasia and the differentiation of brown adipocytes (Bukowiecki et al., 1982, Chondronikola et al., 2016). A previous study reported that increased BAT mass in mid-gestation was not related to increased TGs or protein content (Frontera et al., 2005). The same study also reported an increase of sex steroids (i.e., 17β-estradiol and progesterone) in mid-gestation, which promotes greater water content in BAT (Frontera et al., 2005). This explanation is in agreement with older study that showed increased water retention in pregnant rats resulting in increased tissue weight (Atherton et al., 1982). Furthermore, a previous study reported an increased BAT mass in late-gestation due to the

increased lipid accumulation to prepare for lactation (Villarroya et al., 1986, Abelenda and Puerta, 1987, Ramos et al., 2003).

Although the dietary intervention affected the weights of some organs (heart, kidney and liver), in this study, it did not affect brain weight. This finding is in accordance with that of similar studies (Sellers et al., 2007, Piao et al., 2013). The liver displayed a trend towards increased weight in accordance with weight gain. An increase in liver weight may be due to an increase in intracellular storage of TGs by the action of circulating lipoprotein lipase (LPL) (Yang et al., 2012). Increases in liver weight during mid-gestation may be attributed to several factors, such as, hyperphagia, insulin, insulin-like growth factor and placental lactogen (Freemark et al., 1993, El Khattabi et al., 2006, Augustine et al., 2008, Celton-Morizur et al., 2009). Kidney weights increased across the time points, mainly by the dietary intervention. A previous study reported high-fat diet (HFD) increased renal TG and cholesterol accumulation this might result from lipid synthesis (Jiang et al., 2005). These findings of alteration in liver and kidney weights induced by HFHS in the present study are in accordance with those of a recent study (Showalter et al., 2018). No previous studies reported increases in heart weight induced by an HFHS diet. Such increases could provide evidence for myocardial hypertrophy. However, a recent study reported that maternal obesity-induced diet produced an increased heart weight, hypertension and cardiac dysfunction in adult male offspring (Loche et al., 2018).

3.3.2 Metabolic adaptation to the HFHS and standard housing temperature

This study analysed a number of circulatory plasma metabolites, which previous studies showed an increase in response to diet induced-obesity (Sumiyoshi et al., 2006, Ragab et al., 2015, Kowalski et al., 2017).

In the current study, there was an increase in fasting plasma glucose prior to gestation in the animals housed under thermoneutral temperature conditions and fed the control diet. These results were not accompanied by any change in serum insulin level. Many previous studies reported that a HFHS increased glucose and then insulin levels (Sumiyoshi et al., 2006, Ragab et al., 2015, Kowalski et al., 2017). Researches also showed that maintaining rodents within their thermoneutral zone reduced sympathetic activity (Swoap et al., 2008). In this study, insulin was unaffected by the increased glucose level. Skeletal muscles and adipose tissues are the two major sites that utilise glucose by insulin action. Both sympathetic and parasympathetic innervation supplies skeletal muscles; whereas adipose tissue is supplied by sympathetic innervation and some adrenergic but there is no parasympathetic supply to the adipose tissue (Landsberg, 1992, Bartness and Bamshad, 1998). Glucose metabolism is regulated either by sympathetic or parasympathetic innervation. Sympathetic handling of glucose mediated by sympathetic nervous system (SNS) mediators such as, epinephrine, glucagon and the direct innervation to adipose tissue, muscles and liver (Nonogaki, 2000). The effect of parasympathetic innervation of glucose metabolism is mediated by insulin and the direct innervation to the liver (Bartness and Bamshad, 1998). Sympathetic

innervation, generates a catabolic effect on glucose, while parasympathetic, produces an anabolic effect (Shimazu, 1996). Activation of the splanchnic sympathetic innervation inhibits insulin release from beta cells in the pancreas and stimulate glucagon (Nonogaki, 2000). In this study, fasting insulin level was not elevated with increased fasting glucose level, which suggest a sympathetic handling of glucose. In the fasted state, SNS induces adrenal medullary epinephrine to release glucagon, which promotes hepatic-glycogen hydrolysis and the production of glucose via glycogenolysis (Nonogaki, 2000, Cahill, 2006). The latter process starts 4 hours post-absorption and lasts for 28 hours (Cahill, 2006). Increases in hepatic glucose production in the fasted state is mainly attributed to epinephrine (Shimazu, 1996, Nonogaki and Iguchi, 1997b, Nonogaki and Iguchi, 1997a). Sympathetic activation stimulates glucose utilization in adipose tissue through adrenergic receptors of norepinephrine (Landsberg, 1992, Bartness and Bamshad, 1998). In addition, mild cold promotes elevated glucose uptake in skeletal muscles independent of the action of insulin, mechanism is activated by an increase in sympathetic activity (Landsberg, 1992). In the present study, the adipose tissue mass of the animals housed under a standard housing temperature conditions and fed the control diet was lighter than that of the animals housed under thermoneutral temperature conditions. These findings may be explained by the utilization of some energy in the process of thermogenesis to maintain core body temperature.

In the present study, fasting plasma NEFA was increased during late gestation in the animals fed the HFHS diet, and the increase was not

accompanied by any significant changes in fasting plasma TGs levels. The progressive increase in fasting plasma TGs level and NEFA during the late gestational stage in rat adipose tissue, pointed to the constant decrease in LPL activity and enhanced hepatic triglycerides synthesis in late gestation (Otway and Robinson, 1968, Herrera et al., 1988, Kershaw and Flier, 2004). Decreased LPL activity indicates that fat uptake reduces during late gestation, which together with the enhanced lipolytic activity that occurs at this stage of gestation results in accelerated breakdown of fat (Herrera, 2002). This catabolic condition during late gestation enables maximum fetal growth and maternal hyperlipidemia, which increases plasma NEFA alongside other lipids (Smith et al., 1998, Herrera, 2002, López-Soldado et al., 2017). NEFA may be used for β-oxidation to acyl-CoA and ketone body synthesis (Herrera, 2002). As reported previously, these changes are essential to provide dams with the energy required for mammary glands to prepare for the onset of lactation and for glucose transfer to the foetus for rapid weight growth (Smith et al., 1998, Corvino et al., 2015, Soma-Pillay et al., 2016).

Although the HFHS diet had only modest effects on plasma metabolites, it had a clear effect on fat mass at the three time points. Neither the dietary nor the thermal intervention influenced fasting plasma insulin level at any of the time points, although there was a trend towards a modest elevation in fasting plasma insulin level in the late gestational period in the animals housed under standard housing temperature conditions and fed the HFHS diet. Although the values were numerically higher, they were not statistically significant. Previous studies showed that the sucrose component of the diet

had a greater effect than the high-fat component on plasma insulin levels and that a combination of the two components elicited the strongest effect on plasma insulin levels (Barnard et al., 1970, Musial et al., 2017). Gestational hormones modulate insulin sensitivity in early to mid gestation, especially progesterone, which has an anti-insulin in early to mid-gestational period (day 0 to 14) (Ramos et al., 2003). Late gestation is characterised by insulin resistance (i.e. insulin stimulation of glucose uptake decreased by 50%) (Leturque et al., 1986), hyperinsulinaemia is responsible for 25% reduction in lipolysis at the late gestational period, that results in maintaining and or expanding stored lipids, and reducing β_3-AR in adipocytes (Nonogaki, 2000). In the late gestational period, increase plasma 17β-estradiol level induces insulin resistance by reducing the quantity of peripheral insulin receptor (Gonzalez et al., 2000). In the current study, there was an insignificant increase in fasting plasma TG levels with all study intervention and in fasting NEFA levels at thermoneutral temperature condition at late gestational period. This could be explained by the accelerated breakdown of lipids occur in this stage of gestation and increased hormone sensitive lipase activity. Lipolytic activity is enhanced in fasting state to compensate for the maternal nutritional deprivation and demands (Herrera, 2000, Herrera, 2002). Increase in maternal plasma NEFA and TGs circulating hydrolysis and uptake resulting from an impaired LPL activity (Lopez-Luna et al., 1991, Herrera, 2002). In the late gestational period, NEFA produces ketones, which are an important source for polyunsaturated fatty acids for foetus (Herrera, 2002). This enables lipolysis

to produce lipids for maternal fuel and, transporting the readily available glucose, amino acid and ketones to the foetus (Soma-Pillay et al., 2016).

In the present study, neither diet nor temperature in the pre- and mid-gestation periods alterd fasting plasma TG levels. Although not statistically significant, there was a trend towards raised TG levels in late pregnancy, regardless of the diet or temperature. This increase was accompanied by an increment in fasting NEFA in the animals housed under the standard housing tempreture and fed the HFHS diet. At the last third of gestation, the metabolism switches to catabolic phase with an accelerated rate breakdown of fat deposits because of augmented adipose tissue Lipolytic activity. Previous studies in late pregnant rats showed increased mRNA expression of HSL in WAT (Martineau et al., 2015). Furthermore, it has been shown that LPL activity reduced in rat and human late-gestation (Pujol et al., 2005), thus decreasing the deposit of lipids in maternal adipocytes. This result is in agreement with that of other studies (Sinitskaya et al., 2007, López-Soldado et al., 2017).

3.4 Conclusion

This chapter demonstrated that female rodents exposed to an obesogenic (HFHS) diet become heavier, especially during pregnancy. Despite the modest changes in plasma metabolites, there is a clear change in adipose tissue mass. The dietary intervention led to higher adipose tissue weights. These findings emphasize the subtle but important effect of housing temperature when examining the effects of the HFHS diet.

Chapter 4 - The effect of temperature and dietary intervention on BAT thermogenic capacity

4.1 Introduction and aims

Obesity and metabolic syndrome occur when energy intake continuingly exceeds expenditure. One potential treatment is the activation of brown adipose tissue (BAT), a metabolically active organ that was first identified in rodents and recently found to be present in human (van Marken Lichtenbelt et al., 2009, Cypess et al., 2009, Zingaretti et al., 2009, Saito et al., 2009). Cold exposure activates the sympathetic nervous system (SNS), which releases norepinephrine (NE) and induces thermogenesis through fatty acid (FA) and glucose consumption (Cannon and Nedergaard, 2004). BAT utilizes a large amount of energy to enable thermogenesis via activation of beta-3 adrenergic receptors (β_3-ARs), which is located on brown adipocytes (Virtanen et al., 2009, Cypess et al., 2013a). Thermogenesis is achieved in the presence of a unique protein called mitochondrial uncoupling protein 1 (UCP1) that uncouples respiration from oxidative phosphorylation (Cannon and Nedergaard, 2004). This chapter focuses on studying UCP1 abundance and number of genes that play a critical role in thermogenesis.

Therefore, in this chapter the thermogenic capacity of the interscapular BAT and resulting phenotypic and genotypic alterations in adipose tissue were investigated. Previous studies suggested that gestation affected the thermogenic capacity by inhibiting thermogenesis to enable fat deposition

and ensure sufficient energy for maternal and foetus fuel (Frontera et al., 2005, Soma-Pillay et al., 2016).

The hypothesis in this chapter was that adaptation to standard housing temperature conditions would contribute to an increase in the expression of thermogenic active BAT-related genes and increase the mitochondrial UCP1 abundance and that the thermogenic capacity would decrease in the gestational period for reserve energy to dams and their growing offspring.

4.2 Material and methods

The current study was undertaken at the Division of Child Health in the University of Nottingham, U.K. The primers used were developed and optimised by staff members in the division. Gene expression values were normalized and calculated against the two housekeeping genes (i.e., TBP and YWHAZ) using GeNorm software (Primer Design Ltd, Southampton, Hampshire, UK). A detailed description of the methods and statistical analysis can be found in Chapter 2.

4.3 Results

4.3.1 The effect of housing temperature and diet on interscapular BAT morphology

As described in Chapter 3, the interscapular BAT weight increased in the animal fed the HFHS diet and in those housed under the standard housing temperature. To determine the impact of the HFHS diet and housing temperature, histological sections were analysed. The UCP1 abundance (%) in BAT, adipocyte surface area in micrometre squared (μm^2) and adipocyte number were determined. Representative samples from tissues obtained before gestation (Fig. 4.1), mid gestation (Fig. 4.2) and late gestation (Fig. 4.3) are shown.

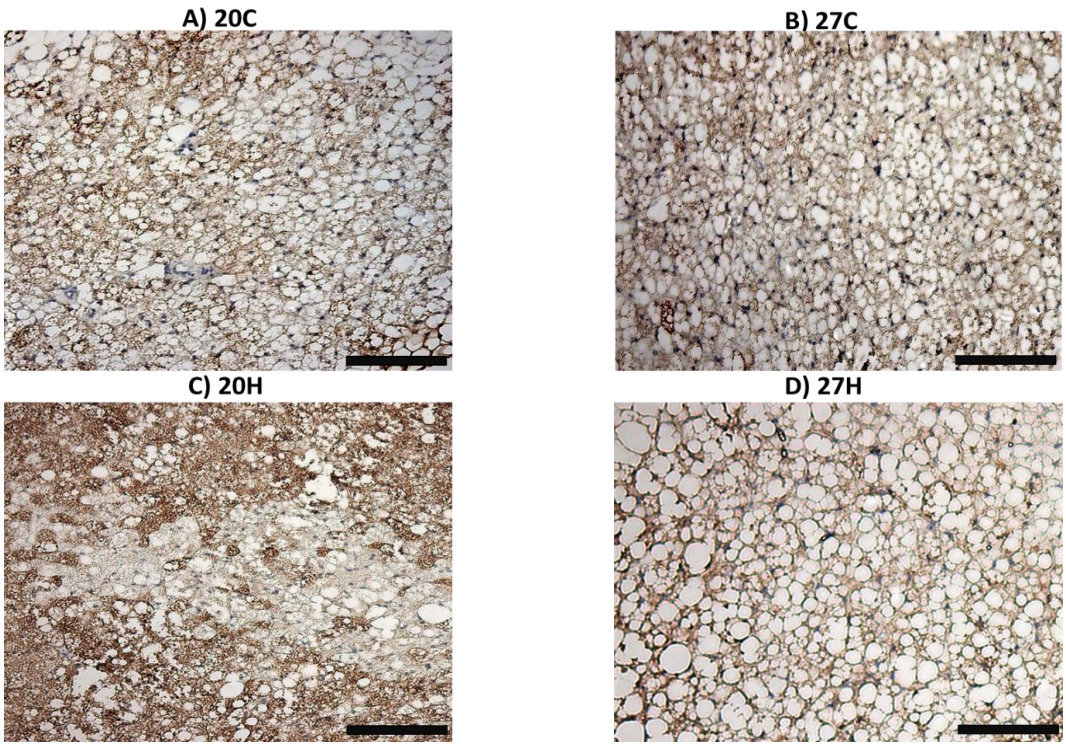


Figure 4.1: Representative examples of the IHC stained histological sections in the pre-gestation.

A) housed under standard housing temperature (20°C) and fed the control diet, B) housed under thermoneutral temperature conditions (27°C) and fed the control diet, C) housed under standard housing temperature and fed the HFHS diet and D) housed under thermoneutral temperature conditions and fed the HFHS diet. HFHS = high fat high sucrose. Scale bar = 300 μm; magnification 10×.

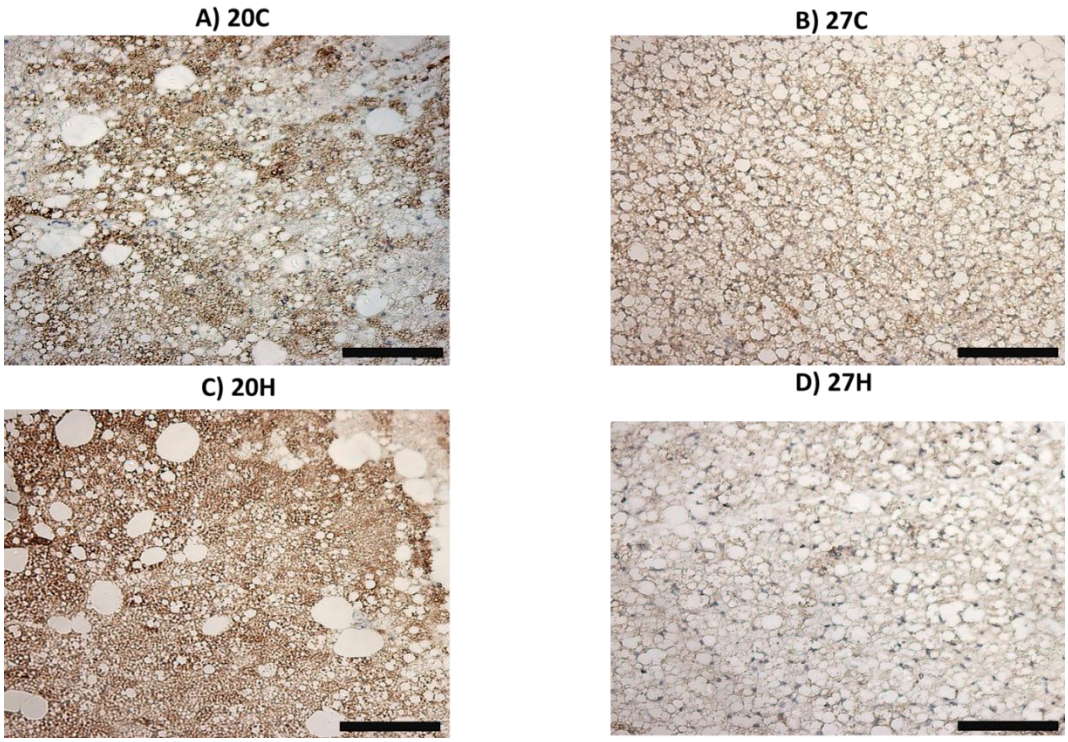


Figure 4.2: Representative examples of the IHC stained histological sections in the mid gestational period (10-days gestation).

A) housed under standard housing temperature (20°C) and fed the control diet, B) housed under thermoneutral temperature conditions (27°C) and fed the control diet, C) housed under standard housing temperature and fed the HFHS diet and D) housed under thermoneutral temperature conditions and fed the HFHS diet. HFHS = high fat high sucrose. Scale bar = 300 μm; magnification 10×.

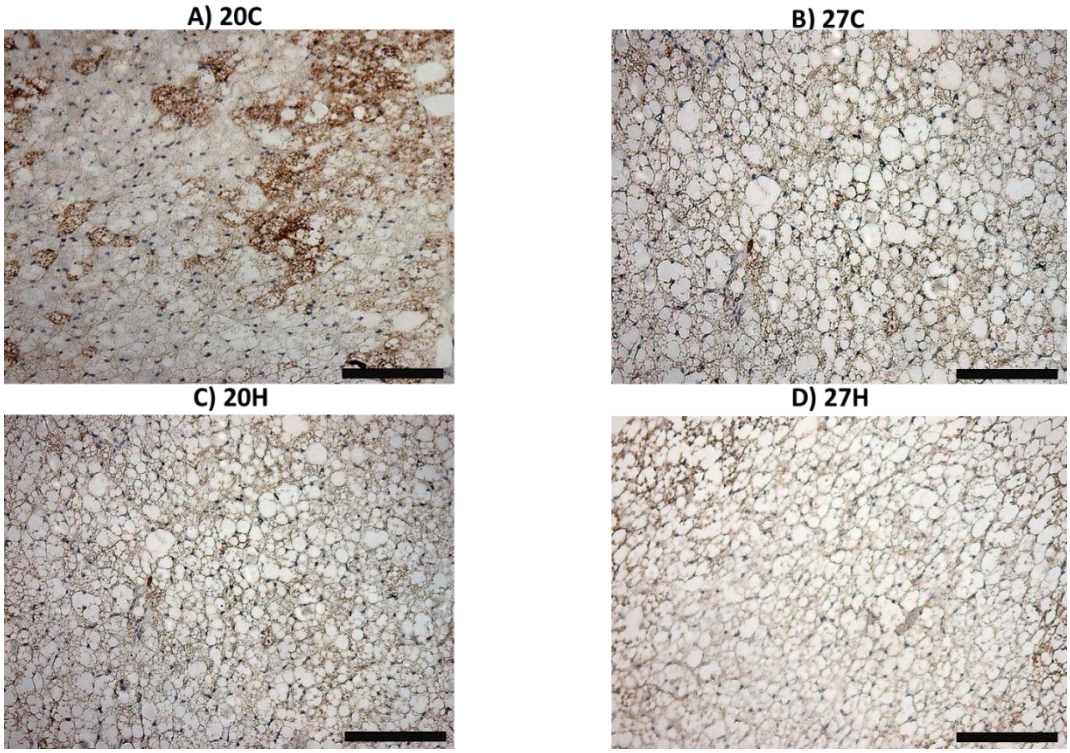


Figure 4.3: Representative examples of the IHC stained histological sections in the late gestational period (19-days gestation).

A) housed under standard housing temperature (20°C) and fed the control diet, B) housed under thermoneutral temperature conditions (27°C) and fed the control diet, C) housed under standard housing temperature and fed the HFHS diet and D) housed under thermoneutral temperature conditions and fed the HFHS diet. HFHS = high fat high sucrose. Scale bar = 300 μm; magnification 10×.

4.3.1.1 Mitochondrial UCP1 abundance

The analysis of the mitochondrial UCP1 abundance in histological sections identified increased UCP1 abundance only in the animals housed under standard housing temperature conditions and fed the HFHS diet prior to gestation. In the mid gestational period, UCP1 abundance increased in the animals housed under standard housing temperature conditions, regardless of the diet (Fig. 4.4).

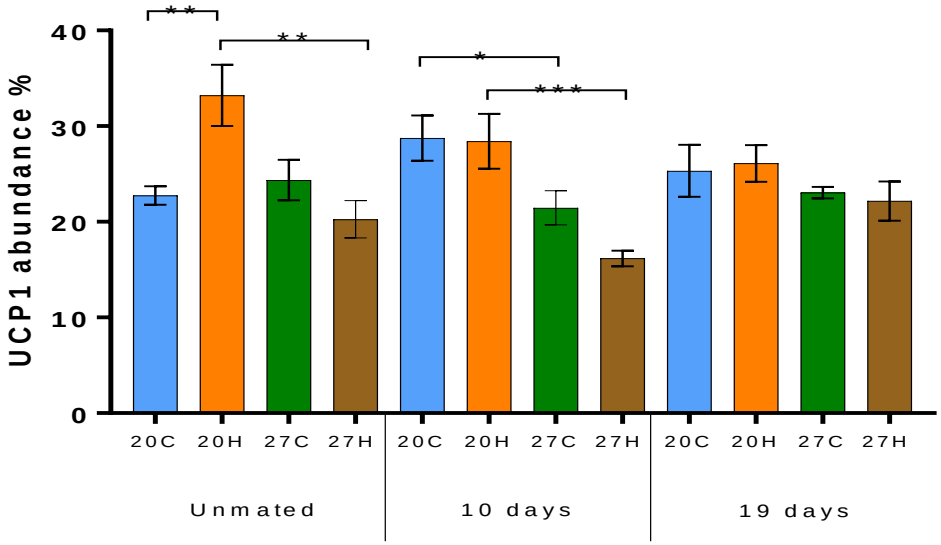


Figure 4.4: The effect of housing temperature and diet on UCP1 abundance (%) at the three time points.

Days: number of days of gestation. The number 20 and 27 denote the temperature in degrees Celsius. H: HFHS diet and C: control diet. In the unmated group 20C, 20H, and 20C (*n* = 6), 27C (*n* = 5). In the 10-day gestation 20C (*n* = 6) and 27H, 20H, 27C and 20H (*n* = 7). In the 19-day gestation group, 20C, 27C and 27H (*n* = 6) and 20H (*n* = 8). The values are mean ± standard error of mean. The superscripts indicate statistical significance ($p < 0.05$). ** = $p \leq 0.01$ and *** = $p \leq 0.001$. For statistical analysis: Two-way ANOVA test was conducted for normally distributed data and the Mann-Whitney test was used for the non-parametric data with fisher LSD post-hoc comparison (20C v 20H, 27C v 27H, 20C v 27C, 20H v 27H) within each of the three the three time points.

4.3.1.2 Adipocyte area and number

To determine the impact of diet and housing temperature on the interscapular tissue, the white adipocytes area and number were measured. The adipocyte area decreased prior to gestation in the animals fed the control diet and housed under thermoneutral temperature conditions. In contrast, adipocyte area increased prior to gestation in the animals housed under standard housing temperature conditions and fed the control diet (Fig. 4.5). Prior to gestation, adipocytes number rose only

in the animals housed under thermoneutral temperature conditions and fed the control diet. Throughout gestation, the adipocyte number decreased in the animals housed under standard housing temperature, regardless of the diet (Fig. 4.6).

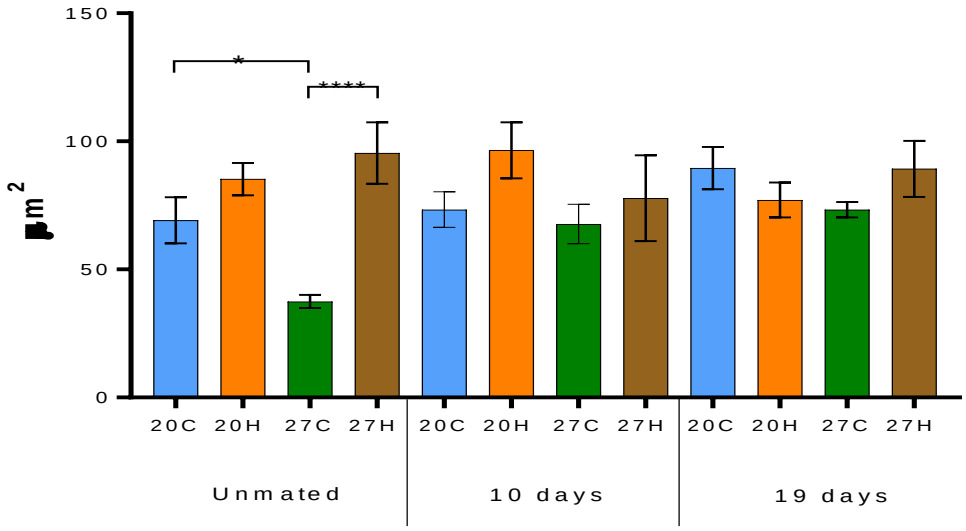


Figure 4.5: The effect of housing temperature and diet on adipocyte area at the three time points.

Days: number of days of gestation. The number 20 and 27 denote the temperature in degrees Celsius. H: HFHS diet and C: control diet. In the unmated group 20C, 20H, and 20C (*n* = 6), 27C (*n* = 5). In the 10-day gestation 20C (*n* = 6) and 27H, 20H, 27C and 20H (*n* = 7). In the 19-day gestation group, 20C, 27C and 27H (*n* = 6) and 20H (*n* = 8). The values are mean ± standard error of mean. The superscripts indicate statistical significance ($p < 0.05$). * = $p < 0.05$ and **** = $p \leq 0.0001$.Statistical analysis: Two way ANOVA test for normally distributed data and Mann-Whitney test for non-parametric data with fisher LSD post-hoc comparison (20C v 20H, 27C v 27H, 20C v 27C, 20H v 27H) within each of the three the three time points.

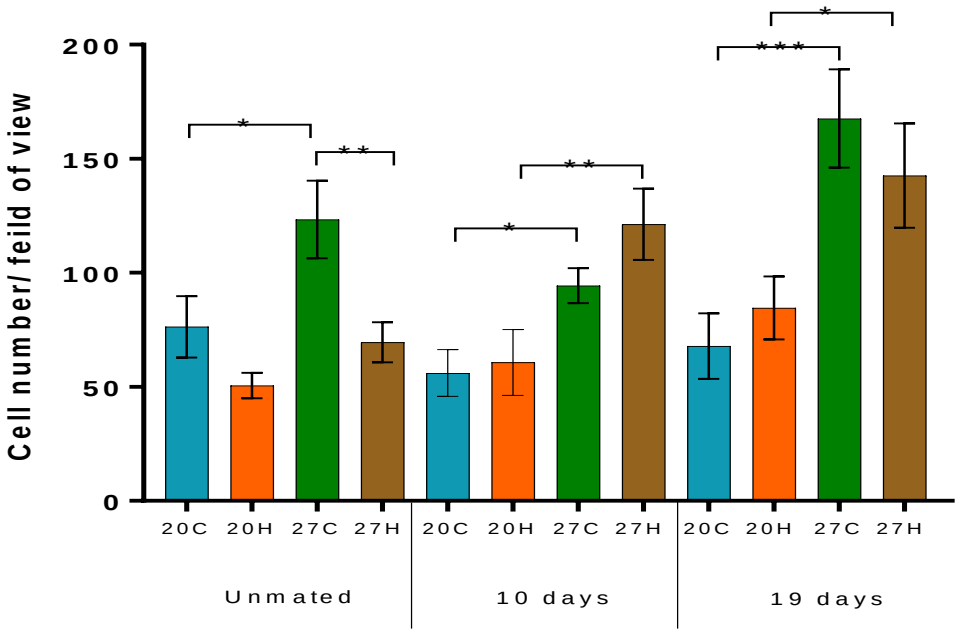


Figure 4.6: The effect of housing temperature and diet on the mean adipocyte count at the three time points.

Days: number of days of gestation. The number 20 and 27 denote the temperature in degrees Celsius. H: HFHS diet and C: control diet. In the unmated group 20C, 20H, and 20C (*n* = 6), 27C (*n* = 5). In the 10-day gestation 20C (*n* = 6) and 27H, 20H, 27C and 20H (*n* = 7). In the 19-day gestation group, 20C, 27C and 27H (*n* = 6) and 20H (*n* = 8). The values are mean ± standard error of mean. The superscripts indicate statistical significance ($p < 0.05$). * = $p < 0.05$, **=≤0.01 and ***= p≤0.001. For statistical analysis: Two-way ANOVA test was conducted for normally distributed data and the Mann-Whitney test was used for the non-parametric data with fisher LSD post-hoc comparison (20C v 20H, 27C v 27H, 20C v 27C, 20H v 27H) within each of the three the three time points.

4.3.2 The effect of housing temperature and diet on the interscapular BAT genotype

4.3.2.1 Brown adipose tissue thermogenesis genes

To determine the interscapular BAT thermogenic capacity, gene expression analysis of a number of key genes (*UCP1, PPARγ, PGC1α, β_3-AR* and *TRPV1α*) associated with BAT-related functions was conducted. The relative mRNA expression of UCP1 was only elevated prior to pregnancy in the animals housed under standard housing temperature conditions and fed the control diet (Fig. 4.7). The relative mRNA expression of PPARγ mRNA expression decreased in the animals housed under standard housing temperature conditions, regardless of the diet, and it increased in the animals housed under thermoneutral temperature conditions and fed the control diet (Fig. 4.8). PGC1α showed increased relative expression before gestation in the animals housed under standard housing temperature and fed the HFHS diet. In the late gestational period, the relative PGC1α mRNA expression increased in the animals housed under standard housing temperature conditions and fed the control diet (Fig. 4.9). There was no difference of the relative mRNA expression of the β_3-ARs or SERCA2b at any of the time points, before gestation, 10 and 19-days of gestation (Figs. 4.10 and 4.11). Neither diet nor temperature affected the relative mRNA expression of TRPV1α, although its expression was increased in the mid gestational period (Fig. 4.12).

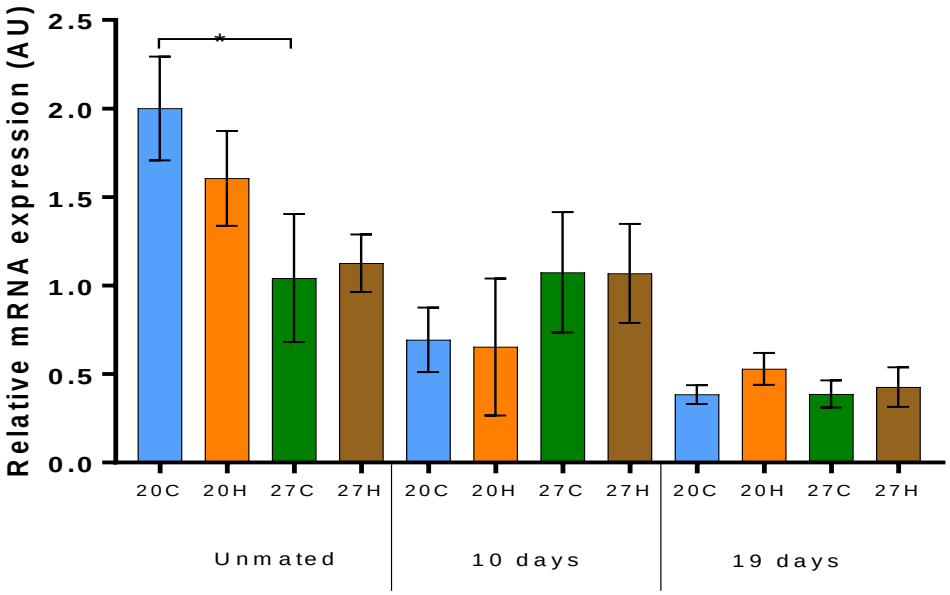


Figure 4.7: The effect of housing temperature and diet on the relative mRNA expression of UCP1 gene in interscapular BAT at the three time points.

Days: number of days of gestation. The number 20 and 27 denote the temperature in degrees Celsius. H: HFHS diet and C: control diet. In the unmated group 20C, 20H, and 20C (*n* = 6), 27C (*n* = 5). In the 10-day gestation 20C (*n* = 6) and 27H, 20H, 27C and 20H (*n* = 7). In the 19-day gestation group, 20C, 27C and 27H (*n* = 6) and 20H (*n* = 8). The gene expression was normalized against TBP/YWHAS to produce the relative expression. The values are mean ± standard error of mean. The superscripts indicate statistical significance ($p < 0.05$). * = $p < 0.05$. For statistical analysis: Two-way ANOVA test was conducted for normally distributed data and the Mann-Whitney test was used for the non-parametric data with fisher LSD post-hoc comparison (20C v 20H, 27C v 27H, 20C v 27C, 20H v 27H) within each of the three the three time points.

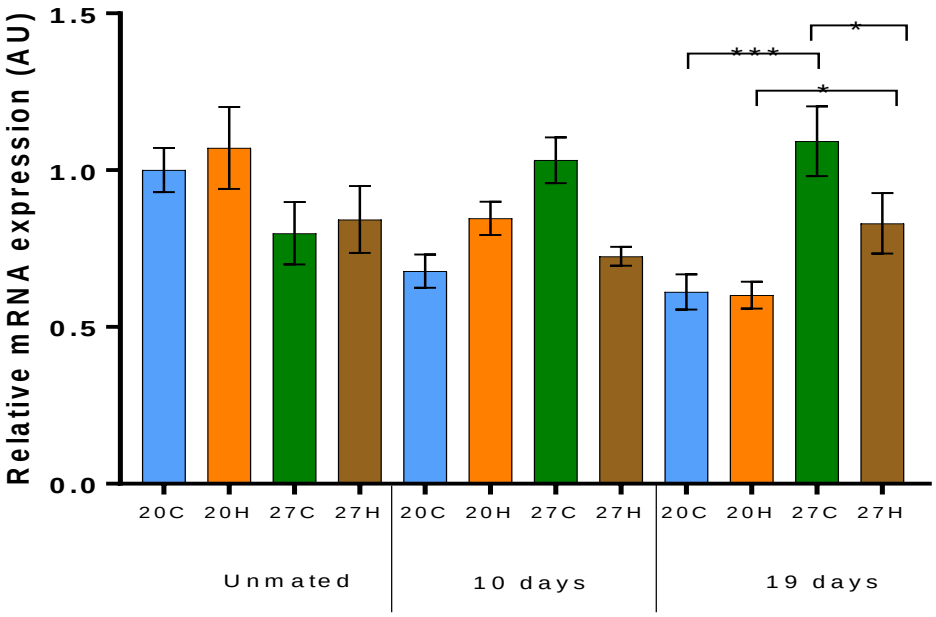


Figure 4.8: The effect of housing temperature and diet on the relative mRNA expression *PPARγ* gene in interscapular BAT at the three time points.

Days: number of days of gestation. The number 20 and 27 denote the temperature in degrees Celsius. H: HFHS diet and C: control diet. In the unmated group 20C, 20H, and 20C (*n* = 6), 27C (*n* = 5). In the 10-day gestation 20C (*n* = 6) and 27H, 20H, 27C and 20H (*n* = 7). In the 19-day gestation group, 20C, 27C and 27H (*n* = 6) and 20H (*n* = 8). The gene expression was normalized against TBP/YWHAS to produce the relative expression. The values are mean ± standard error of mean. The superscripts indicate statistical significance ($p < 0.05$). * = $p < 0.05$, *** = $p \leq 0.001$. For statistical analysis: Two-way ANOVA test was conducted for normally distributed data and the Mann-Whitney test was used for the non-parametric data with fisher LSD post-hoc comparison (20C v 20H, 27C v 27H, 20C v 27C, 20H v 27H) within each of the three the three time points.

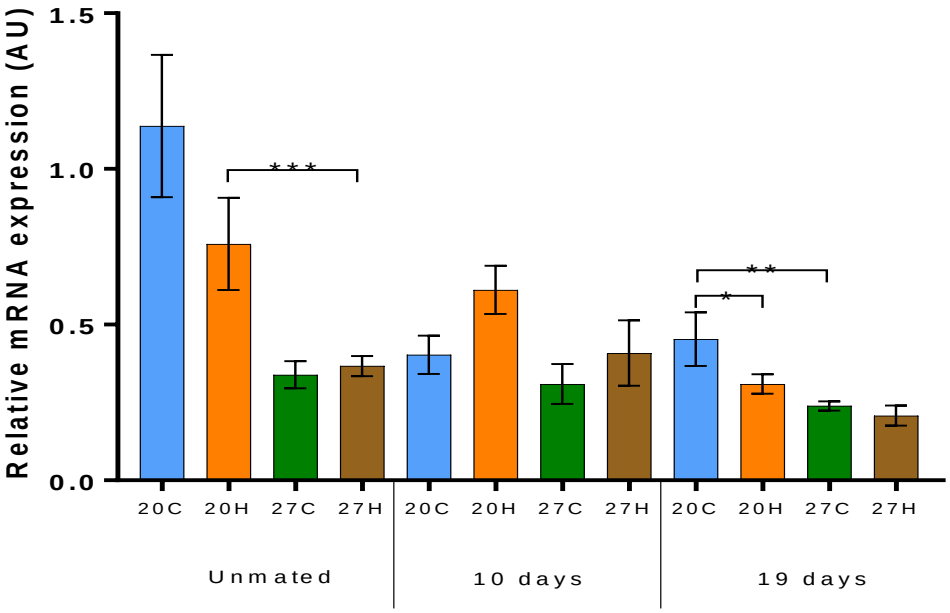


Figure 4.9: The effect of housing temperature and diet on the relative mRNA expression of *PGC1α* gene in interscapular BAT at the three time points.

Days: number of days of gestation. The number 20 and 27 denote the temperature in degrees Celsius. H: HFHS diet and C: control diet. In the unmated group 20C, 20H, and 20C (*n* = 6), 27C (*n* = 5). In the 10-day gestation 20C (*n* = 6) and 27H, 20H, 27C and 20H (*n* = 7). In the 19-day gestation group, 20C, 27C and 27H (*n* = 6) and 20H (*n* = 8). The gene expression was normalized against TBP/YWHAS to produce the relative expression. The values are mean ± standard error of mean. The superscripts indicate statistical significance ($p < 0.05$). * = $p < 0.05$, ** = $p \leq 0.01$ and *** = $p \leq 0.001$. For statistical analysis: Two-way ANOVA test was conducted for normally distributed data and the Mann-Whitney test was used for the non-parametric data with fisher LSD post-hoc comparison (20C v 20H, 27C v 27H, 20C v 27C, 20H v 27H) within each of the three the three time points.

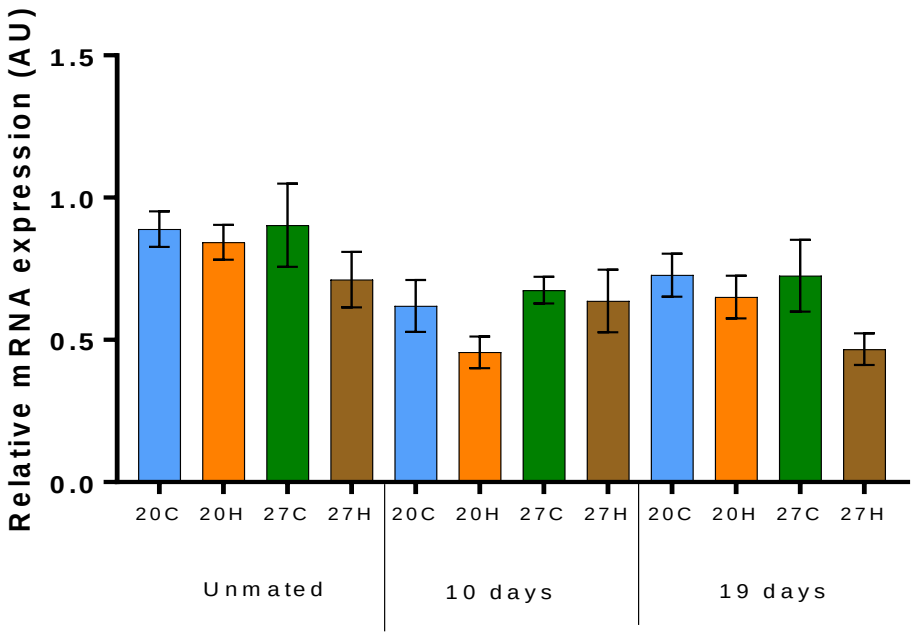


Figure 4.10: The effect of housing temperature and diet on the relative mRNA expression of β_3-ARs gene in interscapular BAT at the three time points.

Days: number of days of gestation. The number 20 and 27 denote the temperature in degrees Celsius. H: HFHS diet and C: control diet. In the unmated group 20C, 20H, and 20C (*n* = 6), 27C (*n* = 5). In the 10-day gestation 20C (*n* = 6) and 27H, 20H, 27C and 20H (*n* = 7). In the 19-day gestation group, 20C, 27C and 27H (*n* = 6) and 20H (*n* = 8). The gene expression was normalized against TBP/YWHAS to produce the relative expression. The values are mean ± standard error of mean. For statistical analysis: Two-way ANOVA test was conducted for normally distributed data and the Mann-Whitney test was used for the non-parametric data with fisher LSD post-hoc comparison (20C v 20H, 27C v 27H, 20C v 27C, 20H v 27H) within each of the three the three time points.

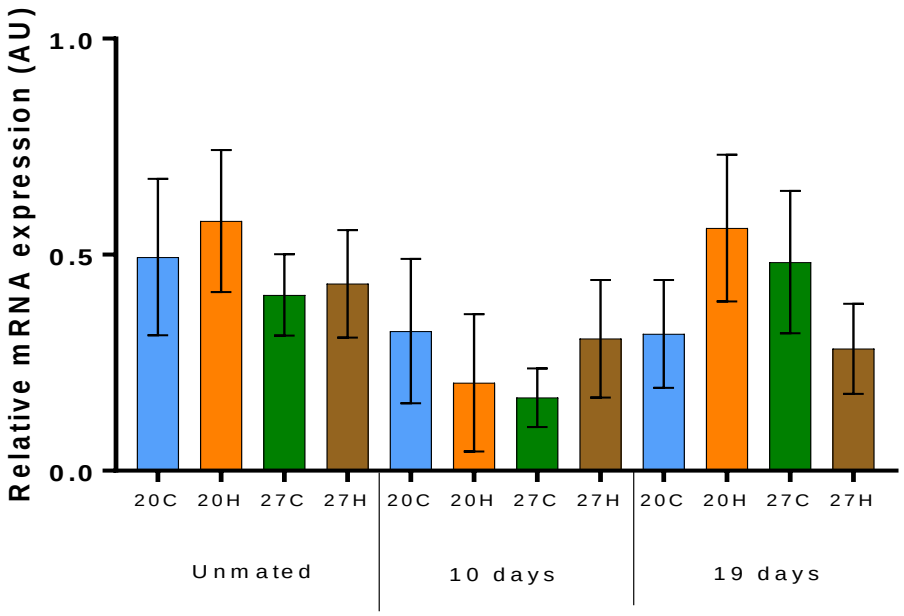


Figure 4.11: The effect of housing temperature and diet on the relative mRNA expression of *SERCA2b* gene in interscapular BAT at the three time points.

Days: number of days of gestation. The number 20 and 27 denote the temperature in degrees Celsius. H: HFHS diet and C: control diet. In the unmated group 20C, 20H, and 20C (*n* = 6), 27C (*n* = 5). In the 10-day gestation 20C (*n* = 6) and 27H, 20H, 27C and 20H (*n* = 7). In the 19-day gestation group, 20C, 27C and 27H (*n* = 6) and 20H (*n* = 8). The gene expression was normalized against TBP/YWHAS to produce the relative expression. The values are mean ± standard error of mean. For statistical analysis: Two-way ANOVA test was conducted for normally distributed data and the Mann-Whitney test was used for the non-parametric data with fisher LSD post-hoc comparison (20C v 20H, 27C v 27H, 20C v 27C, 20H v 27H) within each of the three the three time points.

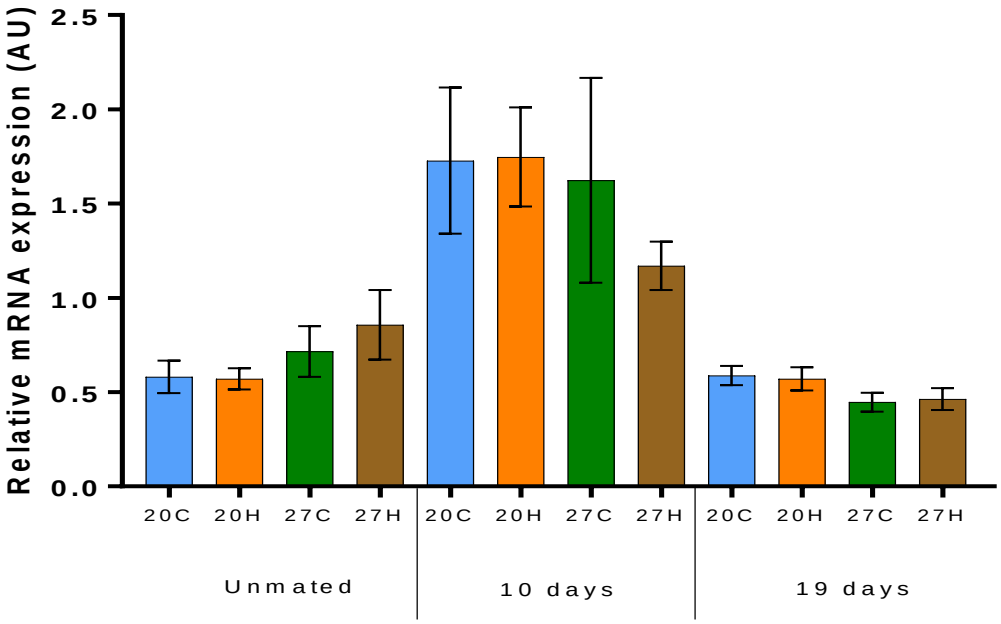


Figure 4.12: The effect of housing temperature and diet on the relative mRNA expression of *TRPV1* gene in interscapular BAT at the three time points.

Days: number of days of gestation. The number 20 and 27 denote the temperature in degrees Celsius. H: HFHS diet and C: control diet. In the unmated group 20C, 20H, and 20C (*n* = 6), 27C (*n* = 5). In the 10-day gestation 20C (*n* = 6) and 27H, 20H, 27C and 20H (*n* = 7). In the 19-day gestation group, 20C, 27C and 27H (*n* = 6) and 20H (*n* = 8). The gene expression was normalized against TBP/YWHAS to produce the relative expression.The values are mean ± standard error of mean. For statistical analysis: Two-way ANOVA test was conducted for normally distributed data and the Mann-Whitney test was used for the non-parametric data with fisher LSD post-hoc comparison (20C v 20H, 27C v 27H, 20C v 27C, 20H v 27H) within each of the three the three time points.

4.3.2.2 Identification of an energy-sensing gene in interscapular BAT

To identify an energy-sensing gene (leptin) was measured in the interscapular BAT. The relative mRNA expression of *leptin* decreased only in the animals housed under standard housing temperature conditions and fed HFHS diet before pre- and mid-gestation points (Figure 4.13).

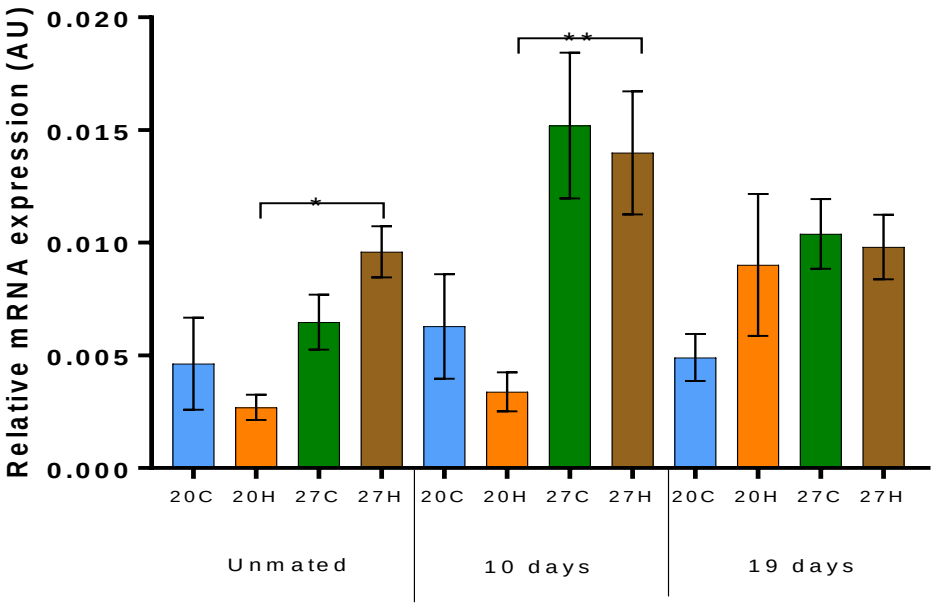


Figure 4.13: The effect of housing temperature and diet on the relative mRNA expression of *leptin gene* in interscapular BAT at the three time points.

Days: number of days of gestation. The number 20 and 27 denote the temperature in degrees Celsius. H: HFHS diet and C: control diet. In the unmated group 20C, 20H, and 20C (*n* = 6), 27C (*n* = 5). In the 10-day gestation 20C (*n* = 6) and 27H, 20H, 27C and 20H (*n* = 7). In the 19-day gestation group, 20C, 27C and 27H (*n* = 6) and 20H (*n* = 8). The gene expression was normalized against TBP/YWHAS to produce the relative expression. The values are mean ± standard error of mean. The superscripts indicate statistical significance ($p < 0.05$). * = $p < 0.05$ and ** = $p \leq 0.01$. For statistical analysis: Two-way ANOVA test was conducted for normally distributed data and the Mann-Whitney test was used for the non-parametric data with fisher LSD post-hoc comparison (20C v 20H, 27C v 27H, 20C v 27C, 20H v 27H) within each of the three the three time points.

4.3.2.3 Fat transporter gene in interscapular BAT

In response to the control diet, the animals housed under thermoneutral temperature conditions showed an increase in *ATGL* mRNA expression pre-gestation. However, in the late gestational period, under standard housing temperature conditions, the mRNA expression of *ATGL* decreased in the animals fed the control diet and increased in those fed the control diet and housed at thermoneutral temperature condition (Fig. 4.14).

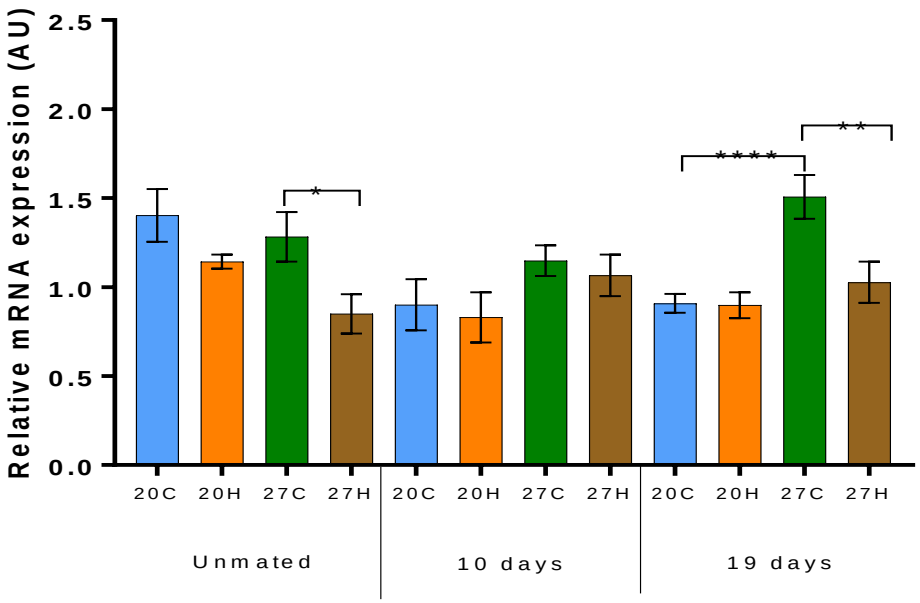


Figure 4.14: The effect of housing temperature and diet on the relative mRNA expression of *ATGL* gene in the interscapular BAT at the three time points.

Days: number of days of gestation. The number 20 and 27 denote the temperature in degrees Celsius. H: HFHS diet and C: control diet. In the unmated group 20C, 20H, and 20C (*n* = 6), 27C (*n* = 5). In the 10-day gestation 20C (*n* = 6) and 27H, 20H, 27C and 20H (*n* = 7). In the 19-day gestation group, 20C, 27C and 27H (*n* = 6) and 20H (*n* = 8). The gene expression was normalized against TBP/YWHAS to produce the relative expression. The values are mean ± standard error of mean. The superscripts indicate statistical significance ($p < 0.05$). * = $p < 0.05$ ** = $p \leq 0.01$ and **** = $p \leq 0.0001$. For statistical analysis: Two-way ANOVA test was conducted for normally distributed data and the Mann-Whitney test was used for the non-parametric data with fisher LSD post-hoc comparison (20C v 20H, 27C v 27H, 20C v 27C, 20H v 27H) within each of the three the three time points.

4.4 Discussion

4.4.1 The effect of the housing temperature and the HFHS on the interscapular BAT phenotype

In this study, the standard housing temperature increased mitochondrial UCP1 abundance in interscapular BAT before and at mid-gestational period. A previous study detected the activation of BAT in animals housed at a temperature below thermoneutrality, (i.e., 27± 1°C °C) for rat (Golozoubova et al., 2004, Rosell et al., 2014). At sub-thermoneutrality, as under standard housing temperature, thermogenesis is required to prevent excessive heat loss (Cannon and Nedergaard, 2004). Mitochondria play an important role in BAT through UCP1-mediated thermogenesis. The standard housing temperature activates sympathetic signalling in BAT, which generates heat by utilising glucose and free FAs (FFAs) using UCP1 (Cannon and Nedergaard, 2004, Fischer et al., 2018). BAT is recognisable by signature phenotypic features, multilocular UCP1 expression and the distinctive brownish colour associated with the iron content of its mitochondria (Golozoubova et al., 2001, Nedergaard et al., 2001, Golozoubova et al., 2006). In this study, when the thermal challenge was eliminated (i.e., under thermoneutral temperature conditions), the abundance of UCP1 declined, as BAT UCP1 abundance declined (Cannon and Nedergaard, 2004). Furthermore, in the present study, the abundance of UCP1 increased in the animals fed the HFHS diet, which provided more FFAs to replenish TGs, which were then utilised in thermogenesis. In a previous study, UCP1-ablation had a dramatic effect on mice, resulting in weight gain and increased fat mass, neither of which was related to an

increase in energy intake (Feldmann et al., 2009). In this study, the mitochondrial UCP1 was not reduced during gestation unlike what was reported in previous studies. A recent mice study reported decreased UCP1 protein but this finding was based on a single IHC slide, without any UCP1 quantification (McIlvride et al., 2017). Furthermore, the same study suggested that gestation decreased thermogenic response, but this was only measured in terminally anaesthetized mice and could be a confounding effect. If there were any decrease in the mitochondrial content during gestation, it could be an indication of decreased mitochondrial biogenesis, which is responsible for the subsequent decrease in the thermogenic response (Frontera et al., 2005).

In general, adipocyte growth mechanisms include hypertrophy (i.e., an increase in cell size) and hyperplasia (i.e., an increase in cell number), with the latter occurring when stored TG exceed the current adipocyte capacity (Reynisdottir et al., 1994, Kaartinen et al., 1995). In response to insulin, existing adipocytes utilise and convert glucose into lipids and store it for later use (Haczeyni et al., 2018). Another reason for adipocytes hypertrophy is adipocytes dysfunction, which may recognised as increased number of hypertrophic adipocytes that is associated with stress signals, chronic inflammation, degeneration of small adipocytes and immune cell recruitment (Haczeyni et al., 2018). Moreover, adipocyte hypertrophy result in reduces adiponectin, which reduces adipocytes hyperplasia (Haczeyni et al., 2018). Both, hypertrophy and hyperplasia are the result of a positive energy balance (Reynisdottir et al., 1994, Kaartinen et al., 1995). In the present study, the adipocyte area increased in the animals housed under

standard housing temperature conditions and decreased under thermoneutral temperature conditions. As white adipose tissue serves as a source of energy storage for mammals, when energy demands cannot be met by circulating fuel, lipolysis mobilise TGs into glycerol and NEFAs, with the latter process regulated by the SNS (Landsberg, 1992, Nonogaki, 2000). Although TGs stored in adipocytes are critical for thermogenesis, previous studies suggested that BAT used glucose and NEFAs in the circulatory system to BAT to restore as a TG rather than using them directly in thermogenesis (Cannon and Nedergaard, 2004, Labbé et al., 2015, Irshad et al., 2017). In response to cold, activation of thermogenesis cascade activate TG hydrolysis to release FFA, which then be used in the mitochondria with the UCP1 in producing heat (respiration) rather than oxidative phosphorylation (Cannon and Nedergaard, 2004). Research also indicated that SNS activity may be inhibiting the stimulation of adipocyte proliferation of α_2-adrenoceptor, which produce a selective stimulation of pre-adipocytes proliferation (Bouloumie et al., 1994, Valet et al., 1998). As lipid stores increase and fat cells enlarge, the number of α_2-adrenoceptor increase, which induces fat cell proliferation (Valet et al., 1998, Bowers et al., 2004, Rooks et al., 2005, Harris, 2012). This finding was consistent with that of an earlier study that reported that denervation-induced an increased in α_2-adrenoceptors and subsequently, fat cells number (Cousin et al., 1993). Furthermore, studies reported that mild cold exposure decreased leptin levels, which stimulates appetite and increases energy intake (Bing et al., 1998, Langeveld et al., 2016), thereby resulting in increased lipid deposition and an increase in adipocyte area.

In this study, although the number of white adipocytes increased in the interscapular area in the animals fed the control diet prior to gestation, they showed a trend towards decreased adipocytes area. Hyperplasia is not only stimulated by exceeding the capacity of existing adipocytes but also by adipogenesis recruiting adipocyte progenitors, which proliferate and differentiate into small early differentiated adipocytes (Faust et al., 1978, de Ferranti and Mozaffarian, 2008, Tchoukalova et al., 2010, Cawthorn et al., 2012a, Cawthorn et al., 2012b). In this study, under thermoneutral temperature conditions, the adipocytes number increased, this could be from the downregulation of the SNS as there is an absence of thermal challenge, thereby, resulting in an increase in the number of adipocytes, this finding is in agreement with that of another study (Cui et al., 2016). Similarly, 11 weeks old hamsters were exposed to unilateral denervation of the inguinal depot (i.e., a subcutaneous adipose fat pad located in the lower abdominal wall), in hamsters increased the adipocyte hyperplasia by 250%, fat pad mass 200% as compared with that in contralateral intact depot (Youngstrom and Bartness, 1998). These changes were accompanied by 80% decrease in NE which support the role of SNS innervation in WAT (Youngstrom and Bartness, 1998).

In the present study, under standard housing temperature conditions, the adipocyte number decreased, it could be as a result of inhibition of the adipocytes proliferation stimulation mediated by the SNS activity, these results are in agreement with those of other studies (Cousin et al., 1993, Youngstrom and Bartness, 1998). Cousin et al. (1993) reported that the number of fat cells markedly increased following denervation of the

retroperitoneal (i.e., visceral fat) depot in rats. Another study found that noradrenalin at the postganglionic SNS-transmitter was decreased by 80% in the denervated depot as compared to the ones with intact sympathetic innervation, these findings suggest that the SNS inhibits adipocyte hyperplasia (Jones et al., 1992). Consistent with the finding of the present study, a previous study suggested that NE activation of β_1-ARs inhibited the proliferation of pre-adipocyte (Schneider et al., 2018).

Overall, the findings in the present study, demonstrate a trend towards a decreased in the number of adipocytes throughout the gestational period in the animals housed under standard housing temperature conditions. To my knowledge, no other studies have reported similar results. Other studies reported increased adiposity as pregnancy progressed (Lopez-Luna et al., 1991, Herrera, 2000, Crew et al., 2018). A previous study in rodents found that leptin increased the fat mass, which resulted in increased adipocyte differentiation via an increase in LPL activity (Machinal-Quelin et al., 2002). Adipose tissue mass is consist of the adipocytes size and number, thus, the association with circulating leptin with the fat pad mass (Zhang et al., 2002). A pervious study found a strong correlation between leptin mRNA level and adipocytes volume in three depots (inguinal, epididymial and retroperitoneal) (Zhang et al., 2002). This correlation is in agreement with the suggestion that leptin production by adipocytes can reflect their volume (Zhang et al., 2002). Such changes (i.e., decrease adipocyte number) might occur in adipocyte under the standard housing temperature conditions, as these present a cold challenge to dams and it is known that LPL activity

decreased in rat gestation (Otway and Robinson, 1968), thus reduced adipocyte proliferation.

4.4.2 The effect of the housing temperature and HFHS diet on the interscapular BAT genotype

In the present study, the mRNA expression of *UCP1* increased under the standard housing temperature conditions. As reported earlier, these conditions represent a considerable cold challenge (Maloney et al., 2014, Fischer et al., 2018, Symonds et al., 2018, L Small, 2018). The standard housing temperature required energy expenditure by mitochondrial UCP1 in thermogenesis (Cannon and Nedergaard, 2004). BAT is heavily innervated by the SNS, which releases NE, that binds to β_3-ARs on the brown adipocytes. The activation of this receptor stimulates the thermogenesis cascade through mitochondrial UCP1 (Cannon and Nedergaard, 2004).

The difference between UCP1 protein abundance and mRNA expression has not been clearly discussed in literature. The protein expression is generally considered to be a function of mRNA expression (Guo et al., 2008). However, at a given time point the availability of both mRNA and protein abundance depends on their life and stability on cellular environment (Hargrove and Schmidt, 1989). Previous study have proposed that protein is more stable than mRNA in most tissue and this was specifically observed in UCP1 mRNA that was degraded at a faster rate than UCP1 proteins (Gospodarska et al., 2015).

In this study, the relative mRNA expression of *PGC1α* gene increased in interscapular BAT in the dams housed under standard housing temperature

conditions. Previous studies demonstrated that in response to cold or FFAs availability, SNS released NE, which act upon β-ARs that function is direct regulators to *PGC1α* expression and activity (Cederberg et al., 2001, Cao et al., 2004). Following the activation of PGC1α by SNS and PGC1α phosphorylation (Cao et al., 2004), the activated *PGC1α* regulated thermogenesis via interactions with PPARα and PPARγ (Puigserver et al., 1998, Hondares et al., 2006, Wulf et al., 2008). With the cooperation of PPARγ, PGC1α induced *UCP1* gene transcription (Puigserver et al., 1998). Mice with deleted PGC1α showed an impaired cold-induced thermogenesis due to the inability to activate thermogenesis genes (Lin et al., 2004). However, in a gain of function experiment, PGC1α expression in WAT induced a variety of genes including *UCP1*, involved in mitochondrial thermogenesis, thereby emphasising the central role of PGC1α in the biological regulation of mitochondria thermogenesis (Lindgren et al., 2004, Austin and St-Pierre, 2012, Satyanarayana, 2016).

The present study showed a trend towards decreased the relative mRNA expression of *PPARγ* under the standard housing temperature conditions and in the late gestational period in the animals fed the control diet. SNS represses the effect on PPARγ expression in brown adipocyte mediated by β-ARs (Lindgren et al., 2004). The effect of NE was observed in both undifferentiated pre-adipocytes that express β_1-ARs and mature brown adipocytes β_3-ARs, with both types of receptors mediating the inhibitory effect (Lindgren et al., 2004).

The current study showed a trend towards increased the relative *ATGL* expression pre- and late-gestational period in the animals fed the control

diet. A previous research demonstrated that dietary and hormonal regulators, such as fasting, insulin and glucocorticoid regulated the ATGL expression (Zimmermann et al., 2004). Fasting increased ATGL expression, whereas feeding and elevated insulin level decreased it (Kershaw et al., 2006). In periods of increased energy demands, ATGL induces the first step of hydrolysing TGs and FFA release (Osuga et al., 2000, Zimmermann et al., 2004). In a previous study, fat storage was increased in several tissues, such as adipose tissue and skeletal muscle, in ATGL-knocked-out mice (Haemmerle et al., 2006). In this study, the rats housed under thermoneutral temperature conditions and fed the control diet, paradoxically, exhibited signs (i.e., excessive movement) of what could viewed as stereotypical distress behaviour (Dawkins, 2011). A possible explanation for the excessive movement is increased sensory motor output, especially that the cage was standard without an exercise wheel or any other stimuli (Dantzer, 1986, Sherwin, 1998). Moreover, a possible increase in stress hormones, such as glucocorticoid could have up-regulated ATGL expression in adipocytes (Xu et al., 2009).

In the present study, in the late gestational period, *ATGL* relative expression was decreased in the animals housed under standard housing temperature conditions. These results are with disagreement of a previous study that reported cold exposure activated ATGL to breakdown TG for thermogenesis (Zechner et al., 2012). However, a recent study reported that ATGL is not critical in BAT thermogenesis and its absence impaired BAT lipolysis yet it did not affect β_3-AR response to cold exposure (Schreiber et al., 2017). Other explanation is rat late gestational period

showed reduced LPL activity and thus, decrease fat uptake from adipose tissue during late gestation, similar explanation was reported in earlier studies (Otway and Robinson, 1968, Herrera et al., 1988, Galan et al., 1994). Such a change correlate to a decrease in the activity of the enzyme in the adipose tissue (Martin-Hidalgo et al., 1994). Therefore, the anabolic condition present in adipose tissue during early gestation switches to catabolic condition during late gestation which coincident with maximal fetal growth (Herrera and Ortega-Senovilla, 2010). The mRNA expression of ATGL should be increased with standard house temperature and its level may be by the pregnancy itself as it acts as a modulatory factor. Previous studies reported the mRNA expression of ATGL mRNA decreased with obesity (Reynisdottir et al., 1994, Large et al., 1999, Lofgren et al., 2002, Viguerie et al., 2005, Jocken et al., 2007). Other studies suggested that genetic variation of ATGL is associated with obesity and type 2 diabetes mellitus (Klannemark et al., 1998, Schoenborn et al., 2006).

In this study, *leptin* relative mRNA expression showed a trend towards decreased expression in the animals housed under standard housing temperature prior to gestation and in the mid-gestational period. Earlier studies reported supressed leptin expression with cold exposure in mice (Trayhurn et al., 1995, Evans et al., 1999). This may be result from the cold induced increased in SNS activity (Puerta et al., 2002). Previous research on rodent demonstrated that the administration of catecholamines and β-AR agonist mimic the effect of cold exposure and subsequently reduced leptin expression in WAT these was mediated through β_3-ARs (Giacobino, 1996, Mantzoros et al., 1996, Trayhurn P, 1998). Although leptin acts

centrally to regulate energy balance and core body temperature, it was reported that leptin or leptin receptor deficient mice showed increased feeding and obesity (McLaughlin and Baile, 1981, Alingh Prins et al., 1986), as well as decreased energy expenditure and core body temperature (Trayhurn et al., 1977, Trayhurn, 1979). Cold exposure enable utilising a substantial amount of energy by lipolysis and thermogenesis. In addition, food intake increases gradually with prolonged cold exposure, which has an inhibitory effect of leptin synthesis and consequently increase intake (Trayhurn P, 1998, Cannon and Nedergaard, 2004). Studies reported that surgically denervated BAT in rodents prevented leptin-induced increases mitochondrial UCP1 (Scarpace and Matheny, 1998). Despite losing their ability to energy expenditure, leptin-deficient mice were not able to maintain their core body temperature under either thermoneutral or cold temperatures (Kaiyala et al., 2016). Leptin replacement in leptin-deficient mice corrected hypothermia (Kaiyala et al., 2016).

In the present study, *TRPV1* mRNA expression in interscapular BAT did not show any differences with the diet or the housing temperature. Nevertheless, it showed a trend towards increased expression in the mid-gestational period, regardless of the dietary intervention. It was reported that TRPV1 is expressed in chorioallantoic placenta in the mid-gestational period in rats and decreases as the pregnancy progresses (Cella et al., 2008, Fonseca et al., 2012).

In the present study, the thermogenic capacity was confirmed by the *UCP1* mRNA expression and the mitochondrial UCP1 abundance. Paradoxically, the mRNA expression of β_3-ARs was not significantly increased under

standard housing temperature conditions. This result is in contrast to that reported elsewhere (Silva, 2005). The discord in the result could be explained by the effect of the housing temperature on the mRNA expression of β_3-ARs. Despite the lack of any effect on the expression of β_3-ARs, the housing temperature may have affected the expression of other types of β-ARs, such as β_1-ARs. The latter may have played a role in lipolysis and thermogenesis. Previous studies supported this idea (Atgie et al., 1997, Rohrer, 1998). A study reported that β_1-AR knockout mice exposed to cold failed to maintain their core body temperature, expressed severe metabolic syndrome in response to high fat diet and pale BAT in histology (Ueta et al., 2012). Another study reported that overexpression of β_1-ARs on adipose tissue played a role in obesity resistance by decreasing lipid accumulation and increasing brite adipocytes (Soloveva et al., 1997).

In this study, as expected, the mRNA expression of *SERCA2b* was unchanged in response to the temperature or dietary interventions in the interscapular BAT. Thus, the presented study found no UCP1-independent thermogenesis in interscapular BAT. To my knowledge, SERCA2B was only investigated among brite adipocytes and never in BAT (Ikeda et al., 2017).

4.5 Conclusions

In rats housed under standard housing temperature representing a cold challenge, phenotypic and genotypic changes occurred that were most likely stimulated by SNS activity. The expression of BAT markers, such as *UCP1* and *PGC1α*, was reduced in the gestational period may be to enable fetal growth and ensure fuel for the dams. These results suggest that the

standard temperature conditions under which rats are housed in research studies do not represent thermoneutral temperature conditions in humans and that this might have consequences for the results of metabolic research.

Chapter 5 – Conclusion

5.1 General aims

This thesis aimed to determine whether standard housing temperature and the high-fat and high-sucrose diet (HFHS) modify the mitochondrial uncoupling protein 1 (UCP1) abundance, mRNA expression of thermogenic-related genes and plasma metabolites in the interscapular brown adipose tissue (BAT) during gestation in rats. This was achieved by assessing the total body weight (TBW), adipose tissue depots weight, plasma metabolites and UCP1 abundance in histological sections. Furthermore, this thesis examined BAT-related genes by measuring their mRNA expression in the interscapular depot. This chapter summarises the key findings and limitations.

5.2 Main methods

Four-week old female rats were fed either a control diet or an obesity-inducing diet (i.e., HFHS). Each of the groups (pre-gestation, 10 and 19-days gestation) were housed in either standard housing temperature (20°C) conditions or thermoneutral temperature (27°C) conditions. The intervention was maintained for six-weeks among all groups; following this, the animals in one group (pre-gestation) were euthanized. The two other animal groups (10 and 19-days gestation) were mated with males of the same intervention conditions. Day one of gestation was indicated by the presence of operculum in the morning. Subsequent to this, the interventions

were maintained and the animals were then euthanized at either 10 or 19-days gestation. Tissue and blood samples were obtained from the three groups. The tissues were processed, sectioned and stained using immunohistochemistry (IHC) to measure the mitochondrial UCP1 abundance. The mRNA expression of the BAT and thermogenesis related genes were also measured. Finally, plasma metabolites were measured to obtain information about BAT metabolism.

5.3 Summary of findings

A summary of the hypotheses, methods and main results are shown in Figure 5.1.

5.3.1 The HFHS diet increased TBW and adiposity

In agreement with previous studies, the present results revealed HFHS diet increased total body weight and adiposity during gestation publications (Murase et al., 2001, Sato et al., 2010, Yang et al., 2012, Cuthbert et al., 2017). In both pre- and intra-gestation groups. Neither diet nor temperature affected BAT mass prior to gestation, however, during gestation, BAT mass was increased by both HFHS diet and standard housing temperature conditions (20°C). Previous studies reported similar results with cold exposure (Bukowiecki et al., 1982, Chondronikola et al., 2016) and with high-fat diet and high-carbohydrate diet (Kanarek and Orthen-Gambill, 1982, Saxton and Eisen, 1984).

5.3.2 Modest effect of HFHS diet and housing temperature on plasma metabolites

Several plasma metabolites were analysed for this study; only modest changes were shown. In late gestation, fasting non-esterified fatty acid (NEFA) levels increased with HFHS diet. An inverse effect of thermoneutral temperature was seen in the pre-gestation group; it increased fasting plasma glucose level, without parallel increase in insulin level. Neither diet nor temperature affected fasting plasma triglycerides (TGs) or insulin levels before or during gestation.

5.3.3 Standard housing temperature modified BAT thermogenic capacity

The mitochondrial UCP1 abundance increased under standard housing temperature conditions before gestation. The mRNA expression of *UCP1* followed a similar pattern. Mid-gestation increased UCP1 abundance under standard housing temperature conditions.

Genes associated with BAT thermogenic capacity showed the expected changes. The mRNA expression of the proximal proliferator-activated receptor (*PPARγ*) modulated only late gestation groups. Further, standard housing temperature decreased the mRNA expression, while the control diet increased the expression. The mRNA expression of the PPARγ coactivator (*PGC1α*) increased under standard housing temperature conditions in pre- and late-gestation groups. Unexpectedly, beta-3 adrenergic receptors (*β3-ARs*) were not modified with any of the interventions at any time point. The expression pattern of the BAT

associated genes suggested that standard housing temperatures stimulate BAT thermogenic capacity.

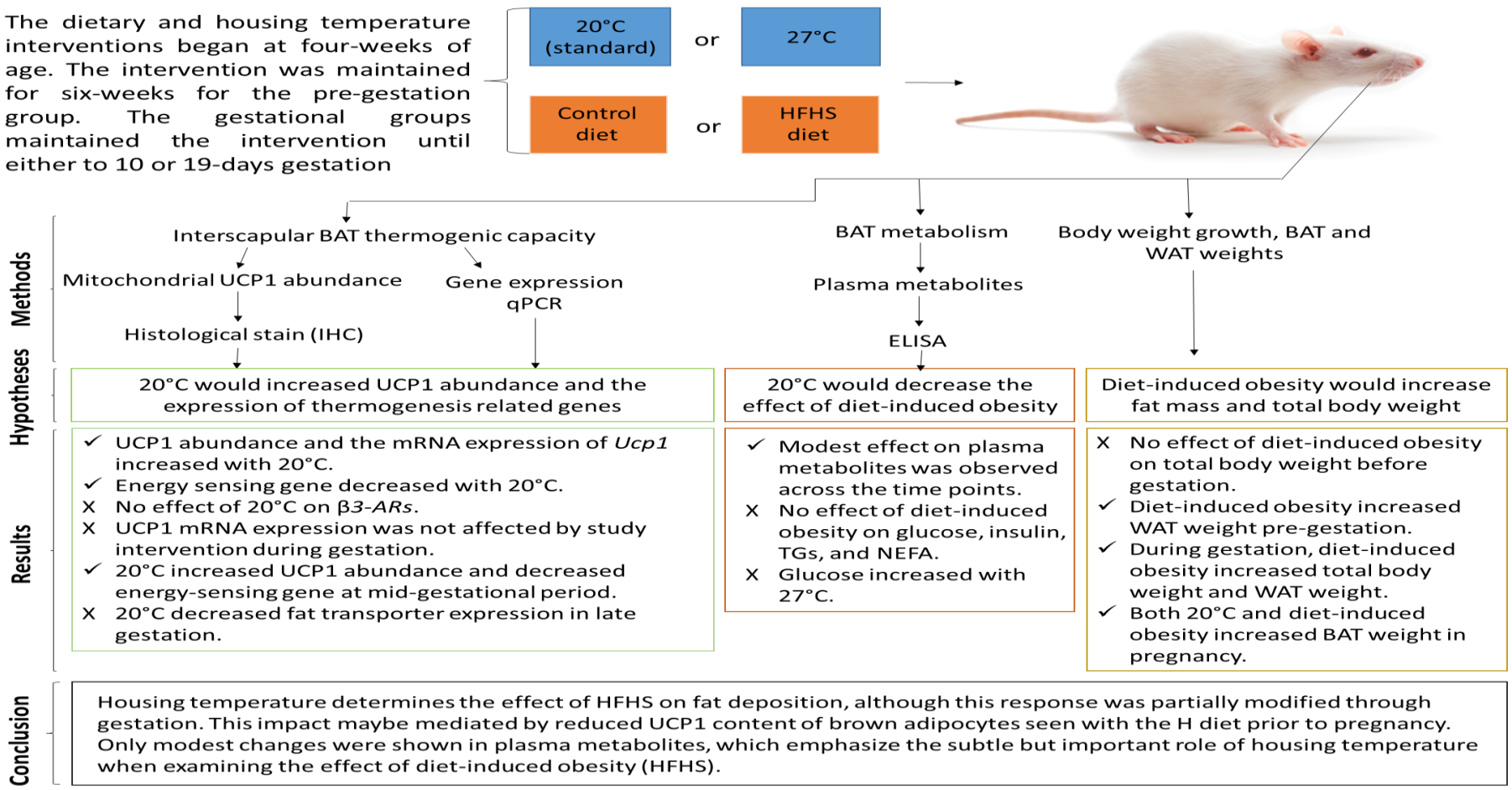


Figure 5.1: Summary of hypotheses, methods, and main results.

Female rats were sampled pre-gestation and at 10 and 19-days of gestation. IHC= immunohistochemistry, qPCR= quantitative polymerase chain reaction and, ELISA= enzyme linked immune assay. Marks indicate whether the hypothesis has been supported (✓) or unsupported (X).

5.4 Study limitations

5.4.1 Rats as a model for human

Despite the rat being considered a good model for the human as described in Chapter 1 (Section 1.4), rats have some differences that could alter research outcomes. While it is simple to manipulate and evaluate the specific dietary composition provided to rats, this likely does not reflect the heterogeneity of human diets or the level of exposure to a physiologically relevant experimental diet (McMullen and Mostyn, 2009). A cafeteria diet partially overcomes these issues, as it is considered to be a more robust model for diet-induced obesity in human subjects. This diet includes 53% of the energy derived from fat and 39% derived from carbohydrates, including foods such as cookies, cereals, cheese, processed meat, chips and crackers (Rothwell and Stock, 1979a, Shafat et al., 2009, Sampey et al., 2011). However, the current study utilised a moderate fat content HFHS diet with 39% of the energy derived from fat (i.e., lard) to enable detection of housing temperature effects. Of note, the difference in housing temperature between the standard and thermoneutral temperatures was only 7°C.

Rats are born immature after a short gestation with an underdeveloped central nervous system and autocrine system. The development of some organs, such as the pancreas, are underdeveloped as compared to larger mammals and humans and they continue to develop in postnatal life (McMullen and Mostyn, 2009). Furthermore, a large litter size poses a major disadvantage in of working with a rat model in prenatal programming studies. The space shared within the uterus results in some differences in

the development environment. For example, rat pups developed at the cervical end of the uterus receive more nutrient rich maternal blood and are born at a heavier weight than their littermates (Ryan and Vandenbergh, 2002, McMullen and Mostyn, 2009). The litter position within the uterus may be also influenced by exposing the foetus to different levels of hormones depending on whether it is positioned next to a male or female (vom Saal et al., 1990). These exposures may cause differences in the phenotype of the pups within a litter (McMullen and Mostyn, 2009).

5.4.2 Challenges in measuring food intake

Rats had unrestricted access to food and water until shortly before euthanasia. The availability of food intake data would enable investigating the relationship between food intake, TBW, adiposity, plasma metabolites, and leptin expression. However, the researchers who conducted the animal study reported food intake measurement consumed a considerable amount of time. Measuring the food intake was reported to be time intensive and exhausting, especially as this measurement included sifting the food from the cage bedding and weighing the food from each cage twice weekly. This became even more challenging during the mating period as female rats did not become pregnant on the same day (i.e. approximately range of 4 days). despite these challenges, food measurements was still partially done for the first cohort of the animal study for the pre-gestation group only.

5.4.3 Limitations of laboratory techniques and power calculation

Although IHC is a relatively simple technique, lack of experience may affect the results. Several trials are commonly needed to determine the appropriate antibody to diluent ratio to produce a clear stained section

without unwanted background stain. To reduce error, this study used the semi-automated BOND-MAX slide processor and secondary antibody as a detection system (Brigati et al., 1988) (as detailed in Chapter 2, Section 2.3.3.2).

This study measured mitochondrial UCP1 in histological sections using IHC and mRNA gene expression. Though these results could be complemented with other UCP1 measures, such as assessing energy expenditure with the housing temperatures by respirometry (i.e., O_2 and CO_2 consumption) and UCP1 tissue protein by immunoblotting (L Small, 2018), there was, unfortunately, insufficient remaining tissue.

Similarly, as plasma inulin was measured in the female rodent, there was insufficient remaining serum samples from the 19-days gestation group to be utilised in an insulin assay. Therefore, the sample number was lower in this group. Omission of samples may reduce the test's reliability, therefore, potentially reducing the statistical significance of the analysis obtained.

Noteworthy, with the study sample size of six rats per group the power is 85%. The power was calculated for UCP1 and may not for the other endpoints in this study such as adiposity and mRNA levels. Therefore, this might reflects the probability of detecting difference when this difference exists (Biau et al., 2008). Sample size calculated to detect difference in the primary outcome (i.e., UCP1). The concern with power can lead to a variety of errors in interpretation of statistical outcomes. This might lead to conclude there is no effect from an intervention when in fact an effect does exist in the animals. This might lead to incorrectly conclude that there is a strong effect when actually is that there is an effect, but it is so small as to

be unimportant. An optimal primary outcome is the one for which there is the most existing evidence of being associated with the intervention of interest. For a certain study aim and hypothesis, there are often several outcome variables that might be considered as related to the intervention of interest. Including several outcomes as primary outcomes would lead to an unfocused research question and study and present problems with interpretation if the intervention effect differed across the outcomes. Having multiple primary outcomes should may increase the chance of reporting a false positive finding (Vetter and Mascha, 2017).

5.4.4 Moderate high-fat content in the HFHS diet

The modest changes in plasma metabolites and the lack of effect of different housing temperature conditions prior to gestation may be due to the relatively short intervention period. Previous maternal obesity studies lasted longer, such as 10-weeks (Niculescu and Lupu, 2009),11-weeks (Fante et al., 2016) and 12-weeks, in addition to the gestational period (Stuart et al., 2018). Another reason the diet did not percipitate weight gain pre-gestation could be the moderate high-fat content in the HFHS diet used. In this study, HFHS diet contained 39% of energy derived from fat rather than a very high-fat diet with approximately 60% of energy derived from fat, utilised in other experimental studies to elicit obesity (Xiao et al., 2015, Cui et al., 2016).

5.5 Future work

The UCP1 expression within the interscapular adipose tissue depots was significantly altered by standard housing temperatures pre-gestation. It would be useful to investigate the same interventions among the offspring

to enable the assessment of the effect of maternal HFHS diet with a longer intervention period, at least 10 weeks prior to gestation. Then studying the effect on offspring at three different developmental windows, at birth, during lactation and post weaning. I would include a larger number of rats and investigate both genders to study the effect of housing temperature and obesity. It would be useful to study the effect of these interventions on UCP1 abundance using western blotting, mitochondrial respiration and respirometery to measure BMR and RMR.

This study utilised an intervention diet with a 4.6 kcal/g, as compared to a control diet that contained 3.1 kcal/g. This HFHS diet showed a modest effect on plasma metabolites and weight gain. Therefore, it would be useful to assess whether the HFHS diet with a higher fat content (60%) and 5.2 kcal/g (Xiao et al., 2015) increases plasma metabolite levels and adiposity under standard and thermoneutral temperature conditions. If plasma metabolites and adiposity levels change from that of the controls, the dietary effect may have masked the standard housing temperature effect.

5.6 Final remarks

This study demonstrated that standard housing temperatures modified BAT thermogenic capacity prior to gestation. In addition, diet-induced obesity increased adiposity and weight gain during gestation. The findings of this study could, in part, help expand current understanding of the metabolic effect of standard housing temperature conditions and clarify the variation of response to dietary intervention in BAT. Thus, efforts to design and test metabolic experiments of rats at thermoneutral temperature conditions could be a benefit.

Reference

ABELENDA, M. & PUERTA, M. L. 1987. Inhibition of diet-induced thermogenesis during pregnancy in the rat. *Pflügers Archiv,* 409**,** 314-317.

ABRAMS, B. & SELVIN, S. 1995. Maternal Weight Gain Pattern and Birth Weight. *Obstetrics & Gynecology,* 86**,** 163-169.

ACHESON, K. J. 1993. Influence of autonomic nervous system on nutrient-induced thermogenesis in humans. *Nutrition,* 9.

ADAMS, N. & BOICE, R. 1983. A longitudinal study of dominance in an outdoor colony of domestic rats. *Journal of Comparative Psychology,* 97**,** 24-33.

AHIMA, R. S. & FLIER, J. S. 2000. Leptin. *Annual Review of Physiology,* 62**,** 413-437.

AHMADIAN, M., ABBOTT, M. J., TANG, T., HUDAK, C. S., KIM, Y., BRUSS, M., HELLERSTEIN, M. K., LEE, H. Y., SAMUEL, V. T., SHULMAN, G. I., WANG, Y., DUNCAN, R. E., KANG, C. & SUL, H. S. 2011. Desnutrin/ATGL is regulated by AMPK and is required for a brown adipose phenotype. *Cell Metab,* 13**,** 739-48.

ALBERTI, K. G., ZIMMET, P. & SHAW, J. 2005. The metabolic syndrome--a new worldwide definition. *Lancet,* 366**,** 1059-62.

ALEIXANDRE DE ARTINANO, A. & MIGUEL CASTRO, M. 2009. Experimental rat models to study the metabolic syndrome. *Br J Nutr,* 102**,** 1246-53.

ALINGH PRINS, A., DE JONG-NAGELSMIT, A., KEIJSER, J. & STRUBBE, J. H. 1986. Daily rhythms of feeding in the genetically obese and lean Zucker rats. *Physiol Behav,* 38**,** 423-6.

ALVAREZ, J. J., MONTELONGO, A., IGLESIAS, A., LASUNCION, M. A. & HERRERA, E. 1996. Longitudinal study on lipoprotein profile, high density lipoprotein subclass, and postheparin lipases during gestation in women. *J Lipid Res,* 37**,** 299-308.

AMICO, J. A., THOMAS, A., CROWLEY, R. S. & BURMEISTER, L. A. 1998. Concentrations of leptin in the serum of pregnant, lactating, and cycling rats and of leptin messenger ribonucleic acid in rat placental tissue. *Life Sci,* 63**,** 1387-95.

ANDREOLLO, N. A., SANTOS, E. F., ARAUJO, M. R. & LOPES, L. R. 2012. Rat's age versus human's age: what is the relationship? *Arq Bras Cir Dig,* 25**,** 49-51.

ARYA, M., SHERGILL, I. S., WILLIAMSON, M., GOMMERSALL, L., ARYA, N. & PATEL, H. R. 2005. Basic principles of real-time quantitative PCR. *Expert Rev Mol Diagn,* 5**,** 209-19.

ATGIE, C., D'ALLAIRE, F. & BUKOWIECKI, L. J. 1997. Role of beta1- and beta3-adrenoceptors in the regulation of lipolysis and thermogenesis in rat brown adipocytes. *Am J Physiol,* 273**,** C1136-42.

ATHERTON, J. C., DARK, J. M., GARLAND, H. O., MORGAN, M. R., PIDGEON, J. & SONI, S. 1982. Changes in water and electrolyte balance, plasma volume and composition during pregnancy in the rat. *J Physiol,* 330**,** 81-93.

ATHUKORALA, C., RUMBOLD, A. R., WILLSON, K. J. & CROWTHER, C. A. 2010. The risk of adverse pregnancy outcomes in women who are overweight or obese. *BMC Pregnancy and Childbirth,* 10**,** 56.

AU-YONG, I. T. H., THORN, N., GANATRA, R., PERKINS, A. C. & SYMONDS, M. E. 2009. Brown Adipose Tissue and Seasonal Variation in Humans. *Diabetes,* 58**,** 2583-2587.

AUGUSTINE, R. A., LADYMAN, S. R. & GRATTAN, D. R. 2008. From feeding one to feeding many: hormone-induced changes in bodyweight homeostasis during pregnancy. *J Physiol,* 586**,** 387-97.

AUSTIN, S. & ST-PIERRE, J. 2012. PGC1α and mitochondrial metabolism – emerging concepts and relevance in ageing and neurodegenerative disorders. *Journal of Cell Science,* 125**,** 4963-4971.

BABOOTA, R. K., SINGH, D. P., SARMA, S. M., KAUR, J., SANDHIR, R., BOPARAI, R. K., KONDEPUDI, K. K. & BISHNOI, M. 2014. Capsaicin induces "brite" phenotype in differentiating 3T3-L1 preadipocytes. *PLoS One,* 9**,** e103093.

BACHMAN, E. S., DHILLON, H., ZHANG, C. Y., CINTI, S., BIANCO, A. C., KOBILKA, B. K. & LOWELL, B. B. 2002. betaAR signaling required for diet-induced thermogenesis and obesity resistance. *Science,* 297**,** 843-5.

BARBERA, M. J., SCHLUTER, A., PEDRAZA, N., IGLESIAS, R., VILLARROYA, F. & GIRALT, M. 2001. Peroxisome proliferator-activated receptor alpha activates transcription of the brown fat uncoupling protein-1 gene. A link between regulation of the thermogenic and lipid oxidation pathways in the brown fat cell. *J Biol Chem,* 276**,** 1486-93.

BARNARD, T., SKÁLA, J. & LINDBERG, O. 1970. Changes in interscapular brown adipose tissue of the rat during perinatal and early postnatal development and after cold acclimation—I. Activities of some respiratory enzymes in the tissue. *Comparative Biochemistry and Physiology,* 33**,** 499-508.

BARND, T., SKALA, J. & LINDBERG, O. 1970. Changes in interscapular brown adipose tissue of the rat during perinatal and early postnatal development and after cold acclimation. I. Activities of some respiratory enzymes in the tissue. *Comp Biochem Physiol,* 33**,** 499-508.

BARRÉ-SINOUSSI, F. & MONTAGUTELLI, X. 2015. Animal models are essential to biological research: issues and perspectives. *Future Science OA,* 1**,** FSO63.

BARTELT, A., BRUNS, O. T., REIMER, R., HOHENBERG, H., ITTRICH, H., PELDSCHUS, K., KAUL, M. G., TROMSDORF, U. I., WELLER, H., WAURISCH, C., EYCHMULLER, A., GORDTS, P. L., RINNINGER, F., BRUEGELMANN, K., FREUND, B., NIELSEN, P., MERKEL, M. & HEEREN, J. 2011. Brown adipose tissue activity controls triglyceride clearance. *Nat Med,* 17**,** 200-5.

BARTNESS, T. J. & BAMSHAD, M. 1998. Innervation of mammalian white adipose tissue: implications for the regulation of total body fat. *Am J Physiol,* 275**,** R1399-411.

BAYOL, S. A., FARRINGTON, S. J. & STICKLAND, N. C. 2007. A maternal 'junk food' diet in pregnancy and lactation promotes an exacerbated taste for 'junk food' and a greater propensity for obesity in rat offspring. *Br J Nutr,* 98**,** 843-51.

BERRY, D. C., JIANG, Y. & GRAFF, J. M. 2016. Mouse strains to study cold-inducible beige progenitors and beige adipocyte formation and function. *Nature Communications,* 7**,** 10184.

BIAU, D. J., KERNÉIS, S. & PORCHER, R. 2008. Statistics in brief: the importance of sample size in the planning and interpretation of medical research. *Clinical orthopaedics and related research,* 466**,** 2282-2288.

BING, C., FRANKISH, H. M., PICKAVANCE, L., WANG, Q., HOPKINS, D. F., STOCK, M. J. & WILLIAMS, G. 1998. Hyperphagia in cold-exposed rats is accompanied by decreased plasma leptin but unchanged hypothalamic NPY. *Am J Physiol,* 274**,** R62-8.

BODEN, G., CHEN, X., MOZZOLI, M. & RYAN, I. 1996. Effect of fasting on serum leptin in normal human subjects. *J Clin Endocrinol Metab,* 81**,** 3419-23.

BOSTROM, P., WU, J., JEDRYCHOWSKI, M. P., KORDE, A., YE, L., LO, J. C., RASBACH, K. A., BOSTROM, E. A., CHOI, J. H., LONG, J. Z., KAJIMURA, S., ZINGARETTI, M. C., VIND, B. F., TU, H., CINTI, S., HOJLUND, K., GYGI, S. P. & SPIEGELMAN, B. M. 2012. A PGC1-alpha-dependent myokine that drives brown-fat-like development of white fat and thermogenesis. *Nature,* 481**,** 463-8.

BOULOUMIE, A., PLANAT, V., DEVEDJIAN, J. C., VALET, P., SAULNIER-BLACHE, J. S., RECORD, M. & LAFONTAN, M. 1994. Alpha 2-adrenergic stimulation promotes preadipocyte proliferation. Involvement of mitogen-activated protein kinases. *J Biol Chem,* 269**,** 30254-9.

BOWERS, R. R., FESTUCCIA, W. T., SONG, C. K., SHI, H., MIGLIORINI, R. H. & BARTNESS, T. J. 2004. Sympathetic innervation of white adipose tissue and its regulation of fat cell number. *Am J Physiol Regul Integr Comp Physiol,* 286**,** R1167-75.

BRAUN, K., OECKL, J., WESTERMEIER, J., LI, Y. & KLINGENSPOR, M. 2018. Non-adrenergic control of lipolysis and thermogenesis in adipose tissues. *J Exp Biol,* 221.

BRIGATI, D. J., BUDGEON, L. R., UNGER, E. R., KOEBLER, D., CUOMO, C., KENNEDY, T. & PERDOMO, J. M. I. 1988. Immunocytochemistry is Automated: Development of A Robotic Workstation Based Upon the Capillary Action Principle. *Journal of Histotechnology,* 11**,** 165-183.

BROOKS, C., WEI, Q., CHO, S. G. & DONG, Z. 2009. Regulation of mitochondrial dynamics in acute kidney injury in cell culture and rodent models. *J Clin Invest,* 119**,** 1275-85.

BUCHANAN, T. A. & XIANG, A. H. 2005. Gestational diabetes mellitus. *J Clin Invest,* 115**,** 485-91.

BUETTNER, R., PARHOFER, K. G., WOENCKHAUS, M., WREDE, C. E., KUNZ-SCHUGHART, L. A., SCHOLMERICH, J. & BOLLHEIMER, L. C. 2006. Defining high-fat-diet rat models: metabolic and molecular effects of different fat types. *J Mol Endocrinol,* 36**,** 485-501.

BUKOWIECKI, L., COLLET, A. J., FOLLEA, N., GUAY, G. & JAHJAH, L. 1982. Brown adipose tissue hyperplasia: a fundamental mechanism of adaptation to cold and hyperphagia. *Am J Physiol,* 242**,** E353-9.

BURGUERA, B., COUCE, M. E., LONG, J., LAMSAM, J., LAAKSO, K., JENSEN, M. D., PARISI, J. E. & LLOYD, R. V. 2000. The long form of the leptin receptor (OB-Rb) is widely expressed in the human brain. *Neuroendocrinology,* 71**,** 187-95.

BUSTIN, S. A., BENES, V., GARSON, J. A., HELLEMANS, J., HUGGETT, J., KUBISTA, M., MUELLER, R., NOLAN, T., PFAFFL, M. W., SHIPLEY, G. L., VANDESOMPELE, J. & WITTWER, C. T. 2009. The MIQE guidelines: minimum information for publication of quantitative real-time PCR experiments. *Clin Chem,* 55**,** 611-22.

BUTLER, J. M. 2005. *Forensic DNA typing [electronic resource] : biology, technology, and genetics of STR markers / John M. Butler,* London, London : Elsevier Academic Press.

BUTTE, N. F. 2000. Carbohydrate and lipid metabolism in pregnancy: normal compared with gestational diabetes mellitus. *Am J Clin Nutr,* 71**,** 1256s-61s.

CAHILL, G. F., JR. 2006. Fuel metabolism in starvation. *Annu Rev Nutr,* 26**,** 1-22.

CAMPFIELD, L. A., SMITH, F. J. & BURN, P. 1996. The OB protein (leptin) pathway--a link between adipose tissue mass and central neural networks. *Horm Metab Res,* 28**,** 619-32.
CANNON, B. & NEDERGAARD, J. 2004. Brown adipose tissue: function and physiological significance. *Physiol Rev,* 84**,** 277-359.
CANNON, B. & NEDERGAARD, J. 2010. Metabolic consequences of the presence or absence of the thermogenic capacity of brown adipose tissue in mice (and probably in humans). *Int J Obes (Lond),* 34 Suppl 1**,** S7-16.
CANNON, B. & NEDERGAARD, J. 2011. Nonshivering thermogenesis and its adequate measurement in metabolic studies. *J Exp Biol,* 214**,** 242-53.
CANNON, B. & NEDERGAARD, J. 2012. Yes, even human brown fat is on fire! *J Clin Invest,* 122**,** 486-9.
CAO, W., DANIEL, K. W., ROBIDOUX, J., PUIGSERVER, P., MEDVEDEV, A. V., BAI, X., FLOERING, L. M., SPIEGELMAN, B. M. & COLLINS, S. 2004. p38 mitogen-activated protein kinase is the central regulator of cyclic AMP-dependent transcription of the brown fat uncoupling protein 1 gene. *Mol Cell Biol,* 24**,** 3057-67.
CAREY, A. L. & KINGWELL, B. A. 2013. Brown adipose tissue in humans: therapeutic potential to combat obesity. *Pharmacol Ther,* 140**,** 26-33.
CATALANO, P. M., TYZBIR, E. D., ROMAN, N. M., AMINI, S. B. & SIMS, E. A. 1991. Longitudinal changes in insulin release and insulin resistance in nonobese pregnant women. *Am J Obstet Gynecol,* 165**,** 1667-72.
CATALANO, P. M., TYZBIR, E. D., WOLFE, R. R., CALLES, J., ROMAN, N. M., AMINI, S. B. & SIMS, E. A. 1993. Carbohydrate metabolism during pregnancy in control subjects and women with gestational diabetes. *Am J Physiol,* 264**,** E60-7.
CATALANO, P. M., TYZBIR, E. D., WOLFE, R. R., ROMAN, N. M., AMINI, S. B. & SIMS, E. A. 1992. Longitudinal changes in basal hepatic glucose production and suppression during insulin infusion in normal pregnant women. *Am J Obstet Gynecol,* 167**,** 913-9.
CATERINA, M. J. 2007. Transient receptor potential ion channels as participants in thermosensation and thermoregulation. *Am J Physiol Regul Integr Comp Physiol,* 292**,** R64-76.
CATERINA, M. J., SCHUMACHER, M. A., TOMINAGA, M., ROSEN, T. A., LEVINE, J. D. & JULIUS, D. 1997. The capsaicin receptor: a heat-activated ion channel in the pain pathway. *Nature,* 389**,** 816-24.
CAWTHORN, W. P., SCHELLER, E. L. & MACDOUGALD, O. A. 2012a. Adipose tissue stem cells meet preadipocyte commitment: going back to the future. *J Lipid Res,* 53**,** 227-46.
CAWTHORN, W. P., SCHELLER, E. L. & MACDOUGALD, O. A. 2012b. Adipose tissue stem cells: the great WAT hope. *Trends Endocrinol Metab,* 23**,** 270-7.
CEDERBERG, A., GRONNING, L. M., AHREN, B., TASKEN, K., CARLSSON, P. & ENERBACK, S. 2001. FOXC2 is a winged helix gene that counteracts obesity, hypertriglyceridemia, and diet-induced insulin resistance. *Cell,* 106**,** 563-73.
CELLA, M., LEGUIZAMÓN, G. F., SORDELLI, M. S., CERVINI, M., GUADAGNOLI, T., RIBEIRO, M. L., FRANCHI, A. M. & FARINA, M. G. 2008. Dual Effect of Anandamide on Rat Placenta Nitric Oxide Synthesis. *Placenta,* 29**,** 699-707.
CELTON-MORIZUR, S., MERLEN, G., COUTON, D., MARGALL-DUCOS, G. & DESDOUETS, C. 2009. The insulin/Akt pathway controls a specific cell division

program that leads to generation of binucleated tetraploid liver cells in rodents. *J Clin Invest,* 119**,** 1880-7.
CHEN, H., SIMAR, D., LAMBERT, K., MERCIER, J. & MORRIS, M. J. 2008. Maternal and postnatal overnutrition differentially impact appetite regulators and fuel metabolism. *Endocrinology,* 149**,** 5348-56.
CHEN, Y., PAN, R. & PFEIFER, A. 2016. Fat tissues, the brite and the dark sides. *Pflugers Archiv,* 468**,** 1803-1807.
CHOMCZYNSKI, P. 1993. A reagent for the single-step simultaneous isolation of RNA, DNA and proteins from cell and tissue samples. *Biotechniques,* 15**,** 532-4, 536-7.
CHOMCZYNSKI, P. & SACCHI, N. 1987. Single-step method of RNA isolation by acid guanidinium thiocyanate-phenol-chloroform extraction. *Anal Biochem,* 162**,** 156-9.
CHONDRONIKOLA, M., VOLPI, E., BØRSHEIM, E., CHAO, T., PORTER, C., ANNAMALAI, P., YFANTI, C., LABBE, S. M., HURREN, N. M., MALAGARIS, I., CESANI, F. & SIDOSSIS, L. S. 2016. Brown Adipose Tissue Is Linked to a Distinct Thermoregulatory Response to Mild Cold in People. *Frontiers in Physiology,* 7.
CHRISTIANSEN, E. & GARBY, L. 2002. Prediction of body weight changes caused by changes in energy balance. *Eur J Clin Invest,* 32**,** 826-30.
CHRISTIE, S., WITTERT, G. A., LI, H. & PAGE, A. J. 2018. Involvement of TRPV1 Channels in Energy Homeostasis. *Frontiers in Endocrinology,* 9**,** 420.
CHU, S. Y., CALLAGHAN, W. M., KIM, S. Y., SCHMID, C. H., LAU, J., ENGLAND, L. J. & DIETZ, P. M. 2007. Maternal obesity and risk of gestational diabetes mellitus. *Diabetes Care,* 30.
CICCARELLI, M., SANTULLI, G., PASCALE, V., TRIMARCO, B. & IACCARINO, G. 2013. Adrenergic receptors and metabolism: role in development of cardiovascular disease. *Frontiers in physiology,* 4**,** 265-265.
CINTI, S. 2001. The adipose organ: morphological perspectives of adipose tissues. *Proc Nutr Soc,* 60**,** 319-28.
CINTI, S. 2006. The role of brown adipose tissue in human obesity. *Nutrition, Metabolism and Cardiovascular Diseases,* 16**,** 569-574.
CINTI, S. 2012. The adipose organ at a glance. *Disease Models & Mechanisms,* 5**,** 588-594.
CINTI, S., FREDERICH, R. C., ZINGARETTI, M. C., DE MATTEIS, R., FLIER, J. S. & LOWELL, B. B. 1997. Immunohistochemical Localization of Leptin and Uncoupling Protein in White and Brown Adipose Tissue*. *Endocrinology,* 138**,** 797-804.
CONNOLLY, E., MORRISEY, R. D. & CARNIE, J. A. 1982. The effect of interscapular brown adipose tissue removal on body-weight and cold response in the mouse. *Br J Nutr,* 47**,** 653-8.
CORKEY, B. E. 2012. Banting lecture 2011: hyperinsulinemia: cause or consequence? *Diabetes,* 61**,** 4-13.
CORVINO, S. B., VOLPATO, G. T., MACEDO, N. C., SINZATO, Y. K., RUDGE, M. V. & DAMASCENO, D. C. 2015. Physiological and biochemical measurements before, during and after pregnancy of healthy rats. *Acta Cir Bras,* 30**,** 668-74.
COUSIN, B., CASTEILLA, L., LAFONTAN, M., AMBID, L., LANGIN, D., BERTHAULT, M. F. & PÉNICAUD, L. 1993. Local sympathetic denervation of white adipose tissue in rats induces preadipocyte proliferation without noticeable changes in metabolism. *Endocrinology,* 133**,** 2255-2262.

COUSIN, B., CINTI, S., MORRONI, M., RAIMBAULT, S., RICQUIER, D., PENICAUD, L. & CASTEILLA, L. 1992. Occurrence of brown adipocytes in rat white adipose tissue: molecular and morphological characterization. *J Cell Sci,* 103 (Pt 4)**,** 931-42.

CREW, R. C., MARK, P. J. & WADDELL, B. J. 2018. Obesity Disrupts Rhythmic Clock Gene Expression in Maternal Adipose Tissue during Rat Pregnancy. *Journal of Biological Rhythms,* 33**,** 289-301.

CUI, X., NGUYEN, N. L. T., ZAREBIDAKI, E., CAO, Q., LI, F., ZHA, L., BARTNESS, T., SHI, H. & XUE, B. 2016. Thermoneutrality decreases thermogenic program and promotes adiposity in high-fat diet-fed mice. *Physiological Reports,* 4**,** e12799.

CUTHBERT, C. E., FOSTER, J. E. & RAMDATH, D. D. 2017. A maternal high-fat, high-sucrose diet alters insulin sensitivity and expression of insulin signalling and lipid metabolism genes and proteins in male rat offspring: effect of folic acid supplementation. *British Journal of Nutrition,* 118**,** 580-588.

CYPESS, A. M., DOYLE, A. N., SASS, C. A., HUANG, T. L., MOWSCHENSON, P. M., ROSEN, H. N., TSENG, Y.-H., PALMER, E. L. & KOLODNY, G. M. 2013a. Quantification of Human and Rodent Brown Adipose Tissue Function Using (99m)Tc-methoxyisobutylisonitrile SPECT/CT and (18)F-FDG PET/CT. *Journal of nuclear medicine : official publication, Society of Nuclear Medicine,* 54**,** 1896-1901.

CYPESS, A. M. & KAHN, C. R. 2010. The Role and Importance of Brown Adipose Tissue in Energy Homeostasis. *Current opinion in pediatrics,* 22**,** 478-484.

CYPESS, A. M., LEHMAN, S., WILLIAMS, G., TAL, I., RODMAN, D., GOLDFINE, A. B., KUO, F. C., PALMER, E. L., TSENG, Y. H., DORIA, A., KOLODNY, G. M. & KAHN, C. R. 2009. Identification and importance of brown adipose tissue in adult humans. *N Engl J Med,* 360**,** 1509-17.

CYPESS, A. M., WEINER, L. S., ROBERTS-TOLER, C., FRANQUET ELIA, E., KESSLER, S. H., KAHN, P. A., ENGLISH, J., CHATMAN, K., TRAUGER, S. A., DORIA, A. & KOLODNY, G. M. 2015. Activation of human brown adipose tissue by a beta3-adrenergic receptor agonist. *Cell Metab,* 21**,** 33-8.

CYPESS, A. M., WHITE, A. P., VERNOCHET, C., SCHULZ, T. J., XUE, R., SASS, C. A., HUANG, T. L., ROBERTS-TOLER, C., WEINER, L. S., SZE, C., CHACKO, A. T., DESCHAMPS, L. N., HERDER, L. M., TRUCHAN, N., GLASGOW, A. L., HOLMAN, A. R., GAVRILA, A., HASSELGREN, P. O., MORI, M. A., MOLLA, M. & TSENG, Y. H. 2013b. Anatomical localization, gene expression profiling and functional characterization of adult human neck brown fat. *Nat Med,* 19**,** 635-9.

DANTZER, R. 1986. Behavioral, physiological and functional aspects of stereotyped behavior: a review and a re-interpretation. *J Anim Sci,* 62**,** 1776-86.

DAWKINS, M. S. 2011. From an animal's point of view: Motivation, fitness, and animal welfare. *Behavioral and Brain Sciences,* 13**,** 1-9.

DE FERRANTI, S. & MOZAFFARIAN, D. 2008. The perfect storm: obesity, adipocyte dysfunction, and metabolic consequences. *Clin Chem,* 54**,** 945-55.

DENMAN, S. E. & MCSWEENEY, C. S. 2005. Quantitative (real-time) PCR. *In:* MAKKAR, H. P. S. & MCSWEENEY, C. S. (eds.) *Methods in Gut Microbial Ecology for Ruminants.* Dordrecht: Springer Netherlands.

DENTON, R. M. 2009. Regulation of mitochondrial dehydrogenases by calcium ions. *Biochim Biophys Acta,* 1787**,** 1309-16.

DESAI, M., JELLYMAN, J. K., HAN, G., BEALL, M., LANE, R. H. & ROSS, M. G. 2014. Rat Maternal Obesity and High Fat Diet Program Offspring Metabolic Syndrome. *American journal of obstetrics and gynecology,* 211**,** 237.e1-237.e13.

DHAKA, A., UZZELL, V., DUBIN, A. E., MATHUR, J., PETRUS, M., BANDELL, M. & PATAPOUTIAN, A. 2009. TRPV1 is activated by both acidic and basic pH. *J Neurosci,* 29**,** 153-8.

DIXEN, K., BASSE, A. L., MURHOLM, M., ISIDOR, M. S., HANSEN, L. H. L., PETERSEN, M. C. H., MADSEN, L., PETROVIC, N., NEDERGAARD, J., QUISTORFF, B. & HANSEN, J. B. 2013. ERRγ enhances UCP1 expression and fatty acid oxidation in brown adipocytes. *Obesity,* 21**,** 516-524.

DULLOO, A. G. & MILLER, D. S. 1984. Energy balance following sympathetic denervation of brown adipose tissue. *Can J Physiol Pharmacol,* 62**,** 235-40.

DUREN, D. L., SHERWOOD, R. J., CZERWINSKI, S. A., LEE, M., CHOH, A. C., SIERVOGEL, R. M. & CAMERON CHUMLEA, W. 2008. Body Composition Methods: Comparisons and Interpretation. *Journal of diabetes science and technology (Online),* 2**,** 1139-1146.

ECKEL, R. H., GRUNDY, S. M. & ZIMMET, P. Z. 2005. The metabolic syndrome. *Lancet,* 365**,** 1415-28.

EL KHATTABI, I., REMACLE, C. & REUSENS, B. 2006. The regulation of IGFs and IGFBPs by prolactin in primary culture of fetal rat hepatocytes is influenced by maternal malnutrition. *Am J Physiol Endocrinol Metab,* 291**,** E835-42.

ENERBÄCK, S. 2010. Human Brown Adipose Tissue. *Cell Metabolism,* 11**,** 248-252.

ENERBACK, S., JACOBSSON, A., SIMPSON, E. M., GUERRA, C., YAMASHITA, H., HARPER, M. E. & KOZAK, L. P. 1997. Mice lacking mitochondrial uncoupling protein are cold-sensitive but not obese. *Nature,* 387**,** 90-4.

ESSER, N., LEGRAND-POELS, S., PIETTE, J., SCHEEN, A. J. & PAQUOT, N. 2014. Inflammation as a link between obesity, metabolic syndrome and type 2 diabetes. *Diabetes Res Clin Pract,* 105**,** 141-50.

EVANS, B. A., PAPAIOANNOU, M., HAMILTON, S. & SUMMERS, R. J. 1999. Alternative splicing generates two isoforms of the beta3-adrenoceptor which are differentially expressed in mouse tissues. *Br J Pharmacol,* 127**,** 1525-31.

FAGUNDES, D. J. & TAHA, M. O. 2004. Modelo animal de doença: critérios de escolha e espécies de animais de uso corrente. *Acta Cirurgica Brasileira,* 19**,** 59-65.

FANTE, T., SIMINO, L. A., REGINATO, A., PAYOLLA, T. B., VITORELI, D. C., SOUZA, M., TORSONI, M. A., MILANSKI, M. & TORSONI, A. S. 2016. Diet-Induced Maternal Obesity Alters Insulin Signalling in Male Mice Offspring Rechallenged with a High-Fat Diet in Adulthood. *PLoS One,* 11**,** e0160184.

FAROOQI, I. S., KEOGH, J. M., KAMATH, S., JONES, S., GIBSON, W. T., TRUSSELL, R., JEBB, S. A., LIP, G. Y. & O'RAHILLY, S. 2001. Partial leptin deficiency and human adiposity. *Nature,* 414**,** 34-5.

FAUST, I. M., JOHNSON, P. R., STERN, J. S. & HIRSCH, J. 1978. Diet-induced adipocyte number increase in adult rats: a new model of obesity. *Am J Physiol,* 235**,** E279-86.

FELDMANN, H. M., GOLOZOUBOVA, V., CANNON, B. & NEDERGAARD, J. 2009. UCP1 ablation induces obesity and abolishes diet-induced thermogenesis in mice exempt from thermal stress by living at thermoneutrality. *Cell Metab,* 9**,** 203-9.

FINN, D. A., BEJANIAN, M., JONES, B. L., SYAPIN, P. J. & ALKANA, R. L. 1989. Temperature affects ethanol lethality in C57BL/6, 129, LS and SS mice. *Pharmacol Biochem Behav,* 34**,** 375-80.

FISCHER, A. W., CANNON, B. & NEDERGAARD, J. 2018. Optimal housing temperatures for mice to mimic the thermal environment of humans: An experimental study. *Mol Metab,* 7**,** 161-170.

FONSECA, B. M., CORREIA-DA-SILVA, G., TAYLOR, A. H., LAM, P. M., MARCZYLO, T. H., KONJE, J. C. & TEIXEIRA, N. A. 2012. Characterisation of the endocannabinoid system in rat haemochorial placenta. *Reprod Toxicol,* 34**,** 347-56.

FORBES, J. M. & COOPER, M. E. 2013. Mechanisms of diabetic complications. *Physiol Rev,* 93**,** 137-88.

FORBES, J. M., COUGHLAN, M. T. & COOPER, M. E. 2008. Oxidative stress as a major culprit in kidney disease in diabetes. *Diabetes,* 57**,** 1446-54.

FRAC 2015.

FREDERICH, R. C., LÖLLMANN, B., HAMANN, A., NAPOLITANO-ROSEN, A., KAHN, B. B., LOWELL, B. B. & FLIER, J. S. 1995. Expression of ob mRNA and its encoded protein in rodents. Impact of nutrition and obesity. *Journal of Clinical Investigation,* 96**,** 1658-1663.

FREEMARK, M., KIRK, K., PIHOKER, C., ROBERTSON, M. C., SHIU, R. P. & DRISCOLL, P. 1993. Pregnancy lactogens in the rat conceptus and fetus: circulating levels, distribution of binding, and expression of receptor messenger ribonucleic acid. *Endocrinology,* 133**,** 1830-42.

FRONTERA, M., PUJOL, E., RODRIGUEZ-CUENCA, S., CATALA-NIELL, A., ROCA, P., GARCIA-PALMER, F. J. & GIANOTTI, M. 2005. Rat brown adipose tissue thermogenic features are altered during mid-pregnancy. *Cell Physiol Biochem,* 15**,** 203-10.

FRUHBECK, G., BECERRIL, S., SAINZ, N., GARRASTACHU, P. & GARCIA-VELLOSO, M. J. 2009. BAT: a new target for human obesity? *Trends Pharmacol Sci,* 30**,** 387-96.

FUKANO, K., OKAMATSU-OGURA, Y., TSUBOTA, A., NIO-KOBAYASHI, J. & KIMURA, K. 2016. Cold Exposure Induces Proliferation of Mature Brown Adipocyte in a ß3-Adrenergic Receptor-Mediated Pathway. *PLoS ONE,* 11**,** e0166579.

GALAN, X., LLOBERA, M. & RAMÍREZ, I. 1994. Lipoprotein lipase and hepatic lipase in Wistar and Sprague-Dawley rat tissues. Differences in the effects of gender and fasting. *Lipids,* 29**,** 333-336.

GALASSI, A., REYNOLDS, K. & HE, J. 2006. Metabolic syndrome and risk of cardiovascular disease: a meta-analysis. *Am J Med,* 119**,** 812-9.

GAO, Y., QIMUGE, N. R., QIN, J., CAI, R., LI, X., CHU, G. Y., PANG, W. J. & YANG, G. S. 2017. Acute and chronic cold exposure differentially affects the browning of porcine white adipose tissue. *animal,* 12**,** 1435-1441.

GARCIA, M. D., CASANUEVA, F. F., DIEGUEZ, C. & SENARIS, R. M. 2000. Gestational profile of leptin messenger ribonucleic acid (mRNA) content in the placenta and adipose tissue in the rat, and regulation of the mRNA levels of the leptin receptor subtypes in the hypothalamus during pregnancy and lactation. *Biol Reprod,* 62**,** 698-703.

GARIBYAN, L. & AVASHIA, N. 2013. Research Techniques Made Simple: Polymerase Chain Reaction (PCR). *The Journal of investigative dermatology,* 133**,** e6-e6.

GESTA, S., TSENG, Y. H. & KAHN, C. R. 2007. Developmental origin of fat: tracking obesity to its source. *Cell,* 131**,** 242-56.
GHASEMI, A. & ZAHEDIASL, S. 2012. Normality tests for statistical analysis: a guide for non-statisticians. *International journal of endocrinology and metabolism,* 10**,** 486-489.
GIACOBINO, J. P. 1996. Role of the beta3-adrenoceptor in the control of leptin expression. *Horm Metab Res,* 28**,** 633-7.
GLASEL, J. A. 1995. Validity of nucleic acid purities monitored by 260nm/280nm absorbance ratios. *Biotechniques,* 18**,** 62-3.
GOLOZOUBOVA, V., CANNON, B. & NEDERGAARD, J. 2006. UCP1 is essential for adaptive adrenergic nonshivering thermogenesis. *Am J Physiol Endocrinol Metab,* 291**,** E350-7.
GOLOZOUBOVA, V., GULLBERG, H., MATTHIAS, A., CANNON, B., VENNSTROM, B. & NEDERGAARD, J. 2004. Depressed thermogenesis but competent brown adipose tissue recruitment in mice devoid of all hormone-binding thyroid hormone receptors. *Mol Endocrinol,* 18**,** 384-401.
GOLOZOUBOVA, V., HOHTOLA, E., MATTHIAS, A., JACOBSSON, A., CANNON, B. & NEDERGAARD, J. 2001. Only UCP1 can mediate adaptive nonshivering thermogenesis in the cold. *Faseb j,* 15**,** 2048-50.
GÓMEZ-AMBROSI, J., FRÜHBECK, G. & ALFREDO MARTíNEZ, J. 2001. Rapid in vivo PGC-1 mRNA upregulation in brown adipose tissue of Wistar rats by a β3-adrenergic agonist and lack of effect of leptin. *Molecular and Cellular Endocrinology,* 176**,** 85-90.
GONZALEZ, C., ALONSO, A., ALVAREZ, N., DIAZ, F., MARTINEZ, M., FERNANDEZ, S. & PATTERSON, A. M. 2000. Role of 17beta-estradiol and/or progesterone on insulin sensitivity in the rat: implications during pregnancy. *J Endocrinol,* 166**,** 283-91.
GOSPODARSKA, E., NOWIALIS, P. & KOZAK, L. P. 2015. Mitochondrial turnover: a phenotype distinguishing brown adipocytes from interscapular brown adipose tissue and white adipose tissue. *J Biol Chem,* 290**,** 8243-55.
GRAHAM, R. C., JR. & KARNOVSKY, M. J. 1966. The early stages of absorption of injected horseradish peroxidase in the proximal tubules of mouse kidney: ultrastructural cytochemistry by a new technique. *J Histochem Cytochem,* 14**,** 291-302.
GREENHILL, C. 2013. Cold exposure increases brown adipose tissue in humans. *Nature Reviews Endocrinology,* 9**,** 566.
GUILAK, F., LOTT, K. E., AWAD, H. A., CAO, Q., HICOK, K. C., FERMOR, B. & GIMBLE, J. M. 2006. Clonal analysis of the differentiation potential of human adipose-derived adult stem cells. *J Cell Physiol,* 206**,** 229-37.
GUILHERME, A., VIRBASIUS, J. V., PURI, V. & CZECH, M. P. 2008. Adipocyte dysfunctions linking obesity to insulin resistance and type 2 diabetes. *Nat Rev Mol Cell Biol,* 9**,** 367-77.
GUO, Y., XIAO, P., LEI, S., DENG, F., XIAO, G. G., LIU, Y., CHEN, X., LI, L., WU, S., CHEN, Y., JIANG, H., TAN, L., XIE, J., ZHU, X., LIANG, S. & DENG, H. 2008. How is mRNA expression predictive for protein expression? A correlation study on human circulating monocytes. *Acta Biochim Biophys Sin (Shanghai),* 40**,** 426-36.
HACZEYNI, F., BELL-ANDERSON, K. S. & FARRELL, G. C. 2018. Causes and mechanisms of adipocyte enlargement and adipose expansion. *Obes Rev,* 19**,** 406-420.

HAEMMERLE, G., LASS, A., ZIMMERMANN, R., GORKIEWICZ, G., MEYER, C., ROZMAN, J., HELDMAIER, G., MAIER, R., THEUSSL, C., EDER, S., KRATKY, D., WAGNER, E. F., KLINGENSPOR, M., HOEFLER, G. & ZECHNER, R. 2006. Defective lipolysis and altered energy metabolism in mice lacking adipose triglyceride lipase. *Science,* 312**,** 734-7.

HAEMMERLE, G., MOUSTAFA, T., WOELKART, G., BUTTNER, S., SCHMIDT, A., VAN DE WEIJER, T., HESSELINK, M., JAEGER, D., KIENESBERGER, P. C., ZIERLER, K., SCHREIBER, R., EICHMANN, T., KOLB, D., KOTZBECK, P., SCHWEIGER, M., KUMARI, M., EDER, S., SCHOISWOHL, G., WONGSIRIROJ, N., POLLAK, N. M., RADNER, F. P., PREISS-LANDL, K., KOLBE, T., RULICKE, T., PIESKE, B., TRAUNER, M., LASS, A., ZIMMERMANN, R., HOEFLER, G., CINTI, S., KERSHAW, E. E., SCHRAUWEN, P., MADEO, F., MAYER, B. & ZECHNER, R. 2011. ATGL-mediated fat catabolism regulates cardiac mitochondrial function via PPAR-alpha and PGC-1. *Nat Med,* 17**,** 1076-85.

HALAAS, J. L., GAJIWALA, K. S., MAFFEI, M., COHEN, S. L., CHAIT, B. T., RABINOWITZ, D., LALLONE, R. L., BURLEY, S. K. & FRIEDMAN, J. M. 1995. Weight-reducing effects of the plasma protein encoded by the obese gene. *Science,* 269**,** 543-6.

HALBERG, N., WERNSTEDT-ASTERHOLM, I. & SCHERER, P. E. 2008. The adipocyte as an endocrine cell. *Endocrinol Metab Clin North Am,* 37**,** 753-68, x-xi.

HAN, T. S. & LEAN, M. E. J. 2016. A clinical perspective of obesity, metabolic syndrome and cardiovascular disease. *JRSM Cardiovascular Disease,* 5**,** 2048004016633371.

HANSSEN, M. J., VAN DER LANS, A. A., BRANS, B., HOEKS, J., JARDON, K. M., SCHAART, G., MOTTAGHY, F. M., SCHRAUWEN, P. & VAN MARKEN LICHTENBELT, W. D. 2016. Short-term Cold Acclimation Recruits Brown Adipose Tissue in Obese Humans. *Diabetes,* 65**,** 1179-89.

HARGROVE, J. L. & SCHMIDT, F. H. 1989. The role of mRNA and protein stability in gene expression. *Faseb j,* 3**,** 2360-70.

HARPSOE, M. C., BASIT, S., BAGER, P., WOHLFAHRT, J., BENN, C. S., NOHR, E. A., LINNEBERG, A. & JESS, T. 2013. Maternal obesity, gestational weight gain, and risk of asthma and atopic disease in offspring: a study within the Danish National Birth Cohort. *J Allergy Clin Immunol,* 131**,** 1033-40.

HARRIS, R. B. 2012. Sympathetic denervation of one white fat depot changes norepinephrine content and turnover in intact white and brown fat depots. *Obesity (Silver Spring),* 20**,** 1355-64.

HATTORI, T., MURASE, T., OHTAKE, M., INOUE, T., TSUKAMOTO, H., TAKATSU, M., KATO, Y., HASHIMOTO, K., MUROHARA, T. & NAGATA, K. 2011. Characterization of a new animal model of metabolic syndrome: the DahlS.Z-Leprfa/Leprfa rat. *Nutrition &Amp; Diabetes,* 1**,** e1.

HAVENAAR, R., MEIJER, J.C., MORTON, D.B., RITSKES_HOITINGA, J., AND ZWART, P., 2001. 2001. Biology and husbandry of laboratory animals. In: Van Zutphen LFM, Baumans V, Beynene AC (Eds.), Principles of laboratory animal Science,.

HE, W., BARAK, Y., HEVENER, A., OLSON, P., LIAO, D., LE, J., NELSON, M., ONG, E., OLEFSKY, J. M. & EVANS, R. M. 2003. Adipose-specific peroxisome proliferator-activated receptor gamma knockout causes insulin resistance in fat and liver but not in muscle. *Proc Natl Acad Sci U S A,* 100**,** 15712-7.

HEATON, J. M. 1972. The distribution of brown adipose tissue in the human. *Journal of Anatomy,* 112**,** 35-39.
HEGYI, K., FULOP, K., KOVACS, K., TOTH, S. & FALUS, A. 2004. Leptin-induced signal transduction pathways. *Cell Biol Int,* 28**,** 159-69.
HERRERA, E. 2000. Metabolic adaptations in pregnancy and their implications for the availability of substrates to the fetus. *Eur J Clin Nutr,* 54 Suppl 1**,** S47-51.
HERRERA, E. 2002. Lipid metabolism in pregnancy and its consequences in the fetus and newborn. *Endocrine,* 19**,** 43.
HERRERA, E., LASUNCION, M. A., GOMEZ-CORONADO, D., ARANDA, P., LOPEZ-LUNA, P. & MAIER, I. 1988. Role of lipoprotein lipase activity on lipoprotein metabolism and the fate of circulating triglycerides in pregnancy. *Am J Obstet Gynecol,* 158**,** 1575-83.
HERRERA, E. & ORTEGA-SENOVILLA, H. 2010. Maternal lipid metabolism during normal pregnancy and its implications to fetal development. *Clinical Lipidology,* 5**,** 899-911.
HIMMS-HAGEN, J. 1984. Nonshivering thermogenesis. *Brain Res Bull,* 12**,** 151-60.
HIROSHIMA, Y., YAMAMOTO, T., WATANABE, M., BABA, Y. & SHINOHARA, Y. 2018. Effects of cold exposure on metabolites in brown adipose tissue of rats. *Molecular Genetics and Metabolism Reports,* 15**,** 36-42.
HOLLOWELL, J., PILLAS, D., ROWE, R., LINSELL, L., KNIGHT, M. & BROCKLEHURST, P. 2014. The impact of maternal obesity on intrapartum outcomes in otherwise low risk women: secondary analysis of the Birthplace national prospective cohort study. *BJOG : an international journal of obstetrics and gynaecology,* 121**,** 343-355.
HONDARES, E., MORA, O., YUBERO, P., RODRIGUEZ DE LA CONCEPCION, M., IGLESIAS, R., GIRALT, M. & VILLARROYA, F. 2006. Thiazolidinediones and rexinoids induce peroxisome proliferator-activated receptor-coactivator (PGC)-1alpha gene transcription: an autoregulatory loop controls PGC-1alpha expression in adipocytes via peroxisome proliferator-activated receptor-gamma coactivation. *Endocrinology,* 147**,** 2829-38.
HOTAMISLIGIL, G. S., SHARGILL, N. S. & SPIEGELMAN, B. M. 1993. Adipose expression of tumor necrosis factor-alpha: direct role in obesity-linked insulin resistance. *Science,* 259**,** 87-91.
HULL, H. R., DINGER, M. K., KNEHANS, A. W., THOMPSON, D. M. & FIELDS, D. A. 2008. Impact of maternal body mass index on neonate birthweight and body composition. *Am J Obstet Gynecol,* 198**,** 416.e1-6.
HWANG, J. J., YECKEL, C. W., GALLEZOT, J.-D., AGUIAR, R. B.-D., ERSAHIN, D., GAO, H., KAPINOS, M., NABULSI, N., HUANG, Y., CHENG, D., CARSON, R. E., SHERWIN, R. & DING, Y.-S. 2015. Imaging human brown adipose tissue under room temperature conditions with (11)C-MRB, a selective norepinephrine transporter PET ligand. *Metabolism: clinical and experimental,* 64**,** 747-755.
IANNACCONE, P. M. & JACOB, H. J. 2009. Rats! *Disease Models & Mechanisms,* 2**,** 206-210.
IKEDA, K., KANG, Q., YONESHIRO, T., CAMPOREZ, J. P., MAKI, H., HOMMA, M., SHINODA, K., CHEN, Y., LU, X., MARETICH, P., TAJIMA, K., AJUWON, K. M., SOGA, T. & KAJIMURA, S. 2017. UCP1-independent signaling involving SERCA2b-mediated calcium cycling regulates beige fat thermogenesis and systemic glucose homeostasis. *Nature medicine,* 23**,** 1454-1465.

IKEDA, K., MARETICH, P. & KAJIMURA, S. 2018. The Common and Distinct Features of Brown and Beige Adipocytes. *Trends Endocrinol Metab,* 29**,** 191-200.

IMAI, T., TAKAKUWA, R., MARCHAND, S., DENTZ, E., BORNERT, J. M., MESSADDEQ, N., WENDLING, O., MARK, M., DESVERGNE, B., WAHLI, W., CHAMBON, P. & METZGER, D. 2004. Peroxisome proliferator-activated receptor gamma is required in mature white and brown adipocytes for their survival in the mouse. *Proc Natl Acad Sci U S A,* 101**,** 4543-7.

IRSHAD, Z., DIMITRI, F., CHRISTIAN, M. & ZAMMIT, V. A. 2017. Diacylglycerol acyltransferase 2 links glucose utilization to fatty acid oxidation in the brown adipocytes. *J Lipid Res,* 58**,** 15-30.

IWASAKI, Y., MORITA, A., IWASAWA, T., KOBATA, K., SEKIWA, Y., MORIMITSU, Y., KUBOTA, K. & WATANABE, T. 2006. A nonpungent component of steamed ginger--[10]-shogaol--increases adrenaline secretion via the activation of TRPV1. *Nutr Neurosci,* 9**,** 169-78.

JAKUS, P. B., SANDOR, A., JANAKY, T. & FARKAS, V. 2008. Cooperation between BAT and WAT of rats in thermogenesis in response to cold, and the mechanism of glycogen accumulation in BAT during reacclimation. *J Lipid Res,* 49**,** 332-9.

JEON, J. Y., STEADWARD, R. D., WHEELER, G. D., BELL, G., MCCARGAR, L. & HARBER, V. 2003. Intact sympathetic nervous system is required for leptin effects on resting metabolic rate in people with spinal cord injury. *J Clin Endocrinol Metab,* 88**,** 402-7.

JIANG, T., WANG, Z., PROCTOR, G., MOSKOWITZ, S., LIEBMAN, S. E., ROGERS, T., LUCIA, M. S., LI, J. & LEVI, M. 2005. Diet-induced obesity in C57BL/6J mice causes increased renal lipid accumulation and glomerulosclerosis via a sterol regulatory element-binding protein-1c-dependent pathway. *J Biol Chem,* 280**,** 32317-25.

JIMENEZ-PREITNER, M., BERNEY, X., ULDRY, M., VITALI, A., CINTI, S., LEDFORD, J. G. & THORENS, B. 2011. Plac8 is an inducer of C/EBPbeta required for brown fat differentiation, thermoregulation, and control of body weight. *Cell Metab,* 14**,** 658-70.

JIMENEZ, M., LEGER, B., CANOLA, K., LEHR, L., ARBOIT, P., SEYDOUX, J., RUSSELL, A. P., GIACOBINO, J. P., MUZZIN, P. & PREITNER, F. 2002. Beta(1)/beta(2)/beta(3)-adrenoceptor knockout mice are obese and cold-sensitive but have normal lipolytic responses to fasting. *FEBS Lett,* 530**,** 37-40.

JOCKEN, J. W. E., LANGIN, D., SMIT, E., SARIS, W. H. M., VALLE, C., HUL, G. B., HOLM, C., ARNER, P. & BLAAK, E. E. 2007. Adipose Triglyceride Lipase and Hormone-Sensitive Lipase Protein Expression Is Decreased in the Obese Insulin-Resistant State. *The Journal of Clinical Endocrinology & Metabolism,* 92**,** 2292-2299.

JOHANNSEN, D. L., KNUTH, N. D., HUIZENGA, R., ROOD, J. C., RAVUSSIN, E. & HALL, K. D. 2012. Metabolic Slowing with Massive Weight Loss despite Preservation of Fat-Free Mass. *The Journal of Clinical Endocrinology and Metabolism,* 97**,** 2489-2496.

JONES, D. D., RAMSAY, T. G., HAUSMAN, G. J. & MARTIN, R. J. 1992. Norepinephrine inhibits rat pre-adipocyte proliferation. *Int J Obes Relat Metab Disord,* 16**,** 349-54.

JORGENSEN, J. O., VAHL, N., DALL, R. & CHRISTIANSEN, J. S. 1998. Resting metabolic rate in healthy adults: relation to growth hormone status and leptin levels. *Metabolism,* 47**,** 1134-9.

JUNG, U. J. & CHOI, M. S. 2014. Obesity and its metabolic complications: the role of adipokines and the relationship between obesity, inflammation, insulin resistance, dyslipidemia and nonalcoholic fatty liver disease. *Int J Mol Sci,* 15**,** 6184-223.

K. PANCHAL, S., POUDYAL, H., IYER, A., NAZER, R., ALAM, A., DIWAN, V., KAUTER, K., SERNIA, C., CAMPBELL, F., WARD, L., GOBE, G., FENNING, A. & BROWN, L. 2011. High-carbohydrate, High-fat Diet–induced Metabolic Syndrome and Cardiovascular Remodeling in Rats. *Journal of Cardiovascular Pharmacology,* 57**,** 611-624.

KAARTINEN, J. M., LANOUE, K. F., MARTIN, L. F., VIKMAN, H. L. & OHISALO, J. J. 1995. Beta-adrenergic responsiveness of adenylate cyclase in human adipocyte plasma membranes in obesity and after massive weight reduction. *Metabolism,* 44**,** 1288-92.

KAHN, B. B. 1996. Lilly lecture 1995. Glucose transport: pivotal step in insulin action. *Diabetes,* 45**,** 1644-54.

KAHN, B. B. & FLIER, J. S. 2000. Obesity and insulin resistance. *J Clin Invest,* 106**,** 473-81.

KAIYALA, K. J., OGIMOTO, K., NELSON, J. T., MUTA, K. & MORTON, G. J. 2016. Physiological role for leptin in the control of thermal conductance. *Molecular Metabolism,* 5**,** 892-902.

KANAREK, R. B. & ORTHEN-GAMBILL, N. 1982. Differential effects of sucrose, fructose and glucose on carbohydrate-induced obesity in rats. *J Nutr,* 112**,** 1546-54.

KAWADA, T., WATANABE, T., TAKAISHI, T., TANAKA, T. & IWAI, K. 1986. Capsaicin-induced beta-adrenergic action on energy metabolism in rats: influence of capsaicin on oxygen consumption, the respiratory quotient, and substrate utilization. *Proc Soc Exp Biol Med,* 183**,** 250-6.

KERSHAW, E. E. & FLIER, J. S. 2004. Adipose tissue as an endocrine organ. *J Clin Endocrinol Metab,* 89**,** 2548-56.

KERSHAW, E. E., HAMM, J. K., VERHAGEN, L. A. W., PERONI, O., KATIC, M. & FLIER, J. S. 2006. Adipose Triglyceride Lipase: Function, Regulation by Insulin, and Comparison With Adiponutrin. *Diabetes,* 55**,** 148.

KLANNEMARK, M., ORHO, M., LANGIN, D., LAURELL, H., HOLM, C., REYNISDOTTIR, S., ARNER, P. & GROOP, L. 1998. The putative role of the hormone-sensitive lipase gene in the pathogenesis of Type II diabetes mellitus and abdominal obesity. *Diabetologia,* 41**,** 1516-22.

KLAUS, S., SEIVERT, A. & BOEUF, S. 2001. Effect of the β3-adrenergic agonist Cl316,243 on functional differentiation of white and brown adipocytes in primary cell culture. *Biochimica et Biophysica Acta (BBA) - Molecular Cell Research,* 1539**,** 85-92.

KLINGENSPOR 2012. M. a. F., T. in Adipose Tissue Biology (ed ME Symonds) *39-69. Springer Science+Business Media*.

KOOIJMAN, S., WANG, Y., PARLEVLIET, E. T., BOON, M. R., EDELSCHAAP, D., SNATERSE, G., PIJL, H., ROMIJN, J. A. & RENSEN, P. C. N. 2015. Central GLP-1 receptor signalling accelerates plasma clearance of triacylglycerol and glucose by activating brown adipose tissue in mice. *Diabetologia,* 58**,** 2637-2646.

KOPECKY, J., CLARKE, G., ENERBACK, S., SPIEGELMAN, B. & KOZAK, L. P. 1995. Expression of the mitochondrial uncoupling protein gene from the aP2 gene promoter prevents genetic obesity. *J Clin Invest,* 96**,** 2914-23.

KOUPIL, I. & TOIVANEN, P. 2008. Social and early-life determinants of overweight and obesity in 18-year-old Swedish men. *Int J Obes (Lond),* 32**,** 73-81.
KOWALSKI, G. M., KRAAKMAN, M. J., MASON, S. A., MURPHY, A. J. & BRUCE, C. R. 2017. Resolution of glucose intolerance in long-term high-fat, high-sucrose-fed mice. *The Journal of endocrinology,* 233**,** 269.
KRAMAROVA, T. V., SHABALINA, I. G., ANDERSSON, U., WESTERBERG, R., CARLBERG, I., HOUSTEK, J., NEDERGAARD, J. & CANNON, B. 2008. Mitochondrial ATP synthase levels in brown adipose tissue are governed by the c-Fo subunit P1 isoform. *Faseb j,* 22**,** 55-63.
L SMALL, H. G. E. A. 2018. Thermoneutral housing does not influence fat mass or glucose homeostasis in C57BL/6 mice. *Journal of Endocrinology,* 239:3 313–324.
LABBÉ, S. M., CARON, A., BAKAN, I., LAPLANTE, M., CARPENTIER, A. C., LECOMTE, R. & RICHARD, D. 2015. In vivo measurement of energy substrate contribution to cold-induced brown adipose tissue thermogenesis. *The FASEB Journal,* 29**,** 2046-2058.
LAIN, K. Y. & CATALANO, P. M. 2007. Metabolic changes in pregnancy. *Clin Obstet Gynecol,* 50**,** 938-48.
LANDSBERG, L. Y., J. B. 1992. Catecholamines and the adrenal medulla. . *n Williams Textbook of Endrocrinology* 8th edn (eds Wilson, J. D. & Foster, D. W.) 621–705 (W.B. Saunders, Philadelphia, 1992).
LANGEVELD, M., TAN, C. Y., SOETERS, M. R., VIRTUE, S., AMBLER, G. K., WATSON, L. P. E., MURGATROYD, P. R., CHATTERJEE, V. K. & VIDAL-PUIG, A. 2016. Mild cold effects on hunger, food intake, satiety and skin temperature in humans. *Endocrine Connections,* 5**,** 65-73.
LANGNAESE, K., JOHN, R., SCHWEIZER, H., EBMEYER, U. & KEILHOFF, G. 2008. Selection of reference genes for quantitative real-time PCR in a rat asphyxial cardiac arrest model. *BMC Molecular Biology,* 9**,** 53.
LARGE, V., REYNISDOTTIR, S., LANGIN, D., FREDBY, K., KLANNEMARK, M., HOLM, C. & ARNER, P. 1999. Decreased expression and function of adipocyte hormone-sensitive lipase in subcutaneous fat cells of obese subjects. *J Lipid Res,* 40**,** 2059-66.
LAW, J., CHALMERS, J., MORRIS, D. E., ROBINSON, L., BUDGE, H. & SYMONDS, M. E. 2018. The use of infrared thermography in the measurement and characterization of brown adipose tissue activation. *Temperature,* 5**,** 147-161.
LEDDY, M. A., POWER, M. L. & SCHULKIN, J. 2008. The Impact of Maternal Obesity on Maternal and Fetal Health. *Reviews in Obstetrics and Gynecology,* 1**,** 170-178.
LEIBEL, R. L., ROSENBAUM, M. & HIRSCH, J. 1995. Changes in energy expenditure resulting from altered body weight. *N Engl J Med,* 332**,** 621-8.
LEPPER, C. & FAN, C. M. 2010. Inducible lineage tracing of Pax7-descendant cells reveals embryonic origin of adult satellite cells. *Genesis,* 48**,** 424-36.
LETURQUE, A., FERRE, P., BURNOL, A. F., KANDE, J., MAULARD, P. & GIRARD, J. 1986. Glucose utilization rates and insulin sensitivity in vivo in tissues of virgin and pregnant rats. *Diabetes,* 35**,** 172-7.
LI, B., NOLTE, L. A., JU, J. S., HAN, D. H., COLEMAN, T., HOLLOSZY, J. O. & SEMENKOVICH, C. F. 2000. Skeletal muscle respiratory uncoupling prevents diet-induced obesity and insulin resistance in mice. *Nat Med,* 6**,** 1115-20.
LI, Y., FROMME, T., SCHWEIZER, S., SCHOTTL, T. & KLINGENSPOR, M. 2014. Taking control over intracellular fatty acid levels is essential for the analysis of

thermogenic function in cultured primary brown and brite/beige adipocytes. *EMBO Rep,* 15**,** 1069-76.

LICINIO, J., CAGLAYAN, S., OZATA, M., YILDIZ, B. O., DE MIRANDA, P. B., O'KIRWAN, F., WHITBY, R., LIANG, L., COHEN, P., BHASIN, S., KRAUSS, R. M., VELDHUIS, J. D., WAGNER, A. J., DEPAOLI, A. M., MCCANN, S. M. & WONG, M.-L. 2004. Phenotypic effects of leptin replacement on morbid obesity, diabetes mellitus, hypogonadism, and behavior in leptin-deficient adults. *Proceedings of the National Academy of Sciences of the United States of America,* 101**,** 4531-4536.

LIDELL, M. E., BETZ, M. J., DAHLQVIST LEINHARD, O., HEGLIND, M., ELANDER, L., SLAWIK, M., MUSSACK, T., NILSSON, D., ROMU, T., NUUTILA, P., VIRTANEN, K. A., BEUSCHLEIN, F., PERSSON, A., BORGA, M. & ENERBACK, S. 2013. Evidence for two types of brown adipose tissue in humans. *Nat Med,* 19**,** 631-4.

LILLIOJA, S., MOTT, D. M., SPRAUL, M., FERRARO, R., FOLEY, J. E., RAVUSSIN, E., KNOWLER, W. C., BENNETT, P. H. & BOGARDUS, C. 1993. Insulin resistance and insulin secretory dysfunction as precursors of non-insulin-dependent diabetes mellitus. Prospective studies of Pima Indians. *N Engl J Med,* 329**,** 1988-92.

LIN, J., WU, P. H., TARR, P. T., LINDENBERG, K. S., ST-PIERRE, J., ZHANG, C. Y., MOOTHA, V. K., JAGER, S., VIANNA, C. R., REZNICK, R. M., CUI, L., MANIERI, M., DONOVAN, M. X., WU, Z., COOPER, M. P., FAN, M. C., ROHAS, L. M., ZAVACKI, A. M., CINTI, S., SHULMAN, G. I., LOWELL, B. B., KRAINC, D. & SPIEGELMAN, B. M. 2004. Defects in adaptive energy metabolism with CNS-linked hyperactivity in PGC-1alpha null mice. *Cell,* 119**,** 121-35.

LINDGREN, EVA M., NIELSEN, R., PETROVIC, N., JACOBSSON, A., MANDRUP, S., CANNON, B. & NEDERGAARD, J. 2004. Noradrenaline represses PPAR (peroxisome-proliferator-activated receptor) γ2 gene expression in brown adipocytes: intracellular signalling and effects on PPARγ2 and PPARγ1 protein levels. *Biochemical Journal,* 382**,** 597-606.

LIU, X., ROSSMEISL, M., MCCLAINE, J., RIACHI, M., HARPER, M. E. & KOZAK, L. P. 2003. Paradoxical resistance to diet-induced obesity in UCP1-deficient mice. *J Clin Invest,* 111**,** 399-407.

LIVAK, K. J. & SCHMITTGEN, T. D. 2001. Analysis of relative gene expression data using real-time quantitative PCR and the 2(-Delta Delta C(T)) Method. *Methods,* 25**,** 402-8.

LOCHE, E., BLACKMORE, H. L., CARPENTER, A. A., BEESON, J. H., PINNOCK, A., ASHMORE, T. J., AIKEN, C. E., DE ALMEIDA-FARIA, J., SCHOONEJANS, J. M., GIUSSANI, D. A., FERNANDEZ-TWINN, D. S. & OZANNE, S. E. 2018. Maternal diet-induced obesity programmes cardiac dysfunction in male mice independently of post-weaning diet. *Cardiovasc Res,* 114**,** 1372-1384.

LOFGREN, P., HOFFSTEDT, J., RYDEN, M., THORNE, A., HOLM, C., WAHRENBERG, H. & ARNER, P. 2002. Major gender differences in the lipolytic capacity of abdominal subcutaneous fat cells in obesity observed before and after long-term weight reduction. *J Clin Endocrinol Metab,* 87**,** 764-71.

LONCAR, D. 1991. Convertible adipose tissue in mice. *Cell Tissue Res,* 266**,** 149-61.

LONG, J. Z., SVENSSON, K. J., TSAI, L., ZENG, X., ROH, H. C., KONG, X., RAO, R. R., LOU, J., LOKURKAR, I., BAUR, W., CASTELLOT, J. J., JR., ROSEN, E. D.

& SPIEGELMAN, B. M. 2014. A smooth muscle-like origin for beige adipocytes. *Cell Metab,* 19**,** 810-20.
LONGHURST, J. C., KAUFMAN, M. P., ORDWAY, G. A. & MUSCH, T. I. 1984. Effects of bradykinin and capsaicin on endings of afferent fibers from abdominal visceral organs. *Am J Physiol,* 247**,** R552-9.
LOPEZ-LUNA, P., MAIER, I. & HERRERA, E. 1991. Carcass and tissue fat content in the pregnant rat. *Biol Neonate,* 60**,** 29-38.
LÓPEZ-SOLDADO, I., ORTEGA-SENOVILLA, H. & HERRERA, E. 2017. Maternal adipose tissue becomes a source of fatty acids for the fetus in fasted pregnant rats given diets with different fatty acid compositions. *European journal of nutrition*.
LOPEZ, M., TOVAR, S., VAZQUEZ, M. J., WILLIAMS, L. M. & DIEGUEZ, C. 2007. Peripheral tissue-brain interactions in the regulation of food intake. *Proc Nutr Soc,* 66**,** 131-55.
LUKASZEWSKI, M.-A., EBERLÉ, D., VIEAU, D. & BRETON, C. 2013. Nutritional manipulations in the perinatal period program adipose tissue in offspring. *American Journal of Physiology - Endocrinology And Metabolism,* 305**,** E1195.
MACDOUGALD, O. A., HWANG, C. S., FAN, H. & LANE, M. D. 1995. Regulated expression of the obese gene product (leptin) in white adipose tissue and 3T3-L1 adipocytes. *Proceedings of the National Academy of Sciences of the United States of America,* 92**,** 9034-9037.
MACHINAL-QUELIN, F., DIEUDONNE, M. N., LENEVEU, M. C., PECQUERY, R. & GIUDICELLI, Y. 2002. Proadipogenic effect of leptin on rat preadipocytes in vitro: activation of MAPK and STAT3 signaling pathways. *Am J Physiol Cell Physiol,* 282**,** C853-63.
MAFFEI, M., HALAAS, J., RAVUSSIN, E., PRATLEY, R., LEE, G., ZHANG, Y., FEI, H., KIM, S., LALLONE, R. & RANGANATHAN, S. 1995. Leptin levels in human and rodent: measurement of plasma leptin and ob RNA in obese and weight-reduced subjects. *Nature medicine,* 1**,** 1155-1161.
MALCOLM, R. D. & ALKANA, R. L. 1983. Temperature dependence of ethanol lethality in mice. *J Pharm Pharmacol,* 35**,** 306-11.
MALONEY, S. K., FULLER, A., MITCHELL, D., GORDON, C. & OVERTON, J. M. 2014. Translating animal model research: does it matter that our rodents are cold? *Physiology (Bethesda),* 29**,** 413-20.
MANTZOROS, C. S., QU, D., FREDERICH, R. C., SUSULIC, V. S., LOWELL, B. B., MARATOS-FLIER, E. & FLIER, J. S. 1996. Activation of beta(3) adrenergic receptors suppresses leptin expression and mediates a leptin-independent inhibition of food intake in mice. *Diabetes,* 45**,** 909-14.
MARK, P. J., SMITH, J. T. & WADDELL, B. J. 2006. Placental and Fetal Growth Retardation Following Partial Progesterone Withdrawal in Rat Pregnancy. *Placenta,* 27**,** 208-214.
MARQUES, C., MEIRELES, M., NORBERTO, S., LEITE, J., FREITAS, J., PESTANA, D., FARIA, A. & CALHAU, C. 2016. High-fat diet-induced obesity Rat model: a comparison between Wistar and Sprague-Dawley Rat. *Adipocyte,* 5**,** 11-21.
MARTIN-GRONERT, M. S. & OZANNE, S. E. 2007. Experimental IUGR and later diabetes. *J Intern Med,* 261**,** 437-52.
MARTIN-HIDALGO, A., HOLM, C., BELFRAGE, P., SCHOTZ, M. C. & HERRERA, E. 1994. Lipoprotein lipase and hormone-sensitive lipase activity and mRNA in rat adipose tissue during pregnancy. *Am J Physiol,* 266**,** E930-5.

MARTINEAU, M. G., RAKER, C., DIXON, P. H., CHAMBERS, J., MACHIRORI, M., KING, N. M., HOOKS, M. L., MANOHARAN, R., CHEN, K., POWRIE, R. & WILLIAMSON, C. 2015. The metabolic profile of intrahepatic cholestasis of pregnancy is associated with impaired glucose tolerance, dyslipidemia, and increased fetal growth. *Diabetes Care,* 38**,** 243-8.

MARTINS, P. N. A. 2003. The importance of experimental microsurgery for transplantation. *Acta Cirurgica Brasileira,* 18**,** 01-06.

MASON, D. Y. & SAMMONS, R. 1978. Alkaline phosphatase and peroxidase for double immunoenzymatic labelling of cellular constituents. *Journal of Clinical Pathology,* 31**,** 454.

MASUZAKI, H., OGAWA, Y., ISSE, N., SATOH, N., OKAZAKI, T., SHIGEMOTO, M., MORI, K., TAMURA, N., HOSODA, K., YOSHIMASA, Y. & ET AL. 1995. Human obese gene expression. Adipocyte-specific expression and regional differences in the adipose tissue. *Diabetes,* 44**,** 855-8.

MATSUMOTO, T., MIYAWAKI, C., UE, H., YUASA, T., MIYATSUJI, A. & MORITANI, T. 2000. Effects of capsaicin-containing yellow curry sauce on sympathetic nervous system activity and diet-induced thermogenesis in lean and obese young women. *J Nutr Sci Vitaminol (Tokyo),* 46**,** 309-15.

MCILVRIDE, S., MUSHTAQ, A., PAPACLEOVOULOU, G., HURLING, C., STEEL, J., JANSEN, E., ABU-HAYYEH, S. & WILLIAMSON, C. 2017. A progesterone-brown fat axis is involved in regulating fetal growth. *Scientific reports,* 7**,** 10671-10671.

MCLAUGHLIN, C. L. & BAILE, C. A. 1981. Ontogeny of feeding behavior in the Zucker obese rat. *Physiol Behav,* 26**,** 607-12.

MCMANUS, L. M. & MITCHELL, R. N. 2014. *Pathobiology of human disease: a dynamic encyclopedia of disease mechanisms*, Elsevier.

MCMULLEN, S. & MOSTYN, A. 2009. Animal models for the study of the developmental origins of health and disease. *Proc Nutr Soc,* 68**,** 306-20.

MILLS, J. L., JOVANOVIC, L., KNOPP, R., AARONS, J., CONLEY, M., PARK, E., LEE, Y. J., HOLMES, L., SIMPSON, J. L. & METZGER, B. 1998. Physiological reduction in fasting plasma glucose concentration in the first trimester of normal pregnancy: the diabetes in early pregnancy study. *Metabolism,* 47**,** 1140-4.

MINOKOSHI, Y., HAQUE, M. S. & SHIMAZU, T. 1999. Microinjection of leptin into the ventromedial hypothalamus increases glucose uptake in peripheral tissues in rats. *Diabetes,* 48**,** 287-91.

MORGAN, K. L., RAHMAN, M. A., MACEY, S., ATKINSON, M. D., HILL, R. A., KHANOM, A., PARANJOTHY, S., HUSAIN, M. J. & BROPHY, S. T. 2014. Obesity in pregnancy: a retrospective prevalence-based study on health service utilisation and costs on the NHS. *BMJ Open,* 4.

MORRONI, M., BARBATELLI, G., ZINGARETTI, M. C. & CINTI, S. 1995. Immunohistochemical, ultrastructural and morphometric evidence for brown adipose tissue recruitment due to cold acclimation in old rats. *Int J Obes Relat Metab Disord,* 19**,** 126-31.

MOY, F. M. & BULGIBA, A. 2010. The modified NCEP ATP III criteria maybe better than the IDF criteria in diagnosing Metabolic Syndrome among Malays in Kuala Lumpur. *BMC public health,* 10**,** 678-678.

MUHLHAUSLER, B. S., MCMILLEN, I. C., ROUZAUD, G., FINDLAY, P. A., MARROCCO, E. M., RHIND, S. M. & ADAM, C. L. 2004. Appetite regulatory neuropeptides are expressed in the sheep hypothalamus before birth. *J Neuroendocrinol,* 16**,** 502-7.

MUND, R. A. & FRISHMAN, W. H. 2013. Brown adipose tissue thermogenesis: beta3-adrenoreceptors as a potential target for the treatment of obesity in humans. *Cardiol Rev,* 21**,** 265-9.

MUNILLA, M. A. & HERRERA, E. 2000. Maternal Hypertriglyceridemia during Late Pregnancy Does Not Affect the Increase in Circulating Triglycerides Caused by the Long-Term Consumption of a Sucrose-Rich Diet by Rats. *The Journal of Nutrition,* 130**,** 2883-2888.

MURASE, T., MIZUNO, T., OMACHI, T., ONIZAWA, K., KOMINE, Y., KONDO, H., HASE, T. & TOKIMITSU, I. 2001. Dietary diacylglycerol suppresses high fat and high sucrose diet-induced body fat accumulation in C57BL/6J mice. *J Lipid Res,* 42**,** 372-8.

MUSIAL, B., VAUGHAN, O. R., FERNANDEZ-TWINN, D. S., VOSHOL, P., OZANNE, S. E., FOWDEN, A. L. & SFERRUZZI-PERRI, A. N. 2017. A Western-style obesogenic diet alters maternal metabolic physiology with consequences for fetal nutrient acquisition in mice. *The Journal of Physiology,* 595**,** 4875-4892.

NEDERGAARD, J., BENGTSSON, T. & CANNON, B. 2007. Unexpected evidence for active brown adipose tissue in adult humans. *Am J Physiol Endocrinol Metab,* 293**,** E444-52.

NEDERGAARD, J., GOLOZOUBOVA, V., MATTHIAS, A., ASADI, A., JACOBSSON, A. & CANNON, B. 2001. UCP1: the only protein able to mediate adaptive non-shivering thermogenesis and metabolic inefficiency. *Biochim Biophys Acta,* 1504**,** 82-106.

NEDERGAARD, J., PETROVIC, N., LINDGREN, E. M., JACOBSSON, A. & CANNON, B. 2005. PPARγ in the control of brown adipocyte differentiation. *Biochimica et Biophysica Acta (BBA) - Molecular Basis of Disease,* 1740**,** 293-304.

NELSON, S. M., MATTHEWS, P. & POSTON, L. 2010. Maternal metabolism and obesity: modifiable determinants of pregnancy outcome. *Hum Reprod Update,* 16**,** 255-75.

NHS 2018. Statistics on Obesity, Physical activity and Diet. England: 2018.

NICE 2006. besity: The Prevention, Identification, Assessment and Management of Overweight and Obesity in Adults and Children. *Centre for Public Health Excellence at NICE (UK); National Collaborating Centre for Primary Care (UK).* NICE Clinical Guidelines, No. 43.

NICULESCU, M. D. & LUPU, D. S. 2009. High fat diet-induced maternal obesity alters fetal hippocampal development. *International journal of developmental neuroscience : the official journal of the International Society for Developmental Neuroscience,* 27**,** 627-633.

NIH 2017. What are some common pregnancy complications

NIVOIT, P., MORENS, C., VAN ASSCHE, F. A., JANSEN, E., POSTON, L., REMACLE, C. & REUSENS, B. 2009. Established diet-induced obesity in female rats leads to offspring hyperphagia, adiposity and insulin resistance. *Diabetologia,* 52**,** 1133-42.

NNODIM, J. O. 1988. Stereological assessment of age-related changes in lipid droplet surface area and vascular volume in rat interscapular brown adipose tissue. *Anat Rec,* 220**,** 357-63.

NONOGAKI, K. 2000. New insights into sympathetic regulation of glucose and fat metabolism. *Diabetologia,* 43**,** 533-49.

NONOGAKI, K. & IGUCHI, A. 1997a. Role of central neural mechanisms in the regulation of hepatic glucose metabolism. *Life Sci,* 60**,** 797-807.

NONOGAKI, K. & IGUCHI, A. 1997b. Stress, acute hyperglycemia, and hyperlipidemia role of the autonomic nervous system and cytokines. *Trends Endocrinol Metab,* 8**,** 192-7.

NOVOSELOVA, T. V., LARDER, R., RIMMINGTON, D., LELLIOTT, C., WYNN, E. H., GORRIGAN, R. J., TATE, P. H., GUASTI, L., THE SANGER MOUSE GENETICS, P., O'RAHILLY, S., CLARK, A. J. L., LOGAN, D. W., COLL, A. P. & CHAN, L. F. 2016. Loss of Mrap2 is associated with Sim1 deficiency and increased circulating cholesterol. *The Journal of Endocrinology,* 230**,** 13-26.

NRC 2011. Committee for the update of the guide for the care and use of laboratory animals, Institute for Laboratory Animal Research Guide for the care and use of laboratory animals (eighth ed.), National Research Council of the National Academies, The National Academies Press, Washington, DC. 2011. .

OKADA, K., LECLAIR, K. B., ZHANG, Y., LI, Y., OZDEMIR, C., KRISKO, T. I., HAGEN, S. J., BETENSKY, R. A., BANKS, A. S. & COHEN, D. E. 2016. Thioesterase superfamily member 1 suppresses cold thermogenesis by limiting the oxidation of lipid droplet-derived fatty acids in brown adipose tissue. *Molecular Metabolism,* 5**,** 340-351.

OKAMATSU-OGURA, Y., FUKANO, K., TSUBOTA, A., UOZUMI, A., TERAO, A., KIMURA, K. & SAITO, M. 2013. Thermogenic Ability of Uncoupling Protein 1 in Beige Adipocytes in Mice. *PLoS ONE,* 8**,** e84229.

OKUMURA, Y., NARUKAWA, M., IWASAKI, Y., ISHIKAWA, A., MATSUDA, H., YOSHIKAWA, M. & WATANABE, T. 2010. Activation of TRPV1 and TRPA1 by black pepper components. *Biosci Biotechnol Biochem,* 74**,** 1068-72.

OSUGA, J.-I., ISHIBASHI, S., OKA, T., YAGYU, H., TOZAWA, R., FUJIMOTO, A., SHIONOIRI, F., YAHAGI, N., KRAEMER, F. B., TSUTSUMI, O. & YAMADA, N. 2000. Targeted disruption of hormone-sensitive lipase results in male sterility and adipocyte hypertrophy, but not in obesity. *Proceedings of the National Academy of Sciences,* 97**,** 787-792.

OTWAY, S. & ROBINSON, D. S. 1968. The significance of changes in tissue clearing-factor lipase activity in relation to the lipaemia of pregnancy. *The Biochemical journal,* 106**,** 677-682.

OVALLE, W. K. 2013. *Netter's essential histology / William K. Ovalle, Patrick C. Nahirney ; illustrations by Frank H. Netter, contributing illustrators, Joe Chovan ... [et al.],* Philadelphia, PA, Philadelphia, PA : Elsevier/Saunders.

OVERTON, J. M. 2010. Phenotyping small animals as models for the human metabolic syndrome: thermoneutrality matters. *Int J Obes (Lond),* 34 Suppl 2**,** S53-8.

PALACÍN, M., LASUNCIÓN, M. A., ASUNCIÓN, M. & HERRERA, E. 1991. Circulating metabolite utilization by periuterine adipose tissue in situ in the pregnant rat. *Metabolism,* 40**,** 534-539.

PANG, X., ZHAO, J., ZHANG, W., ZHUANG, X., WANG, J., XU, R., XU, Z. & QU, W. 2008. Antihypertensive effect of total flavones extracted from seed residues of Hippophae rhamnoides L. in sucrose-fed rats. *J Ethnopharmacol,* 117**,** 325-31.

PARK, A., KIM, W. K. & BAE, K.-H. 2014. Distinction of white, beige and brown adipocytes derived from mesenchymal stem cells. *World Journal of Stem Cells,* 6**,** 33-42.

PELLEYMOUNTER, M. A., CULLEN, M. J., BAKER, M. B., HECHT, R., WINTERS, D., BOONE, T. & COLLINS, F. 1995. Effects of the obese gene product on body weight regulation in ob/ob mice. *Science,* 269**,** 540-3.

PERRY, P. 2007. The Ethics of Animal Research: A UK Perspective. *ILAR Journal,* 48**,** 42-46.
PFAFFL, M. W. 2001. A new mathematical model for relative quantification in real-time RT–PCR. *Nucleic Acids Research,* 29**,** e45-e45.
PIAO, Y., LIU, Y. & XIE, X. 2013. Change Trends of Organ Weight Background Data in Sprague Dawley Rats at Different Ages. *Journal of Toxicologic Pathology,* 26**,** 29-34.
POOLE, S. & STEPHENSON, J. D. 1977. Body temperature regulation and thermoneutrality in rats. *Q J Exp Physiol Cogn Med Sci,* 62**,** 143-9.
PUERTA, M., ABELENDA, M., ROCHA, M. & TRAYHURN, P. 2002. Effect of acute cold exposure on the expression of the adiponectin, resistin and leptin genes in rat white and brown adipose tissues. *Horm Metab Res,* 34**,** 629-34.
PUIGSERVER, P., WU, Z., PARK, C. W., GRAVES, R., WRIGHT, M. & SPIEGELMAN, B. M. 1998. A cold-inducible coactivator of nuclear receptors linked to adaptive thermogenesis. *Cell,* 92**,** 829-39.
PUJOL, E., PROENZA, A., LLADO, I. & ROCA, P. 2005. Pregnancy effects on rat adipose tissue lipolytic capacity are dependent on anatomical location. *Cell Physiol Biochem,* 16**,** 229-36.
RADESKY, J. S., OKEN, E., RIFAS-SHIMAN, S. L., KLEINMAN, K. P., RICH-EDWARDS, J. W. & GILLMAN, M. W. 2008. Diet during early pregnancy and development of gestational diabetes. *Paediatr Perinat Epidemiol,* 22**,** 47-59.
RAGAB, S. M. M., ABD ELGHAFFAR, S. K., EL-METWALLY, T. H., BADR, G., MAHMOUD, M. H. & OMAR, H. M. 2015. Effect of a high fat, high sucrose diet on the promotion of non-alcoholic fatty liver disease in male rats: the ameliorative role of three natural compounds. *Lipids in Health and Disease,* 14**,** 83.
RAMOS-VARA, J. A. 2005. Technical Aspects of Immunohistochemistry. *Veterinary Pathology,* 42**,** 405-426.
RAMOS, M. P., CRESPO-SOLANS, M. D., DEL CAMPO, S., CACHO, J. & HERRERA, E. 2003. Fat accumulation in the rat during early pregnancy is modulated by enhanced insulin responsiveness. *Am J Physiol Endocrinol Metab,* 285**,** E318-28.
RAVELLI, A. C., VAN DER MEULEN, J. H., MICHELS, R. P., OSMOND, C., BARKER, D. J., HALES, C. N. & BLEKER, O. P. 1998. Glucose tolerance in adults after prenatal exposure to famine. *Lancet,* 351**,** 173-7.
RAVELLI, A. C., VAN DER MEULEN, J. H., OSMOND, C., BARKER, D. J. & BLEKER, O. P. 1999. Obesity at the age of 50 y in men and women exposed to famine prenatally. *Am J Clin Nutr,* 70**,** 811-6.
RAVUSSIN, Y., XIAO, C., GAVRILOVA, O. & REITMAN, M. L. 2014. Effect of Intermittent Cold Exposure on Brown Fat Activation, Obesity, and Energy Homeostasis in Mice. *PLoS ONE,* 9**,** e85876.
REISCHL, U. & KOCHANOWSKI, B. 1999. Quantitative PCR. *In:* KOCHANOWSKI, B. & REISCHL, U. (eds.) *Quantitative PCR Protocols.* Totowa, NJ: Humana Press.
REYNISDOTTIR, S., ELLERFELDT, K., WAHRENBERG, H., LITHELL, H. & ARNER, P. 1994. Multiple lipolysis defects in the insulin resistance (metabolic) syndrome. *J Clin Invest,* 93**,** 2590-9.
RICCIOLINI, R., SCALIBASTRI, M., CARMINATI, P. & ARDUINI, A. 2001. The effect of pivalate treatment of pregnant rats on body mass and insulin levels in the adult offspring. *Life Sci,* 69**,** 1733-8.

ROBIDOUX, J., MARTIN, T. L. & COLLINS, S. 2004. Beta-adrenergic receptors and regulation of energy expenditure: a family affair. *Annu Rev Pharmacol Toxicol,* 44**,** 297-323.

ROBINSON, L., OJHA, S., SYMONDS, M. E. & BUDGE, H. 2014. Body mass index as a determinant of brown adipose tissue function in healthy children. *J Pediatr,* 164**,** 318-22.e1.

ROCHA, M., BING, C., WILLIAMS, G. & PUERTA, M. 2003. Pregnancy-induced hyperphagia is associated with increased gene expression of hypothalamic agouti-related peptide in rats. *Regulatory Peptides,* 114**,** 159-165.

RODEL, H. G., PRAGER, G., STEFANSKI, V., VON HOLST, D. & HUDSON, R. 2008. Separating maternal and litter-size effects on early postnatal growth in two species of altricial small mammals. *Physiol Behav,* 93**,** 826-34.

ROHRER, D. K. 1998. Physiological consequences of beta-adrenergic receptor disruption. *J Mol Med (Berl),* 76**,** 764-72.

ROLLS, B. A., GURR, M. I., VAN DUIJVENVOORDE, P. M., ROLLS, B. J. & ROWE, E. A. 1986. Lactation in lean and obese rats: effect of cafeteria feeding and of dietary obesity on milk composition. *Physiol Behav,* 38**,** 185-90.

ROMERO MDEL, M., ROY, S., POUILLOT, K., FEITO, M., ESTEVE, M., GRASA MDEL, M., FERNANDEZ-LOPEZ, J. A., ALEMANY, M. & REMESAR, X. 2014. Treatment of rats with a self-selected hyperlipidic diet, increases the lipid content of the main adipose tissue sites in a proportion similar to that of the lipids in the rest of organs and tissues. *PLoS One,* 9**,** e90995.

RONG, J. X., QIU, Y., HANSEN, M. K., ZHU, L., ZHANG, V., XIE, M., OKAMOTO, Y., MATTIE, M. D., HIGASHIYAMA, H., ASANO, S., STRUM, J. C. & RYAN, T. E. 2007. Adipose mitochondrial biogenesis is suppressed in db/db and high-fat diet-fed mice and improved by rosiglitazone. *Diabetes,* 56**,** 1751-60.

ROOKS, C. R., PENN, D. M., KELSO, E., BOWERS, R. R., BARTNESS, T. J. & HARRIS, R. B. 2005. Sympathetic denervation does not prevent a reduction in fat pad size of rats or mice treated with peripherally administered leptin. *Am J Physiol Regul Integr Comp Physiol,* 289**,** R92-102.

ROSELL, M., KAFOROU, M., FRONTINI, A., OKOLO, A., CHAN, Y.-W., NIKOLOPOULOU, E., MILLERSHIP, S., FENECH, M. E., MACINTYRE, D., TURNER, J. O., MOORE, J. D., BLACKBURN, E., GULLICK, W. J., CINTI, S., MONTANA, G., PARKER, M. G. & CHRISTIAN, M. 2014. Brown and white adipose tissues: intrinsic differences in gene expression and response to cold exposure in mice. *American Journal of Physiology - Endocrinology and Metabolism,* 306**,** E945-E964.

ROSEN, E. D. & MACDOUGALD, O. A. 2006. Adipocyte differentiation from the inside out. *Nat Rev Mol Cell Biol,* 7**,** 885-96.

ROSEN, E. D., WALKEY, C. J., PUIGSERVER, P. & SPIEGELMAN, B. M. 2000. Transcriptional regulation of adipogenesis. *Genes Dev,* 14**,** 1293-307.

ROSENWALD, M., PERDIKARI, A., RULICKE, T. & WOLFRUM, C. 2013. Bi-directional interconversion of brite and white adipocytes. *Nat Cell Biol,* 15**,** 659-67.

ROTHWELL, N. J. & STOCK, M. J. 1979a. Regulation of energy balance in two models of reversible obesity in the rat. *J Comp Physiol Psychol,* 93**,** 1024-34.

ROTHWELL, N. J. & STOCK, M. J. 1979b. A role for brown adipose tissue in diet-induced thermogenesis. *Nature,* 281**,** 31-5.

ROTHWELL, N. J. & STOCK, M. J. 1983. Diet-Induced Thermogenesis. *In:* DRAPER, H. H. (ed.) *Advances in Nutritional Research: Volume 5.* Boston, MA: Springer US.

RYAN, B. C. & VANDENBERGH, J. G. 2002. Intrauterine position effects. *Neurosci Biobehav Rev,* 26**,** 665-78.

RYAN, E. A., O'SULLIVAN, M. J. & SKYLER, J. S. 1985. Insulin action during pregnancy. Studies with the euglycemic clamp technique. *Diabetes,* 34**,** 380-9.

SAIKI, R. K., GELFAND, D. H., STOFFEL, S., SCHARF, S. J., HIGUCHI, R., HORN, G. T., MULLIS, K. B. & ERLICH, H. A. 1988. Primer-directed enzymatic amplification of DNA with a thermostable DNA polymerase. *Science,* 239**,** 487-91.

SAITO, M. 2013. Brown adipose tissue as a therapeutic target for human obesity. *Obesity Research & Clinical Practice,* 7**,** e432-e438.

SAITO, M., OKAMATSU-OGURA, Y., MATSUSHITA, M., WATANABE, K., YONESHIRO, T., NIO-KOBAYASHI, J., IWANAGA, T., MIYAGAWA, M., KAMEYA, T. & NAKADA, K. 2009. High incidence of metabolically active brown adipose tissue in healthy adult humans. *Diabetes,* 58**,** 1526-1531.

SAKAMOTO, T., TAKAHASHI, N., GOTO, T. & KAWADA, T. 2014. Dietary factors evoke thermogenesis in adipose tissues. *Obesity Research & Clinical Practice,* 8**,** e533-e539.

SALAZAR, H., LLORENTE, I., JARA-OSEGUERA, A., GARCIA-VILLEGAS, R., MUNARI, M., GORDON, S. E., ISLAS, L. D. & ROSENBAUM, T. 2008. A single N-terminal cysteine in TRPV1 determines activation by pungent compounds from onion and garlic. *Nat Neurosci,* 11**,** 255-61.

SALDANA, T. M., SIEGA-RIZ, A. M. & ADAIR, L. S. 2004. Effect of macronutrient intake on the development of glucose intolerance during pregnancy. *Am J Clin Nutr,* 79**,** 479-86.

SAM, S. & MAZZONE, T. 2014. Adipose tissue changes in obesity and the impact on metabolic function. *Translational Research,* 164**,** 284-292.

SAMPEY, B. P., VANHOOSE, A. M., WINFIELD, H. M., FREEMERMAN, A. J., MUEHLBAUER, M. J., FUEGER, P. T., NEWGARD, C. B. & MAKOWSKI, L. 2011. Cafeteria diet is a robust model of human metabolic syndrome with liver and adipose inflammation: comparison to high-fat diet. *Obesity (Silver Spring, Md.),* 19**,** 1109-1117.

SAMUEL, V. T., PETERSEN, K. F. & SHULMAN, G. I. 2010. Lipid-induced insulin resistance: unravelling the mechanism. *Lancet,* 375.

SANCHEZ-GURMACHES, J. & GUERTIN, D. A. 2014. Adipocyte lineages: tracing back the origins of fat. *Biochim Biophys Acta,* 1842**,** 340-51.

SATO, A., KAWANO, H., NOTSU, T., OHTA, M., NAKAKUKI, M., MIZUGUCHI, K., ITOH, M., SUGANAMI, T. & OGAWA, Y. 2010. Antiobesity Effect of Eicosapentaenoic Acid in High-Fat/High-Sucrose Diet–Induced Obesity. *Diabetes,* 59**,** 2495.

SATYANARAYANA, A. 2016. Brown adipose tissue and the genetics of obesity.

SAXTON, A. M. & EISEN, E. J. 1984. Genetic analysis of brown adipose tissue, obesity and growth in mice. *Genetics,* 106**,** 705-18.

SCARPACE, P. J. & MATHENY, M. 1998. Leptin induction of UCP1 gene expression is dependent on sympathetic innervation. *Am J Physiol,* 275**,** E259-64.

SCHNEIDER, J. E. & WADE, G. N. 1987. Body composition, food intake, and brown fat thermogenesis in pregnant Djungarian hamsters. *Am J Physiol,* 253**,** R314-20.

SCHNEIDER, M. K., XUE, B. & SHI, H. 2018. Activation of the sympathetic nervous system suppresses mouse white adipose tissue hyperplasia through the β1 adrenergic receptor. *Physiological Reports,* 6**,** e13645.
SCHOENBORN, V., HEID, I. M., VOLLMERT, C., LINGENHEL, A., ADAMS, T. D., HOPKINS, P. N., ILLIG, T., ZIMMERMANN, R., ZECHNER, R., HUNT, S. C. & KRONENBERG, F. 2006. The ATGL gene is associated with free fatty acids, triglycerides, and type 2 diabetes. *Diabetes,* 55**,** 1270-5.
SCHREIBER, R., DIWOKY, C., SCHOISWOHL, G., FEILER, U., WONGSIRIROJ, N., ABDELLATIF, M., KOLB, D., HOEKS, J., KERSHAW, E. E., SEDEJ, S., SCHRAUWEN, P., HAEMMERLE, G. & ZECHNER, R. 2017. Cold-Induced Thermogenesis Depends on ATGL-Mediated Lipolysis in Cardiac Muscle, but Not Brown Adipose Tissue. *Cell metabolism,* 26**,** 753-763.e7.
SEALE, P., BJORK, B., YANG, W., KAJIMURA, S., CHIN, S., KUANG, S., SCIME, A., DEVARAKONDA, S., CONROE, H. M., ERDJUMENT-BROMAGE, H., TEMPST, P., RUDNICKI, M. A., BEIER, D. R. & SPIEGELMAN, B. M. 2008. PRDM16 controls a brown fat/skeletal muscle switch. *Nature,* 454**,** 961-967.
SEGULA, D. 2014. Complications of obesity in adults: A short review of the literature. *Malawi Medical Journal,* 26**,** 20-24.
SELLERS, R. S., MORTON, D., MICHAEL, B., ROOME, N., JOHNSON, J. K., YANO, B. L., PERRY, R. & SCHAFER, K. 2007. Society of Toxicologic Pathology position paper: organ weight recommendations for toxicology studies. *Toxicol Pathol,* 35**,** 751-5.
SENGUPTA, P. 2013. The Laboratory Rat: Relating Its Age With Human's. *International journal of preventive medicine,* 4**,** 624-630.
SHABALINA, I. G., PETROVIC, N., DE JONG, J. M., KALINOVICH, A. V., CANNON, B. & NEDERGAARD, J. 2013. UCP1 in brite/beige adipose tissue mitochondria is functionally thermogenic. *Cell Rep,* 5**,** 1196-203.
SHAFAT, A., MURRAY, B. & RUMSEY, D. 2009. Energy density in cafeteria diet induced hyperphagia in the rat. *Appetite,* 52**,** 34-8.
SHANKAR, K., HARRELL, A., LIU, X., GILCHRIST, J. M., RONIS, M. J. & BADGER, T. M. 2008. Maternal obesity at conception programs obesity in the offspring. *Am J Physiol Regul Integr Comp Physiol,* 294**,** R528-38.
SHARKEY, D., GARDNER, D. S., FAINBERG, H. P., SEBERT, S., BOS, P., WILSON, V., BELL, R., SYMONDS, M. E. & BUDGE, H. 2009. Maternal nutrient restriction during pregnancy differentially alters the unfolded protein response in adipose and renal tissue of obese juvenile offspring. *Faseb j,* 23**,** 1314-24.
SHERWIN, C. M. 1998. Voluntary wheel running: a review and novel interpretation. *Anim Behav,* 56**,** 11-27.
SHI, S. R., KEY, M. E. & KALRA, K. L. 1991. Antigen retrieval in formalin-fixed, paraffin-embedded tissues: an enhancement method for immunohistochemical staining based on microwave oven heating of tissue sections. *J Histochem Cytochem,* 39**,** 741-8.
SHIMAZU, T. 1996. Innervation of the liver and glucoregulation: Roles of the hypothalamus and autonomic nerves. *Nutrition,* 12**,** 65-66.
SHOWALTER, M. R., NONNECKE, E. B., LINDERHOLM, A. L., CAJKA, T., SA, M. R., LONNERDAL, B., KENYON, N. J. & FIEHN, O. 2018. Obesogenic diets alter metabolism in mice. *PLoS One,* 13**,** e0190632.
SILVA, J. E. 2005. Thyroid hormone and the energetic cost of keeping body temperature. *Biosci Rep,* 25**,** 129-48.

SILVER, N., BEST, S., JIANG, J. & THEIN, S. L. 2006. Selection of housekeeping genes for gene expression studies in human reticulocytes using real-time PCR. *BMC Mol Biol,* 7**,** 33.

SIMONDS, S. E., PRYOR, J. T., RAVUSSIN, E., GREENWAY, F. L., DILEONE, R., ALLEN, A. M., BASSI, J., ELMQUIST, J. K., KEOGH, J. M., HENNING, E., MYERS, M. G., JR., LICINIO, J., BROWN, R. D., ENRIORI, P. J., O'RAHILLY, S., STERNSON, S. M., GROVE, K. L., SPANSWICK, D. C., FAROOQI, I. S. & COWLEY, M. A. 2014. Leptin mediates the increase in blood pressure associated with obesity. *Cell,* 159**,** 1404-16.

SINITSKAYA, N., GOURMELEN, S., SCHUSTER-KLEIN, C., GUARDIOLA-LEMAITRE, B., PÉVET, P. & CHALLET, E. 2007. Increasing the fat-to-carbohydrate ratio in a high-fat diet prevents the development of obesity but not a prediabetic state in rats. *Clinical Science,* 113**,** 417.

SMITH, J. L., LEAR, S. R., FORTE, T. M., KO, W., MASSIMI, M. & ERICKSON, S. K. 1998. Effect of pregnancy and lactation on lipoprotein and cholesterol metabolism in the rat. *J Lipid Res,* 39**,** 2237-49.

SOLOVEVA, V., GRAVES, R. A., RASENICK, M. M., SPIEGELMAN, B. M. & ROSS, S. R. 1997. Transgenic mice overexpressing the beta 1-adrenergic receptor in adipose tissue are resistant to obesity. *Mol Endocrinol,* 11**,** 27-38.

SOMA-PILLAY, P., CATHERINE, N.-P., TOLPPANEN, H., MEBAZAA, A., TOLPPANEN, H. & MEBAZAA, A. 2016. Physiological changes in pregnancy. *Cardiovascular Journal of Africa,* 27**,** 89-94.

SPEAKMAN, J. R. & KEIJER, J. 2013. Not so hot: Optimal housing temperatures for mice to mimic the thermal environment of humans. *Molecular Metabolism,* 2**,** 5-9.

STEMMER, K., KOTZBECK, P., ZANI, F., BAUER, M., NEFF, C., MULLER, T. D., PFLUGER, P. T., SEELEY, R. J. & DIVANOVIC, S. 2015. Thermoneutral housing is a critical factor for immune function and diet-induced obesity in C57BL/6 nude mice. *Int J Obes (Lond),* 39**,** 791-7.

STUART, T. J., O'NEILL, K., CONDON, D., SASSON, I., SEN, P., XIA, Y. & SIMMONS, R. A. 2018. Diet-induced obesity alters the maternal metabolome and early placenta transcriptome and decreases placenta vascularity in the mouse†. *Biology of Reproduction,* 98**,** 795-809.

STUEBE, A. M., FORMAN, M. R. & MICHELS, K. B. 2009. Maternal-recalled gestational weight gain, pre-pregnancy body mass index, and obesity in the daughter. *Int J Obes (Lond),* 33**,** 743-52.

SUMITHRAN, P., PRENDERGAST, L. A., DELBRIDGE, E., PURCELL, K., SHULKES, A., KRIKETOS, A. & PROIETTO, J. 2011. Long-term persistence of hormonal adaptations to weight loss. *New England Journal of Medicine,* 365**,** 1597-1604.

SUMIYOSHI, M., SAKANAKA, M. & KIMURA, Y. 2006. Chronic Intake of High-Fat and High-Sucrose Diets Differentially Affects Glucose Intolerance in Mice. *The Journal of Nutrition,* 136**,** 582-587.

SUN, W., LI, C., ZHANG, Y., JIANG, C., ZHAI, M., ZHOU, Q., XIAO, L. & DENG, Q. 2017. Gene expression changes of thermo-sensitive transient receptor potential channels in obese mice. *Cell Biol Int,* 41**,** 908-913.

SWOAP, S. J., LI, C., WESS, J., PARSONS, A. D., WILLIAMS, T. D. & OVERTON, J. M. 2008. Vagal tone dominates autonomic control of mouse heart rate at thermoneutrality. *Am J Physiol Heart Circ Physiol,* 294**,** H1581-8.

SYMONDS, M. E. 2007. Integration of physiological and molecular mechanisms of the developmental origins of adult disease: new concepts and insights. *Proc Nutr Soc,* 66**,** 442-50.
SYMONDS, M. E. 2013. Brown adipose tissue growth and development. *Scientifica (Cairo),* 2013**,** 305763.
SYMONDS, M. E., ALDISS, P., DELLSCHAFT, N., LAW, J., FAINBERG, H. P., POPE, M., SACKS, H. & BUDGE, H. 2018. Brown adipose tissue development and function and its impact on reproduction. *J Endocrinol,* 238**,** R53-r62.
SYMONDS, M. E. & BUDGE, H. 2009. Nutritional models of the developmental programming of adult health and disease: Workshop on 'Nutritional models of the developmental origins of adult health and disease'. *Proceedings of the Nutrition Society,* 68**,** 173-178.
SYMONDS, M. E., SEBERT, S. & BUDGE, H. 2011. The Obesity Epidemic: From the Environment to Epigenetics – Not Simply a Response to Dietary Manipulation in a Thermoneutral Environment. *Frontiers in Genetics,* 2**,** 24.
SZALLASI, A. & BLUMBERG, P. M. 1999. Vanilloid (Capsaicin) receptors and mechanisms. *Pharmacol Rev,* 51**,** 159-212.
TANAKA, T., YOSHIDA, N., KISHIMOTO, T. & AKIRA, S. 1997. Defective adipocyte differentiation in mice lacking the C/EBPbeta and/or C/EBPdelta gene. *Embo j,* 16**,** 7432-43.
TCHOUKALOVA, Y. D., KOUTSARI, C., VOTRUBA, S. B., TCHKONIA, T., GIORGADZE, N., THOMOU, T., KIRKLAND, J. L. & JENSEN, M. D. 2010. Sex- and depot-dependent differences in adipogenesis in normal-weight humans. *Obesity (Silver Spring),* 18**,** 1875-80.
TEQUEANES, A. L., GIGANTE, D. P., ASSUNCAO, M. C., CHICA, D. A. & HORTA, B. L. 2009. Maternal anthropometry is associated with the body mass index and waist:height ratio of offspring at 23 years of age. *J Nutr,* 139**,** 750-4.
THENEN, S. W. & MAYER, J. 1975. Adipose tissue glycerokinase activity in genetic and acquired obesity in rats and mice. *Proc Soc Exp Biol Med,* 148**,** 953-7.
THIRUNAVUKKARASU, V., ANITHA NANDHINI, A. T. & ANURADHA, C. V. 2004. Lipoic acid attenuates hypertension and improves insulin sensitivity, kallikrein activity and nitrite levels in high fructose-fed rats. *J Comp Physiol B,* 174**,** 587-92.
THORNHILL, J. & HALVORSON, I. 1990. Brown adipose tissue thermogenic responses of rats induced by central stimulation: effect of age and cold acclimation. *J Physiol,* 426**,** 317-33.
TOWNSEND, K. & TSENG, Y. H. 2012. Brown adipose tissue: Recent insights into development, metabolic function and therapeutic potential. *Adipocyte,* 1**,** 13-24.
TRAYHURN, P. 1979. Thermoregulation in the diabetic-obese (db/db) mouse. The role of non-shivering thermogenesis in energy balance. *Pflugers Arch,* 380**,** 227-32.
TRAYHURN P, D. J., HOGGARD N, ET AL 1998. Regulation of leptin production : A dominant role for the sympathetic nervous system? . *Proc Nutr Soc 57 :413-419*.
TRAYHURN, P., THOMAS, M. E., DUNCAN, J. S. & RAYNER, D. V. 1995. Effects of fasting and refeeding on ob gene expression in white adipose tissue of lean and obese (oblob) mice. *FEBS Lett,* 368**,** 488-90.
TRAYHURN, P., THURLBY, P. L. & JAMES, W. P. 1977. Thermogenic defect in pre-obese ob/ob mice. *Nature,* 266**,** 60-2.

TURABELIDZE, A., GUO, S. & DIPIETRO, L. A. 2010. Importance of housekeeping gene selection for accurate reverse transcription-quantitative polymerase chain reaction in a wound healing model. *Wound Repair Regen,* 18**,** 460-6.

UETA, C. B., FERNANDES, G. W., CAPELO, L. P., FONSECA, T. L., D'ANGELO MACULAN, F., GOUVEIA, C. H. A., BRUM, P. C., CHRISTOFFOLETE, M. A., AOKI, M. S., LANCELLOTTI, C. L., KIM, B., BIANCO, A. C. & RIBEIRO, M. O. 2012. β(1) Adrenergic receptor is key to cold- and diet-induced thermogenesis in mice. *The Journal of endocrinology,* 214**,** 359-365.

VALET, P., PAGES, C., JEANNETON, O., DAVIAUD, D., BARBE, P., RECORD, M., SAULNIER-BLACHE, J. S. & LAFONTAN, M. 1998. Alpha2-adrenergic receptor-mediated release of lysophosphatidic acid by adipocytes. A paracrine signal for preadipocyte growth. *J Clin Invest,* 101**,** 1431-8.

VAN MARKEN LICHTENBELT, W. D., VANHOMMERIG, J. W., SMULDERS, N. M., DROSSAERTS, J. M., KEMERINK, G. J., BOUVY, N. D., SCHRAUWEN, P. & TEULE, G. J. 2009. Cold-activated brown adipose tissue in healthy men. *N Engl J Med,* 360**,** 1500-8.

VANDESOMPELE, J., DE PRETER, K., PATTYN, F., POPPE, B., VAN ROY, N., DE PAEPE, A. & SPELEMAN, F. 2002. Accurate normalization of real-time quantitative RT-PCR data by geometric averaging of multiple internal control genes. *Genome Biol,* 3**,** Research0034.

VETTER, T. R. & MASCHA, E. J. 2017. Defining the Primary Outcomes and Justifying Secondary Outcomes of a Study: Usually, the Fewer, the Better. *Anesthesia & Analgesia,* 125**,** 678-681.

VIGUERIE, N., VIDAL, H., ARNER, P., HOLST, C., VERDICH, C., AVIZOU, S., ASTRUP, A., SARIS, W. H., MACDONALD, I. A., KLIMCAKOVA, E., CLEMENT, K., MARTINEZ, A., HOFFSTEDT, J., SORENSEN, T. I. & LANGIN, D. 2005. Adipose tissue gene expression in obese subjects during low-fat and high-fat hypocaloric diets. *Diabetologia,* 48**,** 123-31.

VILLARROYA, F., CEREIJO, R., VILLARROYA, J. & GIRALT, M. 2017. Brown adipose tissue as a secretory organ. *Nat Rev Endocrinol,* 13**,** 26-35.

VILLARROYA, F., FELIPE, A. & MAMPEL, T. 1986. Sequential changes in brown adipose tissue composition, cytochrome oxidase activity and GDP binding throughout pregnancy and lactation in the rat. *Biochim Biophys Acta,* 882**,** 187-91.

VILLARROYA, F., IGLESIAS, R. & GIRALT, M. 2007. PPARs in the Control of Uncoupling Proteins Gene Expression. *PPAR Research,* 2007**,** 74364.

VIRTANEN, K. A., LIDELL, M. E., ORAVA, J., HEGLIND, M., WESTERGREN, R., NIEMI, T., TAITTONEN, M., LAINE, J., SAVISTO, N. J., ENERBACK, S. & NUUTILA, P. 2009. Functional brown adipose tissue in healthy adults. *N Engl J Med,* 360**,** 1518-25.

VOM SAAL, F. S., QUADAGNO, D. M., EVEN, M. D., KEISLER, L. W., KEISLER, D. H. & KHAN, S. 1990. Paradoxical effects of maternal stress on fetal steroids and postnatal reproductive traits in female mice from different intrauterine positions. *Biol Reprod,* 43**,** 751-61.

VOSSELMAN, M. J., BRANS, B., VAN DER LANS, A. A., WIERTS, R., VAN BAAK, M. A., MOTTAGHY, F. M., SCHRAUWEN, P. & VAN MARKEN LICHTENBELT, W. D. 2013. Brown adipose tissue activity after a high-calorie meal in humans. *The American journal of clinical nutrition,* 98**,** 57-64.

WABITSCH, M., JENSEN, P. B., BLUM, W. F., CHRISTOFFERSEN, C. T., ENGLARO, P., HEINZE, E., RASCHER, W., TELLER, W., TORNQVIST, H. &

HAUNER, H. 1996. Insulin and cortisol promote leptin production in cultured human fat cells. *Diabetes,* 45**,** 1435-8.
WALDEN, T. B., HANSEN, I. R., TIMMONS, J. A., CANNON, B. & NEDERGAARD, J. 2012. Recruited vs. nonrecruited molecular signatures of brown, "brite," and white adipose tissues. *Am J Physiol Endocrinol Metab,* 302**,** E19-31.
WANG, X., CHE, H., ZHANG, W., WANG, J., KE, T., CAO, R., MENG, S., LI, D., WEIMING, O., CHEN, J. & LUO, W. 2015. Effects of Mild Chronic Intermittent Cold Exposure on Rat Organs. *International Journal of Biological Sciences,* 11**,** 1171-1180.
WARTH, M. R., ARKY, R. A. & KNOPP, R. H. 1975. Lipid metabolism in pregnancy. II. Altered lipid composition in intermediage, very low, low and high-density lipoprotein fractions. *J Clin Endocrinol Metab,* 41**,** 649-55.
WATANABE, T., KAWADA, T., KUROSAWA, M., SATO, A. & IWAI, K. 1988. Adrenal sympathetic efferent nerve and catecholamine secretion excitation caused by capsaicin in rats. *Am J Physiol,* 255**,** E23-7.
WATANABE, T., KAWADA, T., YAMAMOTO, M. & IWAI, K. 1987. Capsaicin, a pungent principle of hot red pepper, evokes catecholamine secretion from the adrenal medulla of anesthetized rats. *Biochem Biophys Res Commun,* 142**,** 259-64.
WERNER, M., CHOTT, A., FABIANO, A. & BATTIFORA, H. 2000. Effect of formalin tissue fixation and processing on immunohistochemistry. *Am J Surg Pathol,* 24**,** 1016-9.
WESTERTERP, K. R. 2004. Diet induced thermogenesis. *Nutrition & Metabolism,* 1**,** 5.
WESTERTERP, K. R., WILSON, S. A. & ROLLAND, V. 1999. Diet induced thermogenesis measured over 24 h in a respiration chamber: effect of diet composition. *Int J Obes Relat Metab Disord,* 23.
WESTSTRATE, J. A. 1989. Diurnal variation in postabsorptive resting metabolic rate and diet-induced thermogenesis. *Am J Clin Nutr,* 50.
WHITAKER, R. C. 2004. Predicting preschooler obesity at birth: the role of maternal obesity in early pregnancy. *Pediatrics,* 114**,** e29-36.
WHITE, M. F. 2002. IRS proteins and the common path to diabetes. *Am J Physiol Endocrinol Metab,* 283**,** E413-22.
WHO 2016. Obesity and overweight.
WHO 2018. Obesity and overweight.
WILSON, K. & WALKER, J. 2010. *Principles and techniques of biochemistry and molecular biology*, Cambridge university press.
WINN, N. C., VIEIRA-POTTER, V. J., GASTECKI, M. L., WELLY, R. J., SCROGGINS, R. J., ZIDON, T. M., GAINES, T. K. L., WOODFORD, M. L., KARASSEVA, N. G., KANALEY, J. A., SACKS, H. S. & PADILLA, J. 2017. Loss of UCP1 exacerbates Western diet-induced glycemic dysregulation independent of changes in body weight in female mice. *American Journal of Physiology - Regulatory, Integrative and Comparative Physiology,* 312**,** R74-R84.
WU, J., BOSTROM, P., SPARKS, L. M., YE, L., CHOI, J. H., GIANG, A. H., KHANDEKAR, M., VIRTANEN, K. A., NUUTILA, P., SCHAART, G., HUANG, K., TU, H., VAN MARKEN LICHTENBELT, W. D., HOEKS, J., ENERBACK, S., SCHRAUWEN, P. & SPIEGELMAN, B. M. 2012. Beige adipocytes are a distinct type of thermogenic fat cell in mouse and human. *Cell,* 150**,** 366-76.

WULF, A., HARNEIT, A., KROGER, M., KEBENKO, M., WETZEL, M. G. & WEITZEL, J. M. 2008. T3-mediated expression of PGC-1alpha via a far upstream located thyroid hormone response element. *Mol Cell Endocrinol,* 287**,** 90-5.

XIAO, C., GOLDGOF, M., GAVRILOVA, O. & REITMAN, M. L. 2015. Anti-obesity and metabolic efficacy of the β3-adrenergic agonist, CL316243, in mice at thermoneutrality compared to 22°C. *Obesity (Silver Spring, Md.),* 23**,** 1450-1459.

XU, C., HE, J., JIANG, H., ZU, L., ZHAI, W., PU, S. & XU, G. 2009. Direct Effect of Glucocorticoids on Lipolysis in Adipocytes. *Molecular Endocrinology,* 23**,** 1161-1170.

YAN, J., YOUNG, M. E., CUI, L., LOPASCHUK, G. D., LIAO, R. & TIAN, R. 2009. Increased glucose uptake and oxidation in mouse hearts prevent high fatty acid oxidation but cause cardiac dysfunction in diet-induced obesity. *Circulation,* 119**,** 2818-28.

YANG, Z.-H., MIYAHARA, H., TAKEO, J. & KATAYAMA, M. 2012. Diet high in fat and sucrose induces rapid onset of obesity-related metabolic syndrome partly through rapid response of genes involved in lipogenesis, insulin signalling and inflammation in mice. *Diabetology & Metabolic Syndrome,* 4**,** 32.

YE, J. 2007. Role of insulin in the pathogenesis of free fatty acid-induced insulin resistance in skeletal muscle. *Endocr Metab Immune Disord Drug Targets,* 7**,** 65-74.

YE, J. 2008. Regulation of PPARgamma function by TNF-alpha. *Biochem Biophys Res Commun,* 374**,** 405-8.

YE, J. 2009. Emerging role of adipose tissue hypoxia in obesity and insulin resistance. *Int J Obes (Lond),* 33**,** 54-66.

YE, J. 2013. Mechanisms of insulin resistance in obesity. *Frontiers of medicine,* 7**,** 14-24.

YE, J., COULOURIS, G., ZARETSKAYA, I., CUTCUTACHE, I., ROZEN, S. & MADDEN, T. L. 2012. Primer-BLAST: A tool to design target-specific primers for polymerase chain reaction. *BMC Bioinformatics,* 13**,** 134-134.

YE, J. & GIMBLE, J. M. 2011. Regulation of stem cell differentiation in adipose tissue by chronic inflammation. *Clin Exp Pharmacol Physiol,* 38**,** 872-8.

YE, J. & MCGUINNESS, O. P. 2013. Inflammation during obesity is not all bad: evidence from animal and human studies. *Am J Physiol Endocrinol Metab,* 304**,** E466-77.

YONESHIRO, T., MATSUSHITA, M., NAKAE, S., KAMEYA, T., SUGIE, H., TANAKA, S. & SAITO, M. 2016. Brown adipose tissue is involved in the seasonal variation of cold-induced thermogenesis in humans. *Am J Physiol Regul Integr Comp Physiol,* 310**,** R999-r1009.

YOSHIOKA, M., DOUCET, E., DRAPEAU, V., DIONNE, I. & TREMBLAY, A. 2001. Combined effects of red pepper and caffeine consumption on 24 h energy balance in subjects given free access to foods. *Br J Nutr,* 85**,** 203-11.

YOSHIOKA, M., LIM, K., KIKUZATO, S., KIYONAGA, A., TANAKA, H., SHINDO, M. & SUZUKI, M. 1995. Effects of red-pepper diet on the energy metabolism in men. *J Nutr Sci Vitaminol (Tokyo),* 41**,** 647-56.

YOUNG, P., ARCH, J. R. & ASHWELL, M. 1984. Brown adipose tissue in the parametrial fat pad of the mouse. *FEBS Lett,* 167**,** 10-4.

YOUNGSTROM, T. G. & BARTNESS, T. J. 1998. White adipose tissue sympathetic nervous system denervation increases fat pad mass and fat cell number. *Am J Physiol,* 275**,** R1488-93.

ZECHNER, R., ZIMMERMANN, R., EICHMANN, T. O., KOHLWEIN, S. D., HAEMMERLE, G., LASS, A. & MADEO, F. 2012. FAT SIGNALS--lipases and lipolysis in lipid metabolism and signaling. *Cell Metab,* 15**,** 279-91.

ZHANG, J. W., TANG, Q. Q., VINSON, C. & LANE, M. D. 2004. Dominant-negative C/EBP disrupts mitotic clonal expansion and differentiation of 3T3-L1 preadipocytes. *Proc Natl Acad Sci U S A,* 101**,** 43-7.

ZHANG, L. L., YAN LIU, D., MA, L. Q., LUO, Z. D., CAO, T. B., ZHONG, J., YAN, Z. C., WANG, L. J., ZHAO, Z. G., ZHU, S. J., SCHRADER, M., THILO, F., ZHU, Z. M. & TEPEL, M. 2007. Activation of transient receptor potential vanilloid type-1 channel prevents adipogenesis and obesity. *Circ Res,* 100**,** 1063-70.

ZHANG, Y., GUO, K. Y., DIAZ, P. A., HEO, M. & LEIBEL, R. L. 2002. Determinants of leptin gene expression in fat depots of lean mice. *Am J Physiol Regul Integr Comp Physiol,* 282**,** R226-34.

ZIMMERMANN, R., STRAUSS, J. G., HAEMMERLE, G., SCHOISWOHL, G., BIRNER-GRUENBERGER, R., RIEDERER, M., LASS, A., NEUBERGER, G., EISENHABER, F., HERMETTER, A. & ZECHNER, R. 2004. Fat mobilization in adipose tissue is promoted by adipose triglyceride lipase. *Science,* 306**,** 1383-6.

ZINGARETTI, M. C., CROSTA, F., VITALI, A., GUERRIERI, M., FRONTINI, A., CANNON, B., NEDERGAARD, J. & CINTI, S. 2009. The presence of UCP1 demonstrates that metabolically active adipose tissue in the neck of adult humans truly represents brown adipose tissue. *Faseb j,* 23**,** 3113-20.

ZORZANO, A., LASUNCION, M. A. & HERRERA, E. 1986. Role of the availability of substrates on hepatic and renal gluconeogenesis in the fasted late pregnant rat. *Metabolism,* 35**,** 297-303.

Appedix: List of suppliers

Abcam	Cambridge, United Kingdom https://www.abcam.com/
ABgene	Abgene House, Blenheim Road, Epsom, KT19 9AP, UK. www.abgene.com
Abbott Laboratories	Vanwall Business Park, Vanwall Road, Maidenhead SL6 4XE. https://nutrition.abbott/uk
ALPCO diagnostic	26-G, Keewaydin Dr, Salem, NH 03079, USA. https://www.alpco.com/
Ambion	850 Lincoln Centre Drive, Foster City, CA 94404, USA. www.ambion.com
Applied Biosystems	Lingley House 120 Birchwood Boulevard, Warrington, Cheshire, WA3 7QH, Uk. www.appliedbiosystems.com
Bio-Rad Ltd.	Life Science Research, Education, Process Separations, Food Science, 2000 Alfred Nobel Drive, Hercules, California 94547, USA. www.bio-rad.com
Charles River Laboratories	Pharmaceutical company. Wilmington, Massachusetts, United States. https://www.criver.com/

Fisher Scientific UK Ltd	Bishop Meadow Road, Loughborough, LE11 5RG, UK. www.fishersci.co.uk
IBM Corporation	Armonk, New York, USA. https://www.ibm.com/ca-en/?ar=1
ImageJ	https://imagej.nih.gov/ij/
GraphPad Software	7825 Fay Avenue, Suite 230, La Jolla, CA, USA. www.graphpad.com
Hamamatsu Photonics (UK) Ltd	10 Tewin Rd, Welwyn Garden City, Hertfordshire, AL7 1BW, UK. www.hamamatsu.com
Harlan UK Ltd	Shaws Farm, Station Road, Blackthorn, Bicester OX25 1TP, UK.
Improvision Ltd	Coventry, UK www.improvision.com
Leica Biosystems	Balliol Business Park West, Newcastle Upon Tyne, NE12 8EW, UK. www.leicabiosystems.com
Leica Microsystems	Larch House, Woodland Business Park, Breckland, Linford Woods, Milton Keynes, MK14 6FG, UK. www.leica-microsystems.com

Larch House, Woodland Business Park, Breckland, Linford Woods, Milton Keynes, MK14 6FG, UK. www.leica-microsystems.com

Menzel-Gläser	Glasbearbeitungswerk GmbH & Co., Saarbrückener Str. 248, D-38116, Braunschweig, Germany. www.menzel.de Glasbearbeitungswerk GmbH & Co., Saarbrückener Str. 248, D-38116, Braunschweig, Germany. www.menzel.de
Nano Drop Technologies	3411 Silverside Rd # 100BC, Wilmington, DE 19810, USA
Nikon UK Ltd	380 Richmond Rd, Kingston upon Thames, Surrey, KT2 5DB, UK. www.europe-nikon.com/en_GB/
Premier Biosoft	3786 Corina Way, Palo Alto, CA 94303, USA. http://www.premierbiosoft.com/
Primer Design	Millbrook Technology Campus, Second Avenue, Southampton, Hampshire, SO15 0DJ, UK. www.primerdesign.co.uk
TechEn Inc	115 Cedar St # N1, Milford, MA 01757, USA. http://www.techen.com/
Qiagen	Qiagen House, Fleming Way, Crawley, West Sussex, RH10 9NQ, UK. www.qiagen.com
Sigma Chemicals	Fancy Rd, Poole BH12 4QH, UK. https://www.sigmaaldrich.com/united-kingdom.html

Simport Scientific	2588 Bernard-Pilon Street, Beloeil, QC J3G 4S5, Canada. www.simport.com
Thermo Scientific	Sarstrabe 1, 51588 Nümbrecht, Germany. www.sarstedt.com
Simport Scientific	2588 Bernard-Pilon Street, Beloeil, QC J3G 4S5, Canada. www.simport.com
VWR	Hunter Boulevard, Magna Park, Lutterworth, Leicestershire, LE17 4XN, UK. www.vwr.com